ABSTRACT

XIE, YU. Preparation and Evaluation of Small Diameter Blood Vessels with Knitted and Electrospun Bilayer Structure. (Under the direction of Martin W. King).

Coronary arterial disease (CAD) and peripheral arterial disease (PAD) are dominant cardio-vascular diseases accounting for 24.2% of the mortality rate in United States. The gold standard biomaterials for use in by-pass surgery are autologous vessels, such as the saphenous vein and the internal mammary artery. However, these vessels may not be available due to aging, previous harvesting or the pre-existing arterial disease (Konig et al, 2009). As a result, an artificial vascular graft is considered an alternative strategy for coronary arterial bypass surgery. Nevertheless, in spite of their successful application for larger vessels, synthetic materials, such as ePTFE and polyester (PET), have not been found to be suitable for small diameter (< 6mm) vascular grafts. Such commercial grafts usually show a low patency rate after implantation generally due to their high thrombogenicity, low radial compliance and limited ability to grow contiguous endothelial cells on the lumenal surface. To address these issues, many attempts have been tried, such as using alternative biodegradable synthetic polymers and natural polymers, coating the surface with collagen and other proteins, seeding endothelial and smooth muscle cells and so forth. And some of these strategies have shown promise to improve some of these issues. In this study, the objective was to design and fabricate a series of multilayer small diameter vessels for the treatment of coronary artery and peripheral artery disease, based on the concept of mimicking native extracellular matrix morphology to improve endothelial cell attachment to the luminal surface, increase compliance and minimize thrombogenicity.

A series of small diameter vascular grafts (approximately 3 mm in diameter) were fabricated using a composite bilayer approach by first knitting 170 denier poly(lactic acid) (PLA) multifilament yarn on a small diameter circular weft knitting machine and then wrapped it with an electrospun poly(lactide-co-caprolactone) (PLCL) thin layer. The results indicated that the bilayer structure had excellent circumferential tensile strength, bursting strength and suture retention resistance. But, the radial compliance did not show any observable improvement as a result of the unique structure. By applying a collagen and elastin coating and crosslinking it with genipin, the vascular grafts showed improvements in above-mentioned mechanical properties and a significant decrease in thrombus formation. Additionally, a more uniform and contiguous distribution of endothelial cells was observed after 7 days on grafts with an internal electrospun layer. However, the additional collagen/elastin impregnation did not result in a significant increase in cell proliferation.

Preparation and Evaluation of Small Diameter Blood Vessels with Knitted and Electrospun Bilayer Structure

by
Yu Xie

A thesis submitted to the Graduate Faculty of
North Carolina State University
in partial fulfillment of the
requirements for the degree of
Master of Science

Textile Engineering

Raleigh, North Carolina

2014

APPROVED BY:

Dr. Martin W. King Committee Chair	Dr. Tushar K. Ghosh

Dr. Rita M. Hanel

DEDICATION

To my beloved family

To my friends

To my advisor Dr. Martin W. King

BIOGRAPHY

Yu Xie was born on September 12th, 1988 in Chongqing, P.R. China. She received her Bachelor of Science degree in Textile Engineering in July 2011 from Southwest University, P.R. China. Yu joined North Carolina State University to start her further study in Textile Engineering in August 2012. As expected, she plans to receive her Master of Science degree in December 2014. With a strong interest in medical textiles, she decides to apply for and enroll in the PhD program, Fiber and Polymer Science at North Carolina State University after her graduation.

ACKNOWLEDGMENTS

I would like to give me sincere gratitude for those who have helped me in this study. First and foremost, I want to give my deepest appreciation to my advisor Dr. Martin W. King for providing me such a great opportunity to work in the area that I am interested in and I am so honored to work with him in the past two years. His ceaseless dedication on research and pursuit for new knowledge are always inspiring and deeply motivating for me. Thanks to his full support and encouragement, this project is able to progress successfully. He did his utmost to advise and guide me, give me suggestions and address problems with me.

I also want to appreciate other members in my advisory committee. Many thanks to Dr. Tushar Ghosh for advising me how to improve the fabricating process and providing me with electrospinning apparatus from his lab. Many thanks to Dr. Rita Hanel for her assistance with the thrombogenicity test and also spending time with me to explain how to analyze the results.

I would like to give my special thanks to William Barnes, Judy Elson, Jennifer Spencer, Dr. Eva Johannes, Ying Guan, Hai Bui and Tri Vu for their kind assistance and dedication with my experimental work. My appreciation also goes to all the group members in Biomedical Textile research group. It is their wise advice and rich experience in the area that has encouraged and helped me to complete this project. I am especially thankful to Xinyue Lu and Ting He for spending their time to assist me with my experimental work.

Last but not least, I must express my sincere and deepest gratitude to my family and particularly my parents for their everlasting love and belief in me. They have encouraged and

supported my time of study here in the USA, and most importantly I appreciate them for their understanding and respect for my decisions. My appreciation also extends to all my great friends here in the USA and back in China who have given me such extensive support and encouragement during my life so far.

TABLE OF CONTENTS

LIST OF TABLES

LIST OF FIGURES

LITERATURE REVIEW

MATERIALS AND METHODS

RESULTS AND DISCUSSIONS

LIST OF ABBRIVIATIONS, TERMS AND DEFINITIONS

CVD	Cardiovascular disease
CAD	Coronary artery disease
PAD	Peripheral artery disease
PLA	Poly(lactic acid)
PLCL	Poly(L-lactide-co-ε-caprolactone)
SEM	Scanning electron microscope
PCI	Percutaneous coronary intervention
CABG	Coronary artery bypass graft surgery
UA/NSTEMI	Unstable angina/non–ST-elevated myocardial infarction
PTA	Percutaneous transluminal angioplasty
ePTFE	Expanded polytetrafluoroethylene
PET	Poly (ethylene terephthalate)
PU	Polyurethane
EC	Endothelial cell
SMC	Smooth muscle cell
RGD	Arginine-glycine-aspartic acid peptide
ECM	Extra-cellular matrix
GAGs	Glycosaminoglycans
FOY	Fully oriented yarn
LSCM	Laser Scanning Confocal Microscope
DMEM	Dulbecco's Modification of Eagle's Medium
TEG	Thromboelastography

FBS	Fetal Bovine Serum
P/S	Penicillin – streptomycin
BAOECs	Bovine aortic endothelial cells
MTT	Thiazolyl Blue Tetrazolium Bromide
PBS	Phosphate buffer solution
DMSO	Dimethyl sulfoxide
DAPI	4′, 6-diamidino-2-phenylindole
Stenosis	Narrowing of arteries
Occlusion	Blockage of arteries
Angioplasty	Coronary artery reconstruction
Patency	An open or unobstructed state of blood vessels
Autograft	A vascular graft that is transplanted from other part of the same patient
Allograft	A vascular graft that is transplanted from another individual of the same species
Xenograft	A vascular graft that is donated from other species
Thrombogenicity	A tendency to produce thrombus or clot
Endothelialization	An formation of endothelial tissue
Neointimal hyperplasia	Thickening of arterial walls and decreased arterial lumen space due to proliferation and migration of vascular smooth muscle cells

CHAPTER 1

INTRODUCTION

1.1 Background

Cardiovascular disease (CVD) is one type of fatal disease that leads to a significant death rate worldwide. CVD is known as any disease of the heart or its blood vessels, including the arteries, veins and capillaries of the brain, kidneys, and the peripheral vasculature (Institute of Medicine Committee, 2010). In fact, particularly in low and middle income countries, around 30% of all deaths are attributable to CVD (WHO, 2008). Also, it is estimated by the World Health Organization (WHO) that about 17.3 million people died from CVD in 2008. The increasing attention on CVD also accounts for its related chronic diseases, namely diabetes, cancer and chronic respiratory disease, which are all regarded as prevalent diseases with high morbidity.

A number of risk factors known to result in CVD and its related chronic diseases have been shown in global health studies. Table 1.1 shows the 10 highest risk factors worldwide that contribute to poor health. Among these the top six risk factors all associated with an increased incidence of cardiovascular disease (CVD). The most common type of CVD includes coronary artery disease, cerebrovascular disease, peripheral arterial disease, rheumatic heart disease, congenital heart disease, deep vein thrombosis (DVT) leading to pulmonary embolism, heart attacks and stroke which are usually acute events (WHO, 2013).

Coronary artery disease (CAD), also known as atherosclerosis, is the most dominant and common type of CVD, accounting for 43.8% of the entire CV mortality rate in the United States in 2008 (National Heart, Lung, and Blood Institute (NHLBI), 2012). Peripheral artery disease (PAD) is another common CVD, which has 3 to 12 percent prevalence worldwide (Hirsch et al., 2006). In 2010, it was estimated that 202 million people around the world were living with PAD (Fowkes et al., 2013). In Europe and North America, an estimated 27 million individuals were affected with approximately 413,000 inpatient admissions annually attributed to PAD (Norgren et al., 2007).

Table 1. 1 Ten Highest Risk Factors Causing Death Worldwide in 2004 (Institute of Medicine Committee, 2010)

Rank	Risk Factor	Deaths (Millions)	% of total
1	High Blood Pressure	7.5	12.8
2	Tobacco Use	5.1	8.7
3	High Blood Glucose	3.4	5.8
4	Physical Inactivity	3.2	5.5
5	Overweight and Obesity	2.8	4.8
6	High Cholesterol	2.6	4.5
7	Unsafe Sex	2.4	4.0
8	Alcohol Use	2.3	3.8
9	Childhood Underweight	2.2	3.8
10	Indoor Smoke from Solid Fuels	2.0	3.3

1.2 Goals and Objectives

The overall goal of this research is to fabricate a series of multilayer small diameter vessels for the treatment of coronary artery and peripheral artery diseases, based on the concept of mimicking native extracellular matrix morphology to improve endothelial cell attachment to the luminal surface, and then studying the mechanical and biological performance of the prototype structures. Weft tubular knitting and electrospinning techniques are to be used for producing a concentric PLA/PLCL bilayer framework of a vascular prosthesis. It is then proposed to subsequently impregnate the structure with a collagen/elastin protein mixture followed by crosslinking with genipin.

The four objectives that will be addressed in this study are listed below:

1) To fabricate a series of multilayer small diameter tubular vascular prostheses with different structures. One layer will be knitted from poly(lactic acid) (PLA) multifilaments and the other concentric layer will be electrospun from an elastomeric poly(L-lactide-co-ε-caprolactone) copolymer. Details of the two different vascular prototypes and their three controls are as follows:

    i) A double layer tubular vessel with an outer knitted structure attached to an inner electrospun layer and impregnated with a cross-linked collagen/elastin coating. (This is the knitted(outside)/electrospun(inside)/impregnated graft.)

    ii) A double layer tubular vessel with an inner knitted structure attached to an outer electrospun layer and impregnated with a cross-linked collagen/elastin coating. (This

is the knitted(inside)/electrospun(outside)/impregnated graft.)

iii) A single layer tubular knitted control vessel impregnated with a cross-linked collagen/elastin coating. (This is the knitted /impregnated graft.)

iv) A double layer tubular control vessel with an inner knitted structure attached to an outside electrospun layer with no impregnated coating. (This is the knitted(inside)/electrospun(outside)/non-impregnated graft.)

v) A single layer tubular knitted control vessel with no impregnated coating. (This is the knitted/non-impregnated graft.)

2) To evaluate the mechanical properties of these designed prototype vascular prostheses and their controls in terms of the following characteristics:

i) Circumferential tensile strength

ii) Bursting strength

iii) Compliance

iv) Suture retention strength.

In particular, the specific objectives were to assess the influence of the following independent variables on the above four mechanical properties of the small diameter prototype vascular grafts:

a) the inclusion of a second PLCL electrospun layer,

b) whether the electrospun layer was on the outside or the inside of the graft, and

c) the impregnated collagen/elastin protein coating with genipin crosslinking.

3) To evaluate the biological properties of these designed prototype vascular prostheses and their controls in terms of their thrombogenicity and endothelial cell attachment and viability. These characteristics will be evaluated through the use of a thromboelastography (TEG), and MTT assay, immunofluorescence and scanning electron microscopy (SEM). In particular, the specific objectives were to assess the influence of the following independent variables on these two biological properties of the small diameter prototype vascular grafts:

a) the inclusion of a second PLCL electrospun layer,

b) whether the electrospun layer was on the outside or the inside of the graft, and

c) the impregnated collagen/elastin protein coating with genipin crosslinking.

4) To determine whether the attachment of an elastomeric electrospun layer and/or the application of an impregnated and cross-linked collagen/elastin coating addressed the problem of raveling of the weft knitted structure.

1.3 Outline of the Thesis

This thesis contains five chapters, and the first chapter provides some background information about the incidence of cardiovascular disease in the world and then lists the goals

and objectives of the study. Second chapter reviews the relevant literatures of the pathology and therapy of two typical cardiovascular diseases, the materials and fabrication methodologies currently used and researched for small diameter vascular graft. The selected materials in this study are discussed and highlighted specifically. The third chapter describes the experimental design, including fabrication methods and physical and biological property evaluations. The fourth chapter reports the result of the characterization of small diameter vascular graft in terms of surface morphology, mechanical and biological performances. Finally, the last chapter gives a summary and conclusions based on the experimental results and lists recommendations for future study.

CHAPTER 2

REVIEW OF LITERATURE

2.1 Coronary artery disease (CAD) and revascularization

Coronary artery disease (CAD) or atherosclerosis, simply known as narrowing (stenosis) of the coronary arteries that supply the myocardium with oxygen and nutrients is generally due to the buildup of plaque on the arterial walls, as shown in Figure 2.1.1. Plaque is mainly composed of cholesterol-rich fatty deposits, collagen, other proteins and excess smooth muscle cells. CAD is a lifetime disease and usually progresses gradually with thickening and narrowing of the arterial wall, resulting in severely restricted blood flow and deficiency of oxygen and vital nutrients supplied to the heart. This pathology is called ischemia. This can lead to some attendant symptoms such as muscle cramp-like chest pain, called angina. Blood clots form more easily on arterial walls roughened by plaque deposits and may result in complete blockage (occlusion) of one or more of the narrowed coronary arteries and cause a heart attack. Arteries may also narrow suddenly as a result of an arterial spasm. (Johns Hopkins Medicine, n.d. (a))

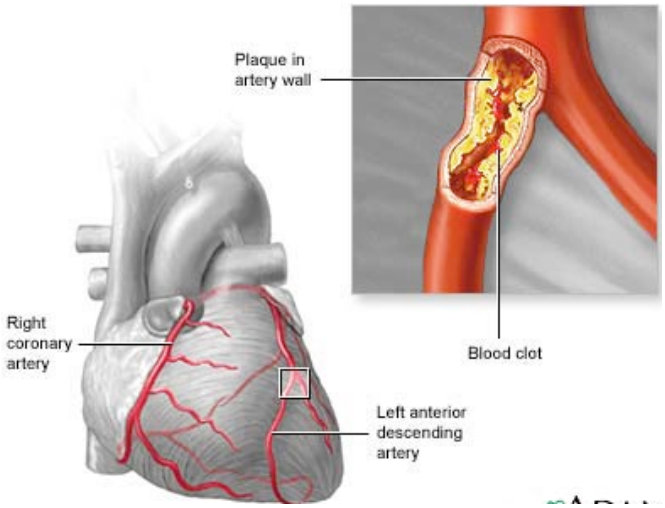

Figure 2. 1 Coronary artery and the causes of atherosclerosis (Copyright © 2010 healthcentral.com)

Coronary artery reconstruction (angioplasty) is also referred to as percutaneous coronary intervention (PCI)) and coronary artery bypass surgery. These are the two primary revascularization treatments for severe CAD. PCI is performed to open blocked coronary arteries without open-heart surgery and to restore arterial blood flow to the heart tissue by inserting a special catheter with a balloon which is inflated once the catheter has been placed within the narrowed arterial segment. The purpose of expanding the balloon catheter is to compress the fatty plaque attached to the arterial wall and make a larger opening inside the artery for improved blood flow, as shown in Figure 2.2 (Johns Hopkins Medicine, n.d.(b)). Coronary artery bypass graft surgery (also called CABG) is a way to redirect blood flow to the heart muscle by means of a substitute vessel grafted so as to bypass the blockage (Figure 2.2). When considering long-term patency, autologous blood vessels are always the best options for CABG surgery. They are usually harvested from the patients' chest, legs, or arms,

most often involving either the internal mammary artery or the saphenous vein depending on availability. These autologous materials are known as the "gold standard" for CABG bypass surgery. Other possible substitute vessels include the radial artery from the lower arm, the gastroepiploic artery from the stomach or the inferior epigastric artery from the abdominal wall (WebMD, n.d.). However, about one-third of patients do not have veins or arteries suitable for grafting due to either their pre-existing vascular disease, or vein stripping, or vein harvesting for a prior vascular procedure (X.W. Wang et al., 2007). As a result there remains a significant need for a small diameter vascular prosthesis.

In 2007, for these two treatment surgeries, PCI or CABG, specific guidelines were established by the American College of Cardiology and the American Heart Association (ACC/AHA) for patients presenting with unstable angina and non-ST-elevated myocardial infarction ("ST" refers to a pattern that shows up on an electrocardiogram). These most recent recommendations are targeting this group of patients who experienced a sudden partial blockage of their coronary artery and identified as being at high risk of death or myocardial infarction (Figure 2. 3) (Hernandez, 2010). In comparison with PCI, the main advantages of CABG are a lower rate of reoperations, greater success with chronically occluded coronary arteries, and protection of the entire vessel proximal to the distal anastomosis (Kalyanasundaram, 2012). More recently, the use of drug-eluting stents, has served to decrease restenosis and the need for repeat procedures.

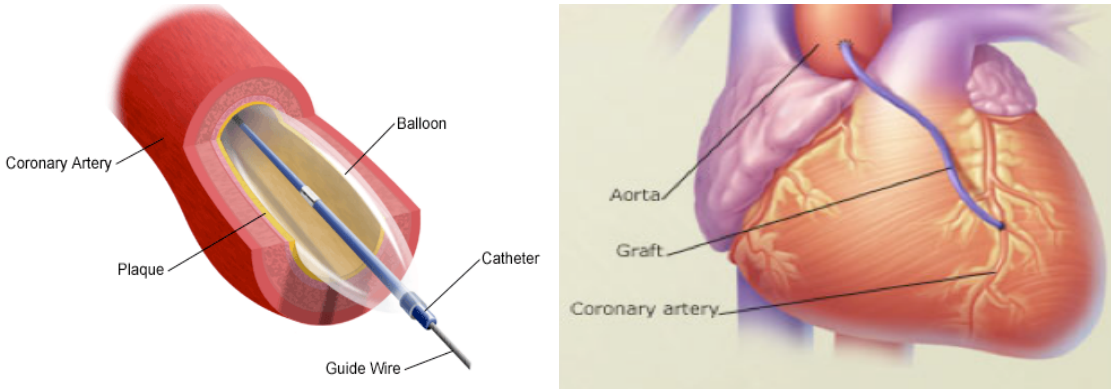

(a) (b)

Figure 2. 2 PCI and CABG surgical therapies for coronary artery disease. (a) Inflation of a balloon in percutaneous coronary intervention (PCI) (Copyright © hopkinsmedicine.org); (b) coronary artery bypass graft surgery (CABG) (Copyright © 2002 WebMD, Inc.)

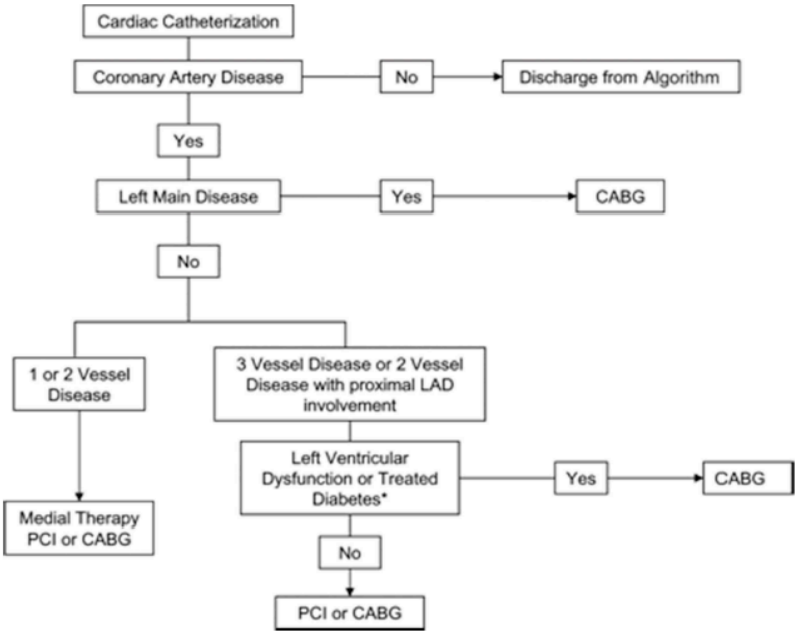

Figure 2. 3 Revascularization strategies for patients presenting with unstable angina/non–ST-elevated myocardial infarction (UA/NSTEMI). (Copyright © 2011 American Heart Association, Inc.)

2.2 Peripheral Arterial Disease (PAD) and revascularization

Peripheral arterial disease (PAD) is generally associated with narrowed or blocked arteries located in the legs. This is similar to the stenosis or occlusion of the coronary arteries due to atherosclerosis, a chronic buildup of hard fatty material on the inside lining of the arterial wall (Figure2.1). This narrowing or blockage ultimately leads to a deficiency of oxygen and nutrients to the lower limbs. The femoral and popliteal arteries are the major vessels that supply blood to the lower extremities and they are a common location for atherosclerotic disease to develop. Apart from the stenosis and occlusion of blood flow, other potential deficits associated with atherosclerosis include claudication pain in the legs, ulcers or wounds that do not heal, and the possibility of infection and gangrene that can lead to amputation (surgical removal) of the foot or leg. (Memorial Health System, 2009)

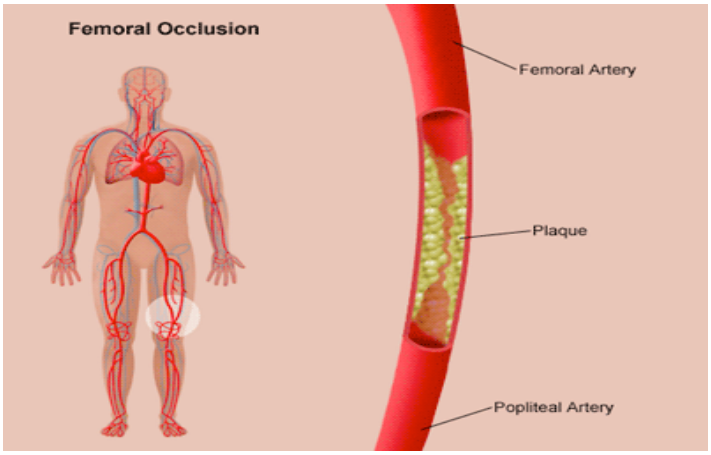

Figure 2. 4 Blockage of the femoral popliteal artery in the leg (Copyright © 2009 Memorial Health System)

The two most common treatments for PAD are percutaneous transluminal angioplasty (PTA) and femoral popliteal bypass. Percutaneous transluminal angioplasty is a minimally invasive procedure used to open the narrowed or stenosed vessel and to restore arterial blood flow to the lower leg by inserting (without a large incision) a special catheter with a tiny balloon into the femoral artery. The balloon is inflated to compress the plaque against the wall of the artery and make the opening larger. It is also possible to insert a stent (a small, expandable metal coil) into the newly opened lumen of the artery to avoid a potential re-stenosis or a repeat blockage. The alternative approach is to perform a femoral popliteal bypass procedure to direct the blood flow around the blocked portion of the artery using a segment of a native or prosthetic vessel similar to coronary artery bypass surgery. A native vessel segment is often the saphenous vein taken from the patient's own leg and implanted with blood flow in the reverse direction to avoid flow disruption from the venous valves. One end of the vein graft is attached above the blockage and the other end is attached below the blockage, rerouting blood flow around the occluded segment through the implanted graft. (Memorial Health System, 2009)

2.3 Small diameter vascular prostheses

Risk factors associated with the buildup of plaque, i.e. high blood pressure and high blood cholesterol, are greatly affected by lifestyle. Therefore, lifestyle changes are most effective in the prevention and/or treatment of atherosclerosis. These will include maintaining a healthy diet, proper exercise, a healthy weight and ensuring emotional health by stress management as well as a reduction in or a cessation of smoking. However, when patients have severe

atherosclerosis, a more immediate way to alleviate their symptoms is by PCI or CABG surgery. In the CABG procedure, autologous arteries or veins from other areas in the body are the preferred grafts of choice. Nevertheless, pre-existing vascular disease, vein stripping, or vein harvesting for a previous vascular procedure may limit the availability of these vascular graft materials. Normal coronary arteries have relatively small luminal diameters in the range of 2-4.5 mm (Dodge et al., 1992). The actual diameter may be different between males and females, between left and right coronary arteries, and between different sites along the length of the artery. The average internal diameter of a typical femoral artery is around 6-8 mm (Vinila et al., 2013), while a distal popliteal artery is found with a finer external diameter of 4-5 mm (Wolf et al., 2006). Thus, the vessels suitable for bypass surgery are usually small diameter prostheses with an inner diameter of less than 6mm.

2.3.1 Vascular prosthesis fabrication

Synthetic prostheses were developed rapidly in response to the limitation of access to biological vascular grafts, such as autografts, allografts and xenografts. Textile structures are most attractive for a number of reasons. Woven and knitted synthetic vascular grafts have been used for 50 years, and most of the current commercial prostheses are still woven and knitted from polyethylene terephthalate (polyester) yarns (King, 1991). The different structures of woven and knitted fabrics as shown in Figure 2.5, each have their own distinct advantages. Woven fabrics involve the interweaving of warp and weft yarns at right angles to each other. The 1/1 plain weave for instance can form a tightly woven, smooth, low porosity surface, which prevents blood leakage and avoids the need for pre-clotting before surgery. As

for warp and weft knitted fabrics, they are more flexible and compliant compared to woven structures. The advantages and disadvantages of each type of structure are summarized in Table 2.1.

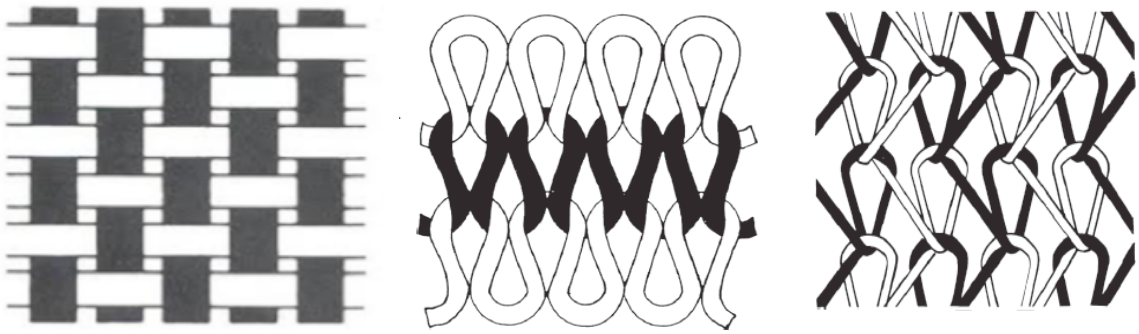

(a) (b) (c)

Figure 2. 5 Woven, weft knitted and warp knitted structures used for vascular prostheses: (a) 1/1 plain weave, (b) single jersey weft knit, (c) single locknit warp knit.

Table 2. 1 Comparison of different polyester (PET) textile structures for vascular grafts. (Chlupac, 2009; King, 2013)

	Woven	Weft-knitted	Warp-knitted
Advantages	Superior biostability, Low permeability, No bleeding	Greater porosity, Tissue ingrowth, Radial compliance	Biostable, Greater porosity, Tissue ingrowth, Radial compliance No raveling
Disadvantages	Low compliance, Limited tissue incorporation,	Dilation over time, Yarns ravel,	Infection risk

Table 2. 1 Continued

	Low porosity, Fraying along cut edges, Infection risk	Infection risk

For many years, researchers have devoted their energy to explore advanced and versatile materials that will serve as permanent, biostable and non-thrombogenic small diameter vascular prostheses. An alternative approach is to follow the concept of tissue engineering that relies on the body's natural regenerative ability to grow viable living tissue using a temporary scaffold to mimic the native ECM. This can be achieved by fabricating biodegradable webs from synthetic and natural polymers, such as polylactide (PLA), polycaprolactone (PCL) and chitosan, using a special spinning technique called electrospinning, which is able to produce fine fibers at the nanoscale. Electrospinning is currently one of the most prevalent methods for fabricating small diameter vascular prostheses. By taking advantage of a high-voltage electrostatic field, the individual filaments are accelerated and attenuated as soon as they are released from the needle containing the polymer solution (Figure 2.6). Typically fibers are deposited on a grounded metal collector and accumulate to form a random nonwoven web. When a high voltage (5-50kV) is applied on the conductive polymer solution in the spinneret nozzle, a repulsive force is generated which overcomes the surface tension of the solution and produces a continuous jet of polymer from the tip of the syringe or spinneret. The solvent evaporates as soon as the

charged jet is accelerated towards the grounded collector and the entanglements of the polymer chains prevent the jet from breaking up which results in fiber formation (Ramakrishna et al, 2006). By electrospinning, fibers can be spun with a range of diameters from several microns down to 100 nm or less at the nanosacle.

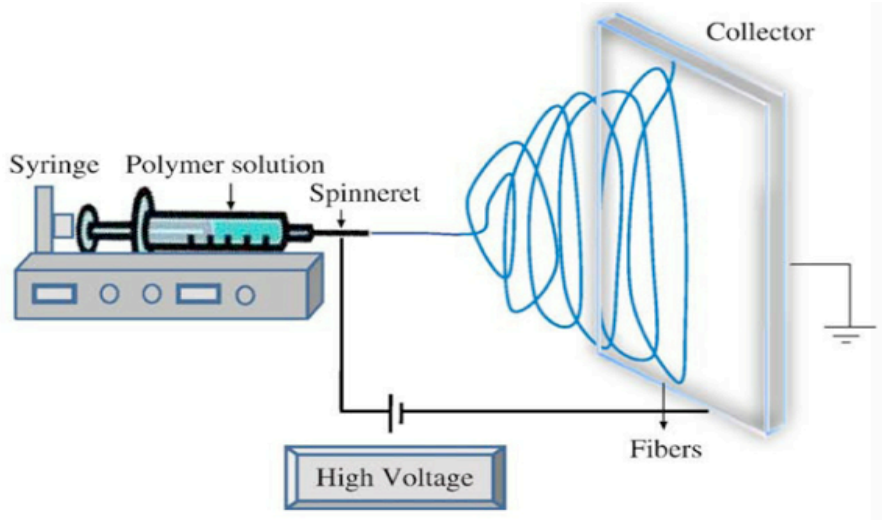

Figure 2. 6 Schematic diagram of electrospinning set-up (Copyright © Zhu, 2013)

Recently a number of researchers have reported the development of small diameter vascular grafts using an electrospining technique. Elecrospun vascular scaffolds have been produced from synthetic polymers likely polycaprolactone PCL (Pektok et al., 2008), poly-L-lactide-cocaprolactone (PLCL) (Inoguchi et al, 2006), and biopolymers, such as chitosan, collagen, elastin and related compounds (Zhao, 2013; McClure, 2010). These are all potential candidates for small diameter vascular prosthesis scaffolds with promising mechanical and

biocompatible properties. By being able to mimic the structure of native artery walls, multi-layered electrospun vessels (McClure, 2010; Valence, 2012) have been shown to have strong potential as a scaffold for vascular tissue regeneration.

2.3.2 Vascular prostheses materials

Early attempts to develop artificial blood vessels have focused on the usage of synthetic materials like expanded polytetrafluoroethylene (ePTFE or Teflon®) and poly(ethylene terephthalate (PET or Dacron®), which have been used commercially as larger diameter vascular grafts (King, 1991). The same materials have also been used in the development of smaller diameter vascular prostheses. For example, non-biodegradable ePTFE with an electronegative luminal surface is antithrombotic and is now widely used for lower limb bypass grafts (7–9 mm) with excellent results (X.W. Wang et al., 2007). Compared with autologous vein grafts, however, they have inferior patency. A five-year study showed that only 45% of ePTFE bypass grafts are patent in the femoropopliteal position while autologous vein grafts have 77% patency (Taylor et al., 1990). PET yarns are usually fabricated by weaving or knitting into vascular tubes. Woven PET vascular grafts have better stability, lower permeability and less bleeding, but they also have the disadvantages of reduced compliance, less tissue incorporation, low porosity and fraying particularly at cut edges. Knitted PET grafts have greater porosity, tissue ingrowth and radial compliance, although they dilate over time (King, 1991). And the risk of infection is the same for both structures. (Chlupac et al., 2009) In spite of its success as a large diameter vascular graft material, PET vascular grafts have not been widely used for lower extremity bypass especially when the

bypass entails vessels below the knee, because of their poor patency rates. In fact, neither ePTFE nor PET grafts have shown satisfactory performance when implanted as a small diameter (< 6mm) graft. Moreover, they do not develop an endothelialized luminal surface spontaneously, while leads to adhesion of platelets and the development of a luminal fibrin layer that can result in thrombosis, decreased flow and occlusion which are the leading causes of vascular graft failure in small diameter prostheses. In addition to inducing acute or subacute graft failure, they may also be a cause of late failure owing to thrombosis superimposed on stenosis due to other causes of vessel narrowing, such as intimal hyperplasia (X.W. Wang et al, 2007).

Several other nonbiodegradable polymer materials have been involved in research on artificial vascular substitutes. In the early 1990s, 4-mm polypropylene grafts (81%) were shown to be more patent than PET (69%) and PTFE (only 20%) *in vivo* at 16 months, with an inner myofibroblast and macrophage layer and a confluent luminal endothelial cell lining when implanted in a canine model (Greisler et al., 1992). Polyurethane (PU), another alternative synthetic graft material has been shown to be more compliant than ePTFE, and thus its mechanical and flow parameters are better matched to those of the native vasculature (X.W. Wang et al., 2007). Preliminary *in vivo* work suggests that these grafts are resistant to degradation and have compliance similar to that of native arteries (Seifalian, 2002; Kannan, 2005). However, over the long term PU's with various chemical formulations have been found to degrade *in vivo* and be carcinogenic. So the long-term biostability and carcinogenicity are still controversial (Tura, 2003). Generally, PUs, with either fibrillar or

foamy structures, have satisfactory compliance, good hemo-compatibility and biocompatibility, lower thrombogenicity, but tend to lack open porosity which limits their potential for capillary ingrowth (Chlupac et al., 2009). Lately, studies of polyurethanes have focused on modifying it by incorporating a diazeniumdiolate-modified nitric oxide (NO)-producing peptide, which can release NO, a potent platelet-inhibiting compound (Figure 2.7) (Jun, 2005; Fleser, 2004). Results showed endothelial cell (EC) growth could be stimulated in the presence of the NO-releasing polyurethane, while smooth muscle cell (SMC) growth was greatly inhibited, suggesting that this NO-generating polyurethane may be a suitable material for small-diameter vascular grafts. Thermoplastic polyurethane (TPU) elastomers with biodegradable chain extenders have proven to be biocompatible with potential benefits for cell proliferation and have therefore been identified as a suitable material for vascular tissue engineering (Baudis et al., 2012).

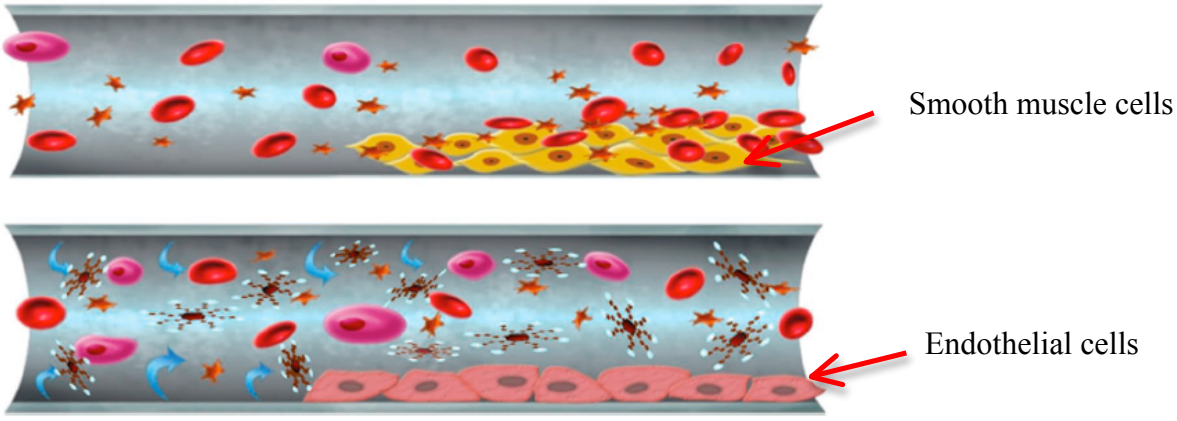

Figure 2. 7 NO-releasing graft inhibits smooth muscle cell (SMC) growth (Copyright © Naghavi, 2013)

Biodegradable polymers have also been studied extensively as scaffolds for vascular tissue engineering because they are able to maintain their strength for relatively long periods of time while allowing the regeneration of new tissue. The most commonly used biodegradable polymer is poly(glycolic acid) (known as PGA). It is an aliphatic polyester that begins to degrade *in vivo* to glycolic acid in around four weeks and is totally metabolized by the human body within six months (Song et al., 2011). PGA scaffolds reinforced with extended PET sleeves have been shown to command relatively high long-term bursting pressures (Niklason et al., 2001). An alternative approach is to produce small-caliber autologous arteries *in vitro* from vascular cells grown on a biodegradable polymer matrix. Niklason et al. showed that PGA scaffolds chemically modified with sodium hydroxide and seeded with bovine SMCs and aortic ECs in a pulsatile perfusion system had an average bursting strength of 2150 ±708 mmHg with 50% dry weight collagen content, which is similar to that for native vessels (Niklason et al., 1999). The thermoplastic polyester, polylactic acid (PLA) is a stronger and stiffer resorbable polymer (Buttafoco et al, 2006), which is often copolymerized with other compounds, such as glycolide and caprolactone in order to render it more flexible or hydrophilic (Cleland, 2001; S.H. Lee, 2003). A bilayer tubular scaffold made up of aligned PLA nanofibers on the inner surface and randomly oriented fibers of poly(caprolactone) (PCL) in the outer layer was designed to mimic the morphology of native vessels and provide larger pores for smooth muscle cells (SMCs) to penetrate (Shalumon et al., 2013). An electrospun small diameter tubular scaffold measuring 4.5 mm in inner diameter was composed of polylactide (PLA) fibers in the outer layer and silk fibroin-gelatin fibers on the inner layer gave appropriate characteristics for a blood vessel for tissue engineering (S. Wang

et al., 2009). Poly(caprolactone) (PCL) because of its flexible nature and high compliance is usually used for preparing materials that match the mechanical properties of blood vessels. Flexible and elastic materials can be obtained by forming block copolymers consisting of PCL and PLA blocks. Vascular tissue engineering scaffolds prepared from these PCLLA block copolymers show significantly more flexibility and less plastic deformation than PLA/PGA scaffolds (S.J. Lee, 2008; Chong, 2007; Xu, 2004). Poly(trimethylene carbonate) (PTMC) is another flexible biodegradable and biocompatible polymer with a low elastic modulus at body temperature (Engelberg & Kohn, 1991). It has therefore been recommended for soft tissue engineering applications (Song et al, 2011). Tubular scaffolds (Buttafoco et al, 2006) were fabricated from a copolymer of trimethylene carbonate (TMC). By culturing both endothelial cells on the luminal surface and smooth muscle cells on the external layer of the constructs, they obtained good cell adhesion and demonstrated that these structures resembled natural blood vessels. In addition, research on the *in vivo* enzymatic degradation of PTMC indicated a surface erosion process with excellent biocompatibility and no toxic side effects after implantation (Z. Zhang et al., 2006).

A number of copolymers materials have also been evaluated as vascular grafts scaffolds. Polyglactin or Vicryl (PG910) is a copolymer of polyglycolic and polylactic acid, which has been thermally treated to increase the level of crystallinity and slow down absorption so as to allow sufficient time for arterial regeneration (Kannan et al., 2005). By combining Vicryl (PG910) with PDS in a 74%: 26% ratio, a biocomponent graft was developed which gave 100% patency at 1 year in a rabbit aorta model (Greisler et al., 1988).

More recently a biodegradable copolymer of poly(ethylene glycol)/poly(lactic acid) (PELA) has been extruded into porous grafts with sufficient hydrophilicity to enhance neoarterial regeneration within the scaffold (Kannan et al., 2005). A study comparing 6 mm PELA coated polyurethane (PU) with commercial ePTFE grafts found that the PELA–PU grafts were patent and pulsatile with a uniform intimal lining of endothelial cells when implanted in a carotid artery model for 3 months (Izhar et al., 2001). Compliance values were closer to those of the native vessel compliance than with the ePTFE graft. A novel biopolymer, namely bacteria derived polyhydroxy butyrate (PHB) is a crystalline, hydrophobic, stiff polymer which is resistant to aneurysmal dilation. By coating it with a PLA sheath, it has shown more resistance to degradation and hence a reduced risk of aneurysm formation (Shum-Tim et al., 1999).

Natural polymers such as silk fibroin (SF) and Type Ⅰ collagen have certain advantages as scaffold materials, namely a reduced risk for tissue toxicity or a severe host inflammatory or host immune response. They can support cell adhesion and proliferation, and be easily metabolized by endogenous enzymes during degradation without significantly adverse effects for the host tissues. For example, an electrospun silk fibroin tubular construct was combined with a Type I collagen gel to produce a biomimetic small-caliber blood vessel with physiological compliance and superior burst pressure and cytocompatibility (Marelli et al., 2012). Similarly, a tubular vessel measuring 1.5 mm in diameter and 10 mm in length was woven from silk fibroin yarns and implanted in the abdominal aorta of rats (Enomoto et al., 2010). The 1-year patency of these fibroin grafts was significantly higher than that of

commercial ePTFE grafts. Endothelial cells and smooth muscle cells migrated into the fibroin graft soon after implantation and they became well organized into distinct adventitial and medial layers.

Chitosan, extracted and purified from shellfish, is another natural material that has been applied to small diameter vascular prostheses. A small 2 mm diameter vascular prosthesis has been fabricated from biodegradable chitosan and found to have good biocompatibility in terms of cell compatibility, inflammatory reaction, and platelet adhesion (Kong et al, 2012).

2.3.3 Modifications to vascular prostheses

To improve the unacceptably poor patency rates of synthetic polymers, alternative strategies have been proposed that include functionalizing the luminal surface of grafts so as to stimulate tissue regeneration. The applications of coatings, chemical and protein modifications, and cell seeding on otherwise inert materials have demonstrated improved endothelialization, reduced thrombogenicity, inhibited a severe inflammatory response and the risk of neointimal hyperplasia (Ravi & Chaikof, 2010).

For example, graphitized carbon is biocompatible and has been used in biomedical applications such as heart valves to reduce thrombogenicity. However when a carbon coated ePTFE graft, was developed, it did not show significantly improved patency compared to a standard ePTFE graft of the same caliber (Kapfer et al., 2006). On the other hand, fibronectin has been bound to the surface of ePTFE grafts and found capable of improving graft healing in a dog carotid model (Nishibe et al., 2001). Recent studies have documented that a cell

adhesion peptide sequence, called P15, found in Type I collagen, can increase endothelial cell adhesion to ePTFE *in vivo* via integrin-specific binding (C. Li et al., 2005). In fact, endothelial cell attachment can be significantly improved on surfaces coupled to other potent adhesion peptides, such as the RGD sequence, compared with simply coating grafts with fibronectin (Krijgsman et al., 2002). Heparin coating of polyester (PET), ePTFE and polyurethane graft materials has been shown to exhibit better patency and significantly reduced thrombosis compared to their uncoated controls (Walpoth, 1998; Bosiers, 2006). The application of a polyethylene glycol (PEG)-hirudin/iloprost coating to a 4 mm diameter ePTFE prosthesis followed by implantation in a pig model led to superior patency and reduced intimal hyperplasia (Heise et al, 2006). Alternatively, a coating of the anti-platelet drug, dipyridamole, improved the patency rate of a 5 mm polyurethane (PU) vascular prosthesis in both a goat and sheep carotid artery study (Aldenhoff et al., 2001). However, in order to increase growth factor production and encourage smooth muscle cell proliferation and the growth of viable endothelial cells, ePTFE grafts were coated with anti-CD34 antibodies and implanted in pigs. While the antibodies were able to capture endothelial progenitor cells and increase endothelial cell coverage, the amount of intimal hyperplasia increased significantly at the distal anastomosis at 4 weeks (Rotmans et al., 2005)

Seeding the lumen of a prosthetic graft with endothelial cells (ECs) is an alternative way to develop surface modification. There are three possible sources of endothelial cells following *in vivo* implantation: i) trans-anastomotic migration from the adjoining native artery, ii) transmural tissue and capillary ingrowth through the prosthetic wall, and iii) a blood-borne

source from circulating progenitor cells (Chlupac et al., 2009). Alternative sources of endothelial cells, either from fat tissue or an omentum biopsy, have been used in an attempt to improve the outcome of a single stage cell seeding method (Alobaid et al., 2005). A two-stage seeding technique has also been studied for coronary artery revascularization using a 4mm diameter ePTFE vascular graft seeded with venous endothelial cells (Laube et al., 2000). This approach involves modifying the prosthesis surface by coating it with peptides having an RGD sequence, matrix proteins such as fibronectin, growth factors such as fibroblast growth factor or endothelial cell growth factor, or applying a combination of these coatings before EC seeding so as to enhance retention of the ECs on exposure to pulsatile blood flow (X.W. Wang et al., 2007). Precoating an ePTFE femoro-popliteal bypass graft with fibrin has recently shown encouraging results *in vivo* with 69 % and 61 % for overall 5-year and 10-year patency rates respectively (Deutsch et al., 2009). More recently, endothelial progenitor cells (EPCs) isolated from peripheral blood and bone marrow have been used for seeding prosthetic vascular grafts. For instance, a 4 mm diameter polyester (PET) graft with preclotted autologous bone marrow blood was implanted in a canine carotid model and exhibited 80% coverage of the luminal surface with endothelial-like cells at 4 weeks (Muneera et al, 2008).

2.4 Poly(lactic acid) (PLA) and Poly(L-lactide-co-ε-caprolactone) (PLCL)

Poly (lactic acid) (PLA) is a thermoplastic aliphatic polyester synthesized by ring-opening polymerization of lactic acid (Table 2.2). Lactic acid monomer is obtained from the fermentation of sugar feed stocks (Lunt, 1998), which are derived from renewable resources,

such as corn starch, tapioca root and sugar cane (Wikipedia, n.d.). PLA has the potential for use in a wide range of applications, such as thermoformed bottles, apparel, furnishings, carpets, fiberfill insulation, packaging and housewares. (Jamshidian et al, 2010). As for medical devices applications, PLA and its derivatives have been approved by the U.S. Food and Drug Administration (FDA) as polymer materials for human clinical use in a number of specific end uses, such as orthopedic pins and bone plates (Thomas et al, 2013).

Poly (L-lactide-co-ε-caprolactone) (PLCL) is a copolymer of lactic acid and ε-caprolactone synthesized through ring-opening polymerization. The inclusion of the caprolactone monomer imparts elastomeric properties to the copolymer, which, with ease of elongation, makes it an attractive candidate for soft tissue applications requiring both elasticity and degradability. At the same time, the more crystalline L-lactic acid sequences account for the copolymers with superior mechanical strength and biocompatibility. With a higher molecular weight, these copolymers are suitable for applications requiring strong, degradable elastomeric biomaterials (Grijpma, 1991; Chung, 2009; Chung 2010). Different blend ratios of the two monomers contribute to different physical states for the PLCL copolymer (Table 2.3). PLCL has been used primarily in the biomedical area. For example, a tubular PLCL scaffold has been found to have a slow rate of degradation when implanted *in vivo* (Jeong et al, 2004).

Table 2. 2 Properties of Poly(lactic acid) (PLA) (Clarinval& Halleux, 2005)

Polymer	Chemical formula	Molecular formula	Density (g/cm^3)	Glass transition point (Tg)	Melting point （Tm)
PLA	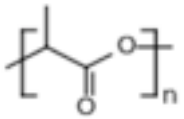	$(C_3H_4O_2)_n$	1.210-1.430	40-70 °C	130-180 °C

Table 2. 3 Molecular weight and physical state of different blend ratios of PLCL copolymers (Keun Kwon et al, 2005)

Polymer	Monomer blend ratio (LL/CL)	Copolymer composition (LL/CL)	Molecular weight (Mn)	Physical state at 25℃
PLL	100/0	100/0	4.5×10^5	Hard solid
PLCL 70/30	70/30	74/26	2.0×10^5	Hard solid
PLCL 50/50	**50/50**	**50/50**	**2.6×10^5**	**Elastomer**
PLCL 30/70	30/70	31/69	1.5×10^5	Gummy solid
PCL	0/100	0/100	1.8×10^5	Hard solid

2.5 Collagen and elastin

Members of the collagen family are the most abundant proteins present in extracellular matrix (ECM). They play vital roles in maintaining the stability of tissues and organs, ensuring the structural integrity of connective tissues as well as serving as a communicating layer when found in the interstitial tissue of parenchymal organs (Gelse et al, 2003).

Furthermore, collagen is one of the main proteins present in the vascular ECM of a native artery with its multi-layer structure (Figure 2.8). The innermost layer of endothelial cells (ECs) is attached to a thin basal lamina. This is followed by a subendothelial layer made of Type IV collagen and elastin. The thick medial layers of smooth muscle cells (SMCs) in a matrix of Types I and III collagen, elastin, and proteoglycans, while the outermost adventitial layer is made of fibroblasts and epithelial cells. Collagens, which are layed down in layers called lamina, supply the arterial wall with sufficient strength. In addition, they serve as a mediator for biological responses, which are primarily produced by smooth muscle cells in the media and by the fibroblasts in the adventitia (Boccafoschi et al, 2005).

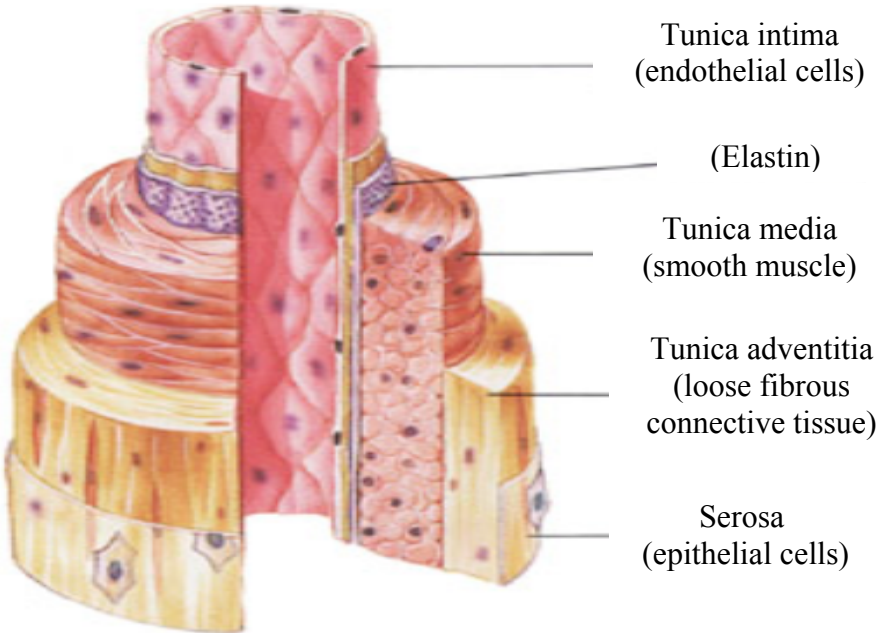

Figure 2. 8 Structure of a native artery (Copyright © Fox, 2013)

As early as the 1970s and before, various forms of collagens were utilized for various medical applications. The types of gels, films, membranes, fibers and sponge already available on the market are summarized in Table 2.4 below.

Table 2. 4 Various forms of collagen and their medical applications (Chvapil, 1997)

Form of Collagen	Applications
Solution	Plasma expander
	Vehicle for drug delivery system
Gel	Vitreous body
	Cosmeticum
Flour	Hemostatic agent
Fiber	Suture material
	Weaving blood vessels
	Valve prosthesis
Film, membrane, tape	Corneal replacement
	Hemodialysis
	Artificial kidneys
	Membrane oxygenators
	Wound dressing
	Hernia repair
	Patches (aneurysm, bladder)
Sponge, felt	Wound dressing
	Bone-cartilage substitute
	Surgical tampons
	Vaginal contraceptive
Tubing	Vessel prostheses
	Reconstructive surgery of hollow organs (esophagus, trachea)

The first attempt to use collagen gels in engineering vascular substitutes was reported by Weinberg and Bell (1986). With the aim of mimicking the multilayer structure of a native

artery, bovine smooth muscle cells were seeded on a collagen gel followed by the injection of endothelial cells on the luminal area and the seeding of fibroblasts on the outer surface. A polyester (PET) mesh was integrated into the structure to provide improved mechanical properties. Since that time, numerous research studies on collagen's biological performance have confirmed its suitability as a structural component of a vascular prosthesis primarily due to its low antigenicity, low cytotoxicity and low inflammatory response (Nicolas & Gagnieu, 1997). In addition, it is suitable as a tissue engineering scaffold material because of its superior cell adhesion and proliferation (Boccafoschi et al., 2005) and its ability to biodegrade (Goissis et al., 1999).

Two dimensional collagen webs and collagen melt component matrices have been fabricated as tissue engineering scaffolds either by electrospinning (Yin, 2013; McClure, 2012; Huang, 2012), gel casting (Kumar, 2013; Bian, 2012) or wet spinning (Siriwardane, 2012; DeRosa, 2011). Pure collagen matrices made by these technologies are not usually able to withstand normal physiologic pressures because they are either hydrogels, or they contain denatured collagen, which is common with electrospun fabrics (Cen, 2008; Y.Z. Zhang, 2007; Caves, 2010). To improve their mechanical performance so as to function as a vascular graft, the collagen-based material needs either to be reinforced by fabricating a multilayer polymer/collagen structure (McClure, 2012; Huang, 2012) or to be stabilized using a cross-linking agent (Ming-Che, 1994; H. Li, 2012).

In addition to collagen, elastin is also an essential protein component in the ECM of arteries that supports cell growth and proliferation. A continuous layer of elastin in the artery wall

provides a suitable surface for the attachment of a monolayer of endothelial cells (ECs) and the infiltration of smooth muscle cells (SMCs) that represent the tunica intima and tunica media respectively (Figure 2.8). Due to its extensively crosslinked structure, elastin contributes to a stable and durable material that provides native arteries with the ability to expand and recover. In fact, elastin is the essential component of soft tissue responsible for two vital characteristics: compliance and favorable cellular interactions, which are currently the two main issues that need to be addressed in the development of small diameter vascular grafts (Almine et al, 2010). In addition to maintaining circumferential stability, elastin as a signaling molecule plays a crucial role in controlling cell activity, including cell migration, proliferation, differentiation and gene expression. Cell interactions with elastin are achieved by cell-surface receptors, such as the elastin/laminin receptor, glycosaminoglycans (GAGs) and several amino acid sequences within the elastin protein molecule.

As an attractive biomedical material, elastin protein can serve as a coating material for synthetic polymer-based devices or can be fabricated into fibrous scaffolds via electrospinning or gel casting. Coating several different synthetic vascular materials with elastin peptides has been found to significantly decrease platelet aggregation by 50%, reduce surface induced platelet activation and reduce platelet adhesion (Almine et al, 2010). Similarly, polyurethane catheters and ePTFE vascular prostheses coated with an elastin peptide or an elastin-mimetic protein have been shown to reduce platelet deposition and significantly increase patency in an *in vivo* study (Jordan & Chaikof, 2007). Recently, elastin has been co-electrospun with biodegradable synthetic and natural polymers to produce tissue

engineering vascular scaffolds. Electrospun mixtures of soluble bovine elastin, Type I collagen and various synthetic polymers, such as PLGA, poly(L-lactide) (PLLA), PCL and PLCL have been found to support positive bovine endothelial cells proliferation (Almine et al, 2010). In summary, it is concluded that because of the positive endothelial cell interactions and the reduced thrombogenicity, elastin-based coatings and elastin containing electrospun grafts provide promising biomaterials for small diameter vascular applications.

CHAPTER 3

MATERIALS AND METHODS

3.1 Fabrication of Small Diameter Vascular Prostheses

As described in Chapter 1 this study involved the fabrication and evaluation of a series of different prototype small diameter tubular scaffolds. Five different samples and controls were made in total, and the different fabrication and testing techniques that were used are described in this chapter.

3.1.1 Tubular Weft Knitting of PLA Multifilament Yarn

A poly(L-lactic acid) (PLA) fully oriented yarn (FOY) with a round cross-section, 170 denier and 18 filaments (170/18) was melt spun at Fiber Innovation Technology Inc. (Johnson City, TN, USA) and drawn at the College of Textiles, North Carolina State University. The PLA polymer, containing 98% L- and 2% D-isomers, was supplied by NatureWorks LLC (Minnetonka, MN, USA). A laboratory single feed circular weft knitting machine Model ST3AH/ZH manufactured by Lamb Knitting Inc. (Chicopee, MA, USA) with 16 needles was used to fabricate the knitted single jersey tubular structures with a working speed of 1300-1500 rpm. Two separate multifilament yarns were folded together and used as the feed yarn for the knitting process. The tension was adjusted to achieve a constant relatively tight structure.

In order to stabilize the structures, each knitted tube was mounted onto a stainless steel mandrel with a diameter of 3.2 mm and heat-set in an oven at 80℃ for 5 minutes. After heat setting, the knitted tubes were stored in a refrigerator at 4℃.

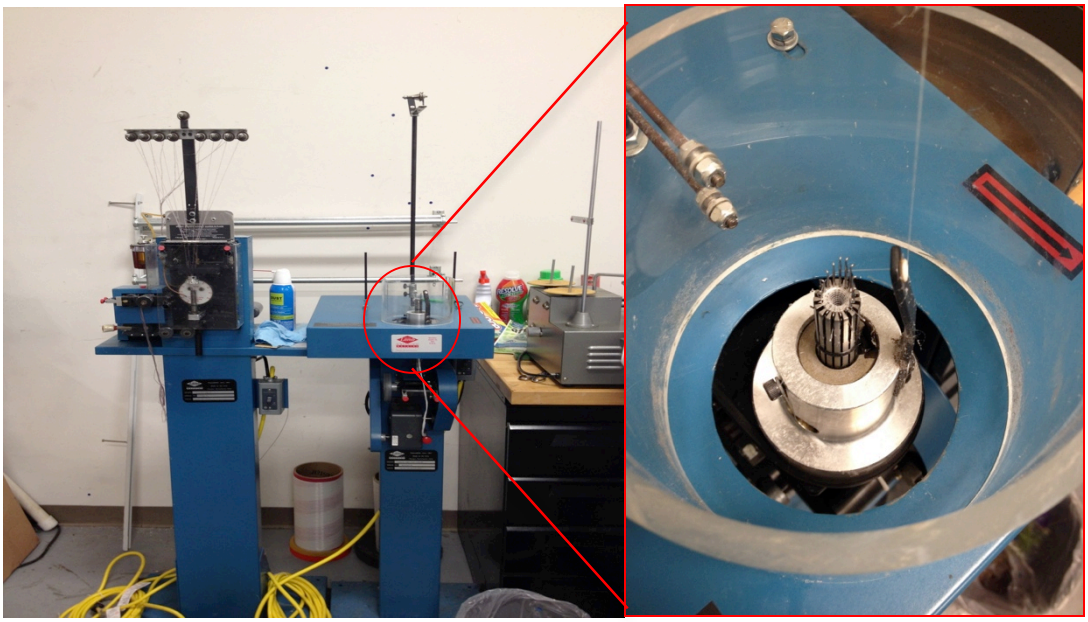

Figure 3. 1 Lamb weft knitting machine and its working mechanism.

3.1.2 PLCL Copolymer Electrospinning

To obtain a composite bilayer structure with one layer of nanofibers for endothelial cell proliferation, nonwoven electrospinning was selected to fabricate the thin nanofiber layer by direct deposition of a 50:50 poly(L-lactide-co-ε-caprolactone) polymer (PLCL, Mw=310960) onto the PLA knitted tubes mounted on a mandrel. The PLCL polymer was obtained as a

polymerized solid bulk copolymer from the Biomaterials Division Research Center at the Korea Institute of Science & Technology (Seoul. South Korea). It had been synthesized by L-lactide, e-caprolactone and 1,6-hexanediol with stannous octoate as the catalyst as described by Soo Hyun Kim et al (2008). This copolymer was dissolved in acetone (Fisher Scientific) because acetone is less toxic than other commonly used solvents such as methylene chloride and 1,1,1,3,3,3-hexafluoro-2-propanol (HFIP). The mixed polymer solution was magnetically stirred at 300 rpm for 3-4 hours to obtain a homogeneous solution. The prepared solution was stored at room temperature and used within three days. The complete set-up for electrospinning in the laboratory is shown in Figure 3.2. A 3 ml plastic syringe with a 20 Ga stainless steel blunt-ended needle (inner diameter, 0.6 mm) was fixed horizontally onto a pumping system (New Era Pump Systems, Inc., Farmingdale, NY), and raised to the same height as the collecting mandrel (now covered with a PLA knitted tube). A DC high voltage supply (Gamma High Voltage Research) was used to generate a high voltage between the needle and the collecting mandrel. In order to ensure that the electrospun layer contained continuous and uniform nanofibers, several parameters crucial to the electrospinning process were modified prior to selecting the optimum conditions. They included the polymer solution concentration, applied voltage, flow rate and the distance between the needle tip and the collecting mandrel. The parameters used in the preliminary trials are indicated in Table 3.1. Every tube was electrospun for 25-30 minutes to obtain a planned thickness. The trial samples were viewed by SEM imaging, and the processing parameters were then calculated.

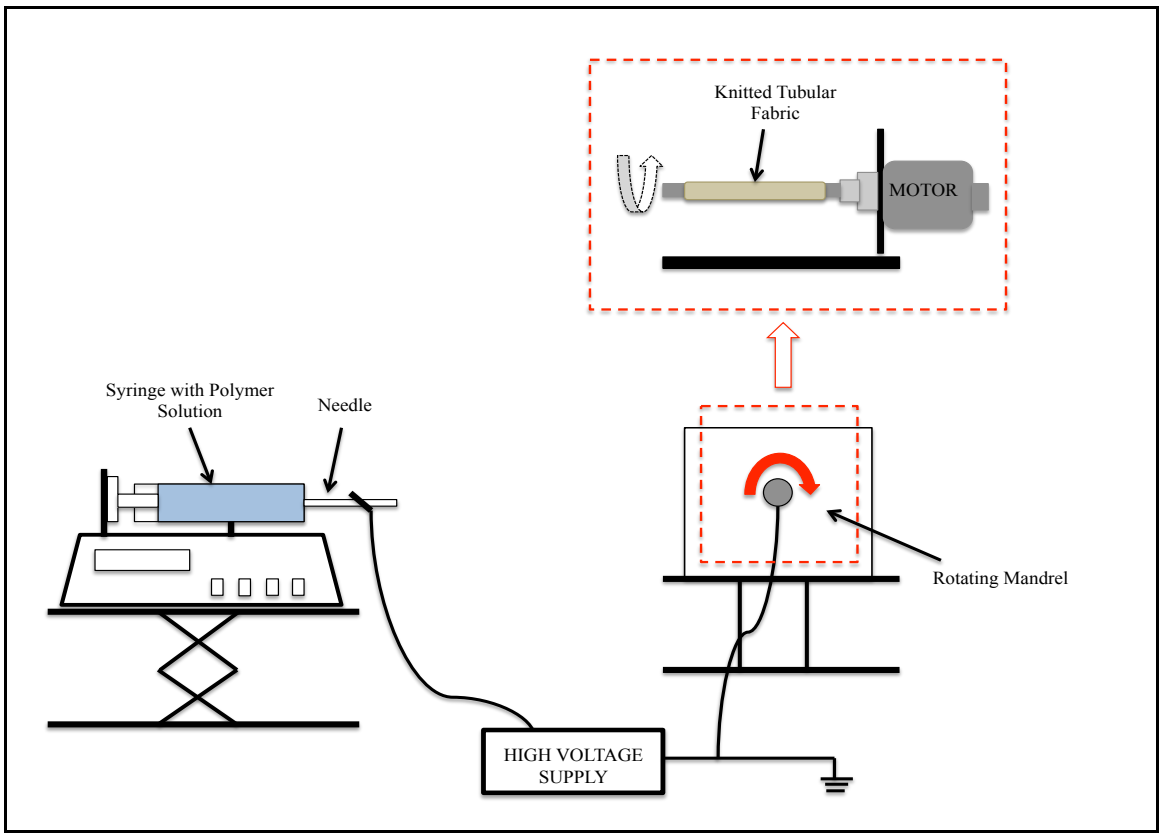

Figure 3. 2 Schematic drawing of electrospinning set-up

Table 3. 1 Variables during preliminary electrospinning trials

Variable Parameters	
Polymer solution concentration (w/v)	8%, 12%, 15%
Applied voltage (kV)	5, 10, 15
Flow rate (ml/h)	2
Distance between needle and mandrel (cm)	3, 6, 10
Mandrel rotation speed (rpm)	200

3.1.3 Inversion Procedure

To obtain the desired structure with the electrospun layer inside of knitted layer, it was necessary to invert the bilayer structure or turn the prototype samples inside out. This was accomplished by using a sewing needle and thread. One end of the bilayer tube was sewn together with a needle and thread, and then the needle was passed through the center of the hollow tube to the other end. By pulling on the needle, the electrospun layer was slowly and progressively turned inside of knitted layer. A mandrel was sometimes required to maintain the shape of the tube since the elastomeric layer was prone to stick together during the turning process.

3.1.4 Collagen/Elastin Impregnation

In order to determine whether thrombus formation could be minimized and increased cell attachment and proliferation could be improved certain of the prototype bilayer structures were impregnated with a mixture of Type 1 collagen and elastin. This was not simply the application of a surface coating, but the composite tubes were immersed in the protein solution so that it filled the gaps between the two layers as well as between the fibers. A 1:1 ratio by weight of the collagen / elastin mixture was selected because the percentage content of these proteins is approximately 1:1 in native arteries (Daamen et al, 2003). A collagen / elastin solution concentration of 0.5% was prepared by first dissolving 0.3 g bovine neck ligament elastin (ES61) from Elastin Products Company Inc. (MI, USA) in 90 ml 0.1M acetic acid for 3 hours. This was followed by adding 30 ml calf skin Type 1 collagen (C806, Elastin Products Company, Inc., MI, USA) and dissolving by stirring for another 3 hours.

The 0.1M acetic acid was prepared by diluting 2.86mL acetic acid (Fisher) in 497.14 ml deionized water. Prior to impregnation, 1.9 ml glycerine (Fisher) was added to the above solution (2%) in order to impart improved flexibility and pliability to the composite tube (Hoffman & Schankereli, 1992).

A 50 cc syringe and an 18Ga needle were used to apply the mixed solution above into the composite structure. After filling the syringe with the 0.5% collagen/elastin solution, the needle was placed into one end of the tubular graft, and the solution was injected into the lumen of the tube, followed by a gentle massage to ensure it penetrated the entire inner surface area. The graft was then permitted to dry for about 1 hour at room temperature. The impregnating and drying steps were repeated for a total of three times. All the impregnated grafts were allowed to air-dry overnight prior to further processing.

3.1.5 Genipin Crosslinking

In this study a natural cross-linking molecule was selected to increase the mechanical strength after protein impregnations by promoting collagen-elastin bonding. Genipin (Figure 3.3) is a chemical compound called geniposide isolated from the fruit of the *Gardenia jasminoides* plant. It can spontaneously react with the primary amine groups on amino acids and proteins to form a dark blue pigment (Sung et al, 2000). A possible mechanism for the reaction of the amino group with collagen is illustrated in Figure 3.4. Genipin was selected due to its significantly lower toxicity compared with other chemical cross-linking agents such as glutaraldehyde, and its superior biocompatibility compared to glutaraldehyde and epoxy compounds when utilized for cross-linking of biomaterials (Bi et al, 2011). It has been

demonstrated that genipin is approximately 10,000 times less cytotoxic and around 5,000 times more effective in promoting cell growth than glutaraldehyde (Mekhail et al, 2011).

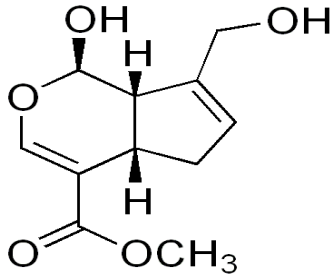

Figure 3. 3 Chemical structure of genipin

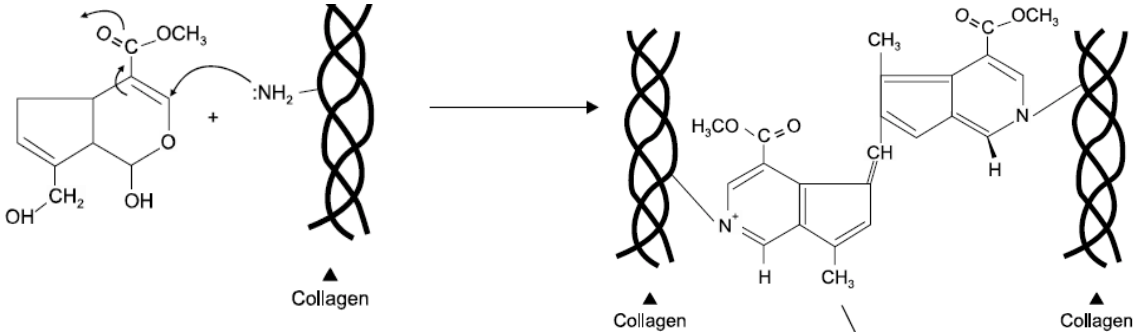

Figure 3. 4 Schematic illustration of proposed mechanism of amine group cross-linking with genipin (Chang, 2001; Yoo, 2011)

A 1% genipin crosslinking solution was prepared by dissolving genipin powder (Wako Pure Chemical Industries, Ltd., Japan) in 1X (0.01M) phosphate buffered saline (PBS, pH 7.4). The mixture was magnetically stirred at a speed of 60 rpm at 30℃ for 3 hours. A 50 cc

syringe filled with genipin solution was injected inside the lumen of those prototype tubes which had been impregnated with the collagen / elastin mixture. They were then gently massaged. A second repeat application of the genipin solution was applied using the same procedure after three hours. All the cross-linked tubes were then placed in a desiccator and vacuum dried for 72 hours, followed by sealing and storing them in glass bottles.

3.1.6 Morphology by Scanning Electron Microscopy (SEM)

The surface morphology and cross-sectional views of the samples were observed using a Phenom G1 scanning electron microscope (Phenom, Netherlands) after sputter coating with gold-palladium in a SC7620 mini sputter coater (Quorum Technologies Inc, Ontario, Canada). Both the outside surface and cross-sectional views of the tubular grafts were imaged.

3.1.7 Measurement of Wall Thickness

The wall thickness of both the bilayer tubes and the single layer knitted tubes were measured by imaging under a Nikon Eclipse 50i POL (Nikon Inc., NY, USA), optical microscope, which was calibrated with a stage micrometer at 100X magnification prior to making the observations. Each sample was cut into a short ring around 1mm in length and set vertically on a glass slide. At least three images were captured from each sample. The Java-based image processing program, ImageJ, was used to analyze the images.

3.2 Mechanical Properties of Tubular Samples

The ISO Standard 7198 "Cardiovascular Implants — Tubular Vascular Prostheses", describes the test methods to be used for measuring the circumferential tensile strength, the bursting strength, the suture retention strength and the compliance of vascular prostheses regardless of their diameter. All five prototype samples were investigated according to this international standard.

3.2.1 Circumferential Tensile Strength

The circumferential tensile test for tubular samples was performed on an Instron Model 5584 mechanical tester (MA, USA). A 2 kN load cell was used with a crosshead speed of 200 mm/min, according to ISO 7198. The tubular grafts were cut into 7 mm lengths. At least five specimens were tested for each sample and all tests were run to failure. A special frame was designed and utilized to mount and hold the tubular structures in the testing equipment. The frame is shown in Figure 3.4. It is comprised of two steel plates (2mm thick) with a pair of arms that are mounted in the upper and lower jaw respectively. Each pair of arms holds a steel alloy pin measuring around 1.2 mm (3/64 inch) in diameter. Prior to each test these pins are inserted parallel to one another inside the hollow lumen of the tubular specimen. This ensures that as the jaws move apart the tubular specimen is loaded in a vertical direction uniformly across its length. To allow the two assemblies to come as close as possible to each other before the test started, the inside distance between the two arms on one plate was set greater than the outside distance of that on the another plate (Figure 3.5). The whole set-up for circumferential tensile test is illustrated in Figure 3.6.

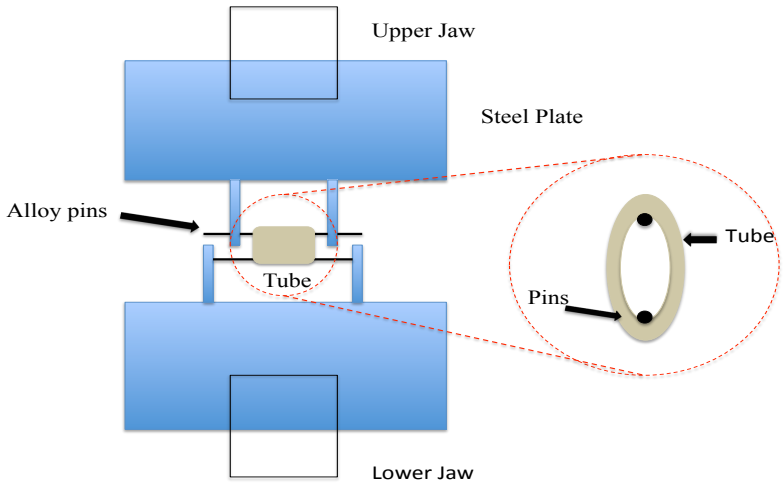

Figure 3. 5 Frame designed to mount tubular structure for testing

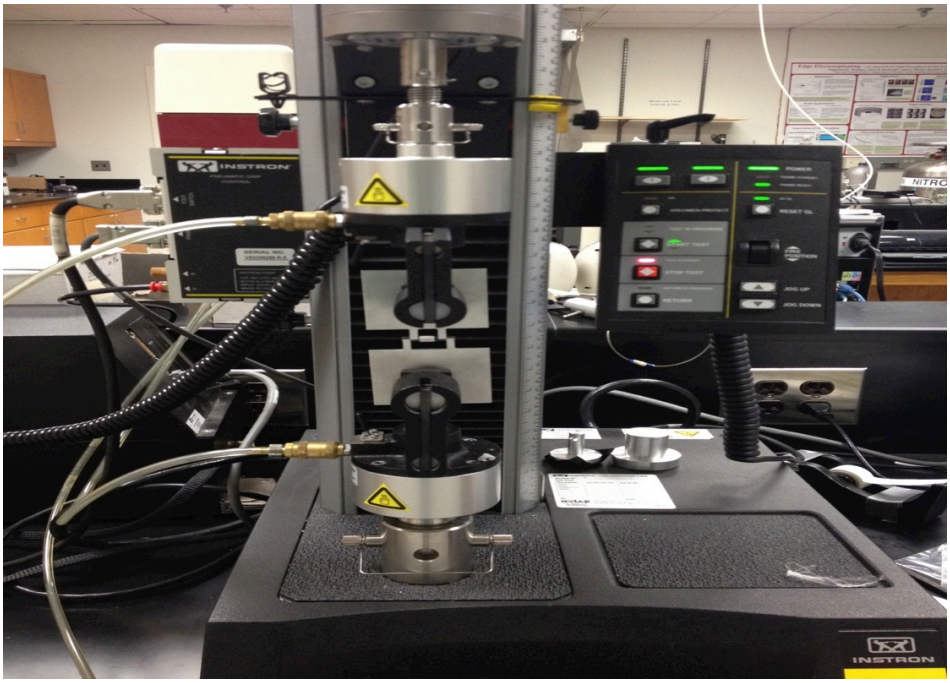

Figure 3. 6 Set-up of circumferential tensile test

The gauge length was set by assuming the width of the tubular structure was half the circumference of the tube when it was flat, as calculated by the following equation:

Gauge length (mm) = π × inner diameter of the tube / 2

The values for the peak load (N) at failure were converted into peak stress (MPa) using the following equation:

$$\text{Peak Stress (MPa)} = \text{Force/Area}(\text{N/mm}^2) = \frac{\text{load (N)}}{\text{thickness (mm)} \times \text{length (mm)} \times 2}$$

The values of extension at maximum load (mm) were converted into strain (%) using the following equation:

Strain (%) = [Extension (mm)/gauge length (mm)] × 100%

3.2.2 Bursting Strength

The bursting strength of the bilayer and single layer prototype samples was determined by following the method described in the ISO Standard 7198 "Cardiovascular Implants - Tubular Vascular Prostheses". It was adapted from the ASTM D3787 Standard Test Method for Bursting Strength of Textiles - Constant Rate of Traverse (CRT) Ball Burst Test, which needs specimens to be at least 12.5 cm in diameter. The ISO Standard Method can operate with much smaller sized specimens. In fact the tubular samples were opened longitudinally and cut into 10mm lengths, which gave around 10mm x 10mm square areas of fabric. The specimens were clamped horizontally in the sample frame in a compression cage, and a

vertical pin with a hemispherical tip measuring 3mm diameter was used to create the bursting force as the crosshead was displaced. The compression cage was easily mounted on the Instron Model 5584 mechanical tester (MA, USA), as seen in Figure 3.7. A 2 kN load cell was used and the crosshead speed was set at 305 mm/min, as indicated the standard test method. The failure point of the test was set differently for the samples with and without the electrospun layer. The former samples were run until the displacement was 10 mm, while the latter samples were stressed until they reached 50% of the peak load. At least five specimens from each sample group were tested and the peak load (or force) was recorded as the bursting strength. Then the bursting strengths of the five samples were converted into bursting stress (MPa) using the following equation where R is the half diameter of the pin.

$$\text{Stress at Burst(MPa)} = \text{Bursting Force (N)/Area(mm}^2\text{)} = \frac{\text{load (N)}}{2\pi R^2}$$

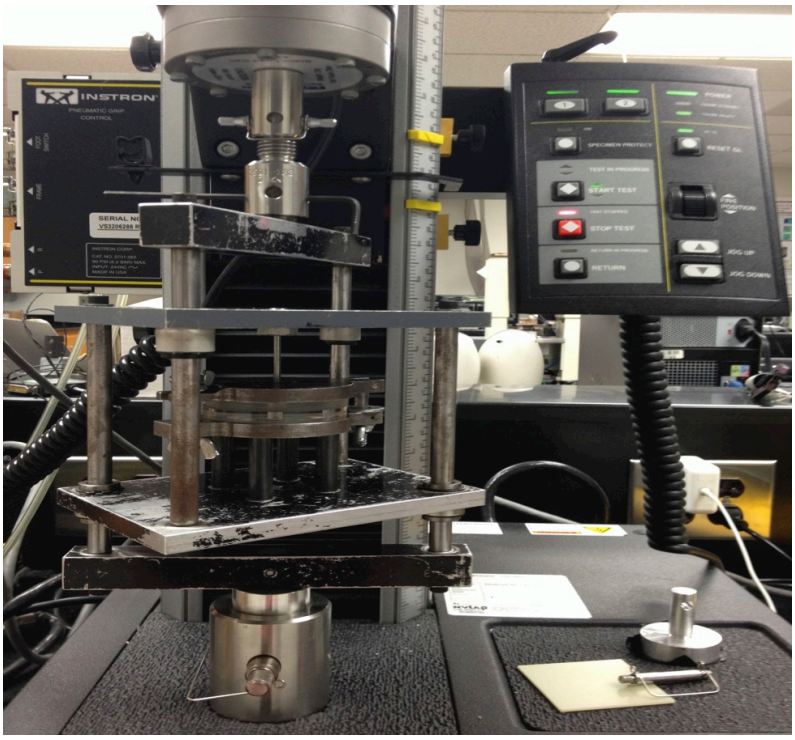

Figure 3. 7 The compression cage and sample frame ready for the ball bursting test.

3.2.3 Suture Retention Strength

Suture retention strength testing was conducted according to the ISO Standard 7198 "Cardiovascular Implants - Tubular Vascular Prostheses" with the objective of comparing the performance of the bilayer and single layer structures. It was important to observe whether the suture would slide out of the specimen or cause the weft knitted structure to ravel during the test. A Test Resources Model 311Q (Shakopee, MN, USA) mechanical tester with a 25 lb. load cell was used to determine the suture retention force for each of the graft samples at a crosshead speed of 300 mm/min. Each specimen was cut into a 20 mm length and a 2-0 braided nylon suture was sutured through the thickness of the specimen at a distance of 2 mm

from the cut edge. Then the suture and the non-sutured end of the specimen were clamped to the top and bottom jaws to the tester as shown in Figure 3.8. The maximum load was recorded as the suture retention strength for at least 5 specimens from each sample group.

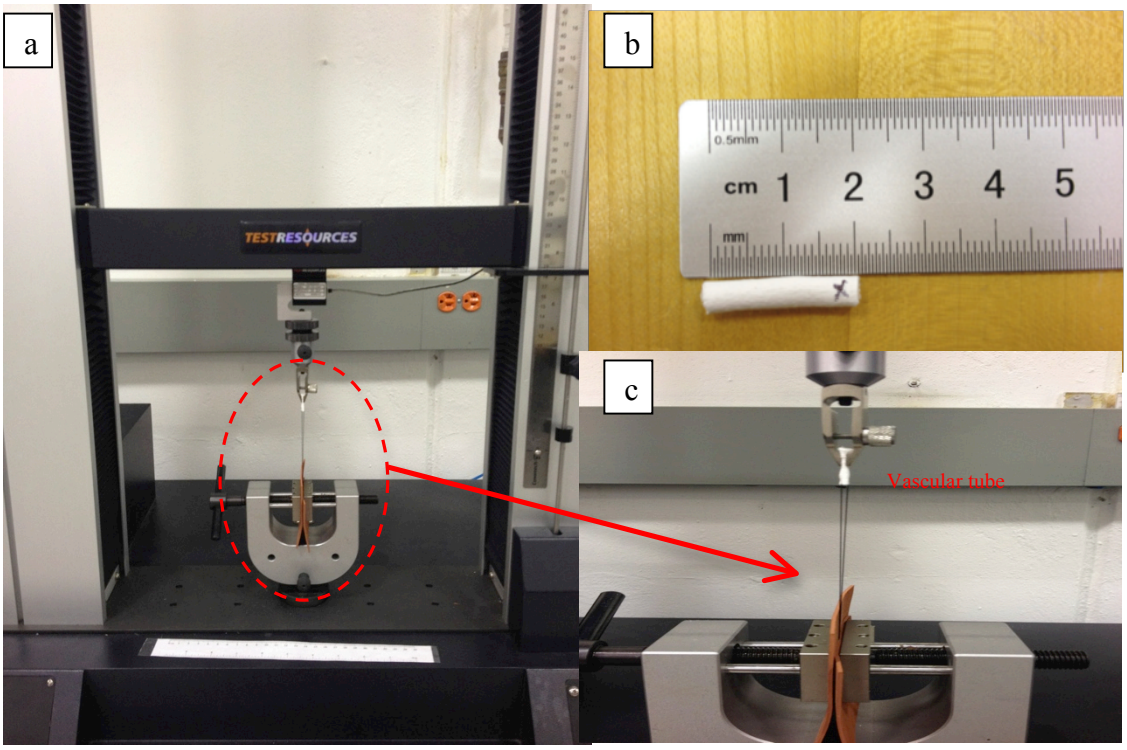

Figure 3. 8 Suture retention strength testing. (a) Test Resources mechanical tester. (b) Tubular specimens cut into 20 mm lengths. (c) Tubular specimen and 2-0 suture clamped to the top and bottom jaws respectively.

3.2.4 Compliance

Compliance is a crucial property for small diameter vascular prostheses. In this study, compliance was performed according to the ISO 7198 Standard Test Method on an

Endurance dynamic mechanical simulation system Model 100451 (Bose Corporation, MN, USA) in the Collage of Textiles at Donghua University, Shanghai, China. Each test specimen was cut into a 5 cm length and mounted on the test machine with a 3 mm diameter polyurethane tube inserted inside and clamped at both ends as shown in Figure 3.9. On applying a 100 mL/min rate of water flow and a 1 Hz pulsatile frequency, the diameter of each specimen was measured over three pressure ranges, namely 50-90 mmHg, 80-120 mmHg and 110-150 mmHg, corresponding to hypotensive, normotensive and hypertensive blood pressures. The changes in external diameter in response to these pressures were recorded by a laser micrometer. At least three specimens from each sample group were tested. The internal radius and final compliance were calculated from the following two formulae (ISO, 1998):

$$R_p = (D_p/2) - t \qquad (1)$$

$$\%Compliance = \frac{(R_{p2} - R_{p1})/R_{p1}}{P_2 - P_1} \times 10^4 \qquad (2)$$

where:

R_p is the pressurized internal radius;

D_p is the measured pressurized external diameter;

t is the graft wall thickness;

P_1 is the lower pressure (diastolic) value, in mmHg;

P_2 is the higher pressure (systolic) value, in mmHg.

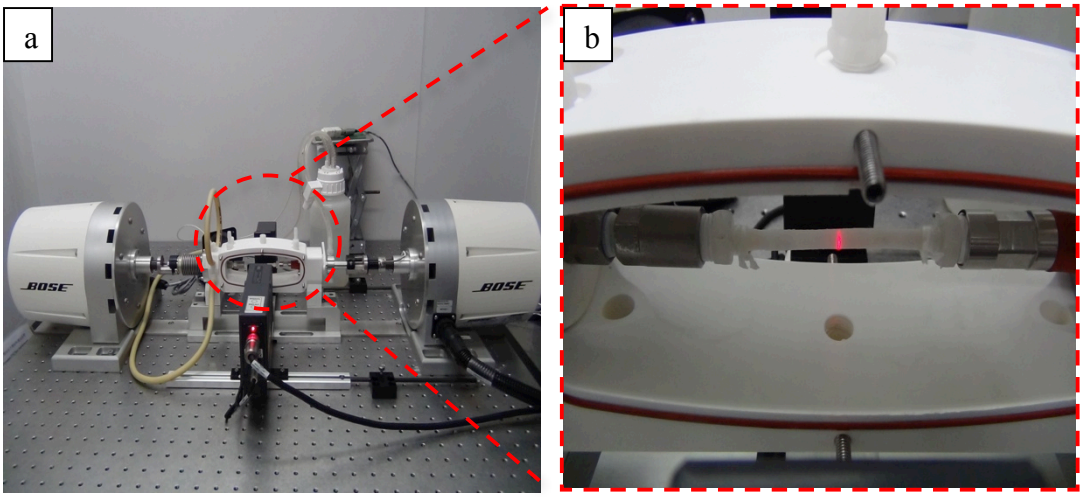

Figure 3. 9 Compliance testing setup. (a) Bose Endurance dynamic mechanical simulation system; (b) The diameter of the mounted and pressurized test specimen being measured with a laser micrometer.

3.3 Thrombogenicity

The level of thrombogenicity was measured to study the tendency of the different small diameter graft samples to produce thrombus or form blood clots when in direct contact with blood. In particular the test was conducted for the purpose of comparing the rate and overall strength of thrombus formation for the collagen / elastin impregnated samples with the untreated grafts by thromboelastography (TEG). The experiment was performed on a TEG 5000 Hemostasis Analyzer System (Haemonetics Corporation, MA, USA) in the College of

Veterinary Medicine at North Carolina State University. Because of the scope of this experiment, the bilayer structures with and without collagen / elastin impregnation were compared with a commercial 3 mm diameter ePTFE vascular prosthesis, which served as the positive control. Each specimen, approximately 6 mm in length, was mounted tightly onto the pin in each TEG testing apparatus and evaluated under three different conditions; namely sterile water, canine citrated plasma and canine citrated whole blood (Figure 3.10). When testing with water a volume of either 330 μL or 360 μL of sterile water was added to the cups that contained a test specimen or no test specimen respectively. For the plasma test, 310 μL of canine citrated plasma and 20 μL of calcium chloride ($CaCl_2$) were added to the cups with samples, while 340 μL of canine citrated plasma and 20 μL of $CaCl_2$ were added to the plain cup with no sample. For the blood test, whole blood was used within 30 minutes of collection from three different dog donors and used to test three specimens of each sample. The volumes of canine citrated whole blood and $CaCl_2$ were the same as for the plasma test conditions described above. The 4 TEG values, reaction time (R), clot formation time (K), maximal amplitude (MA) and angle (α), were entered into the following formula to derive the coagulation index (CI) (Donahue & Otto, 2005):

$$CI = 0.1227(R) + 0.0092(K) + 0.1655(MA) - 0.0241(\alpha) - 5.0220$$

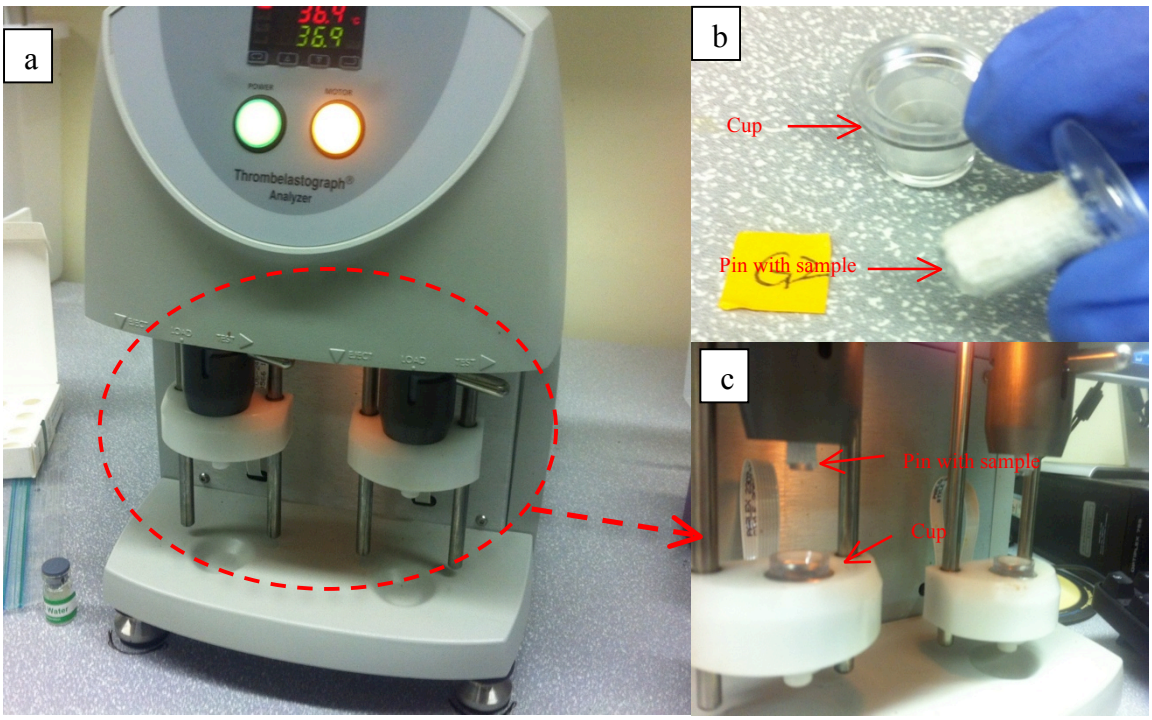

Figure 3. 10 Thromboelastography tester. (a) Test machine with 2 cups running for a test. (b) Impregnated bilayer sample fitted onto the pin and ready to start the test. (c) Cups and pins were placed on the test machine.

3.4 Biological Performances of Vascular Grafts

3.4.1 Sample Preparation

Four groups of vascular grafts were involved in biological performance evaluation, namely, knitted (outside)/electrospun (inside)/impregnated grafts, knitted (inside)/electrospun (outside)/impregnated grafts, knitted/ impregnated grafts and knitted (inside)/electrospun (outside) grafts. All the grafts were cut into 10 mm lengths with one pointed end to indicate the location of cell seeding as shown in Figure 3.11. They were then placed one graft per

well into 24 well cell culture plates. After sterilizing for 12 hours in ethylene oxide followed by aeration for 48 hours, the tubular specimens were immersed in 70% ethanol for 10 minutes followed by three washes (30 minutes each) in 1X PBS (0.01M). After all the washes, the final waste liquid was tested for pH value to ensure it lay between 7.0 and 7.4 using a digital pH meter Model 611(Orion Research Inc., FL, USA). Finally all the washed specimens were immersed in cell culture medium overnight in an incubator at 37℃ and 5% CO_2. The cell culture medium consisted of 89% high glucose DMEM (Dulbecco's modified eagle medium), 10% US origin fetal bovine serum (FBS) and 1% penicillin- streptomycin (P/S), all available from Life Technologies, Thermo Fisher Scientific Inc. (NY, USA).

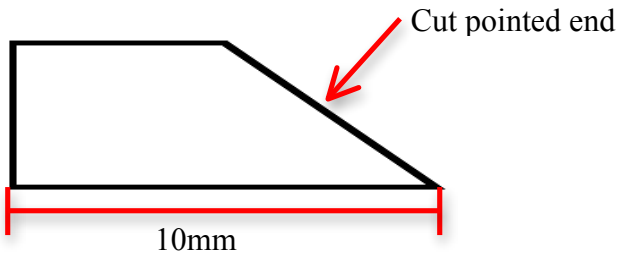

Figure 3. 11 Pointed end was cut to identify the location for cell seeding.

3.4.2 Seeding Bovine Aortic Endothelial Cells on Tubular Samples

Bovine aortic endothelial cells (BAOECs) passage 2, available from Cell Applications Inc. (San Diego, CA, USA), were cultured to obtain to expand the cells and obtain a sufficient quantity for cell seeding. Passage 5 cells were used for the tubular graft seeding experiments.

A volume of 20 μ L of 5 x 10^5 cells/ml was seeded with medium at the pointed end of each tube and then incubated at 37℃ for 30 minutes to allow for cells adhesion. Positive controls were also seeded into empty wells. Then 1 ml of the cell culture medium (89% DMEM+10%FBS+1%P/S) was added to each well. The cells were then cultured at 37℃ with 5% CO_2 for 7 days and the medium was changed every other day.

3.4.3 Cytotoxicity by MTT Assay

An MTT assay was used to evaluate the extent of cell proliferation on all four tubular samples at Day 1, 3 and 7 as described below. To accomplish this it was first necessary to prepare a 5 mg/ml MTT solution by dissolving Thiazolyl Blue Tetrazolium Bromide (MTT) (Sigma-Aldrich, MO, USA) powder in RPMI-1640 medium, to shake so as to completely dissolve the MTT salt and then filter any remaining solids. An MTT assay culture medium was then prepared with 89% RPMI-1640 (Sigma-Aldrich), 10% FBS and 1% P/S, but with no phenol red indicator. Prior to the assay, cell culture medium was aspirated from each well and the cultured tubular samples were washed in culture medium. Then, 500μl fresh assay culture medium and 50μl 5 mg/ml MTT stock solution were added to each well. Negative controls and positive controls consisting of 500μl growth medium and 50 μl MTT, 500μl growth medium and 50 μl MTT with cultured cells were included. The plates were then incubated in the dark at 37^{o}C for at least 4 hours until the purple formazan color had formed in the mitochondria of the living cells. After incubation, 425 μl of medium was removed from each well and replaced by 250μl dimethyl sulfoxide (DMSO) (Sigma-Aldrich). To dissolve the solid MTT formazan, all the plates were shaken and then incubated at 37℃ for

10 minutes. After the converted dye had dissolved, 100µl of the solution was transferred from each well to a new 96-well plate. The solution in each 24-well plate was transferred into 2-3 wells in 96-well plate. Deionized water was added to the 96-well plate as a blank control. The absorbance was then read at 540nm through a microplate reader (Genios, Tecan US Inc. Durham, NC, USA). Five specimens were tested for each sample group.

3.4.4 Cell Proliferation and Migration by Immunofluorescence Assay

In order to visualize the distribution of the endothelial cells (BAOECs) on the inner lumen of the tubular grafts, the extent of cell proliferation and migration on the different structures was examined by an immunofluorescence technique and observed through laser scanning confocal microscopy (LSCM) after 7 days of culture. The specimens with cells were rinsed 3 times in 1X PBS (0.01M) containing Ca^{2+} (which would allow the cells to adhere to the scaffolds) and fixed at room temperature in 3.0% glutaraldehyde and 10X (0.1M) PBS at room temperature for 10 minutes. The specimens were then rinsed 3 times with 1X PBS (0.01M) containing Ca^{2+}, 5 minutes each time. After fixation, the cells on the specimens were permeabilized by immersing in 0.3% Triton-X 100 in PBS for 5min, followed by three washes with 1X PBS (0.01M) plus Ca^{2+}. To identify the cell nuclei, the specimens were stained by 4′, 6-diamidino-2-phenylindole(DAPI), 1:1000 diluted by 1X PBS (0.01M) with Ca^{2+}. After DAPI was added, the samples were incubated in the dark for 15 minutes and washed three times (two minutes per time) with 1X PBS (0.01M). The visible cell seeding surfaces of the specimens were viewed by a Zeiss Model LSM 710 laser scanning confocal microscope (Carl Zeiss MicroImaging, NY, USA) and 3D images were obtained with Zen

software (Carl Zeiss MicroImaging, NY, USA) after capturing a series of thinly sliced images on the microscope. Excitation of a 405 nm diode (λex) and emission absorbance at 410-523 nm (λem) was used (DAPI: λex=340nm, λem=488nm). Different depths of observation were scanned so as to visualize the different structures of the bilayer and single layer grafts based on cell density.

3.4.5 Cell Morphology and Attachment by SEM

Scanning electronic microscopy (SEM) was utilized for characterization of cell attachment on the electrospun and weft knitted surfaces. The cell-cultured tubular grafts were harvested at Day 7 and prepared for SEM imaging. First, the specimens were moved to new glass vials and washed by 0.1M PBS (10X). Then, they were fixed in 3.0% glutaraldehyde solution with 0.1M PBS (10X) at pH 7.4 and 4^{o}C for 48 hours. After fixation, the specimens were washed 3 times in 0.1M PBS, at pH 7.4 for 30 minutes each, followed by dehydration through a graded series of aqueous ethanol solutions, namely 30%, 50% and finally 70% ethanol for 30 minutes each at 4^{o}C. Prior to SEM imaging, the specimens were dehydrated further with 95% ethanol at 4^{o}C and 3 treatments with 100% ethanol 30 minutes each. The first time was at 4^{o}C while the second and third times were at room temperature. Then, all the specimens were dried at the critical point in a Samdri-795 critical point drier, Tousimis Research Corporation (Rockville, MD, USA) for 15 minutes. The dried samples were cut into flat specimens and mounted on aluminum stubs with carbon tape. They were then sputter coated five times with gold/palladium in a Hummer® 6.2 sputtering system (Anatech LTD, California). The five times included the 4 sides using the retroactive support plus the top surface of each specimen.

The thickness of the coating was 30Å each time. The sputter-coated specimens were stored in a vacuum desiccator until they were examined in a JEOL JSM-5900LV scanning electron microscope (JEOL USA, Inc. Peabody, MA, USA) at a 15kV accelerating voltage. The images were taken at the seeded end of the tubular grafts, as well as on the electrospun surfaces and weft knitted structure at magnifications of 500x and 1000x.

3.5 Statistics

All values were calculated and reported in terms of the mean and standard deviation. All statistical comparisons were performed initially by using the ANOVA statistic. Then, if differences were identified, comparisons between the test groups and the control were analyzed using a standard t-test. A p-value of ≤ 0.05 was assumed to be statistically significant.

CHAPTER 4

RESULTS AND DSICUSSIONS

4.1 Fabrication and Characterization of the Small Diameter Vascular Grafts

The initial weft knitted tubular structure was successfully knitted and heat-set using two ends of poly (L-lactic acid) 170 denier multifilament FOY yarns as described in Section 3.1.1.

4.1.1 Effect of Solution Concentration on Electrospinning

To select the best solution concentration for producing the electrospun layer, the appearance and uniformity of the web morphologies spun from three different PLCL polymer concentrations, 8%, 12% and 15%(w/v), were compared using SEM images. The flow rate for all three concentrations was kept constant at 2 ml/h, while the collection distance from the needle tip to the rotating mandrel was controlled at 6 cm, and the applied voltage held at 10kV. As the concentration of the polymer solution increased, more uniform fibers were formed, as presented in Figure 4.1.

At 8% (w/v) polymer concentration, a few fibers were produced together with a large number of beads (Figure 4.1 (a)), which suggested that a certain amount of acetone solvent did not evaporate by the time the polymer arrived on the collector surface. When the polymer concentration was increased to 12% (w/v), there was less bead formation with fewer fibers fusing together (Figure 4.1(b)). It was also observed that the fibers had greater uniformity and a more discrete appearance when spun from solutions with a higher polymer concentration. In fact when the polymer concentration reached 15% (w/v), the fibers were the

most uniform and no beads were formed (Figure 4.1(c)). Therefore, it was not recommended to electrospin this PLCL polymer at lower concentrations because this led to bead formation and incomplete solvent evaporation before the fibers reached the collector (Zong et al, 2002).

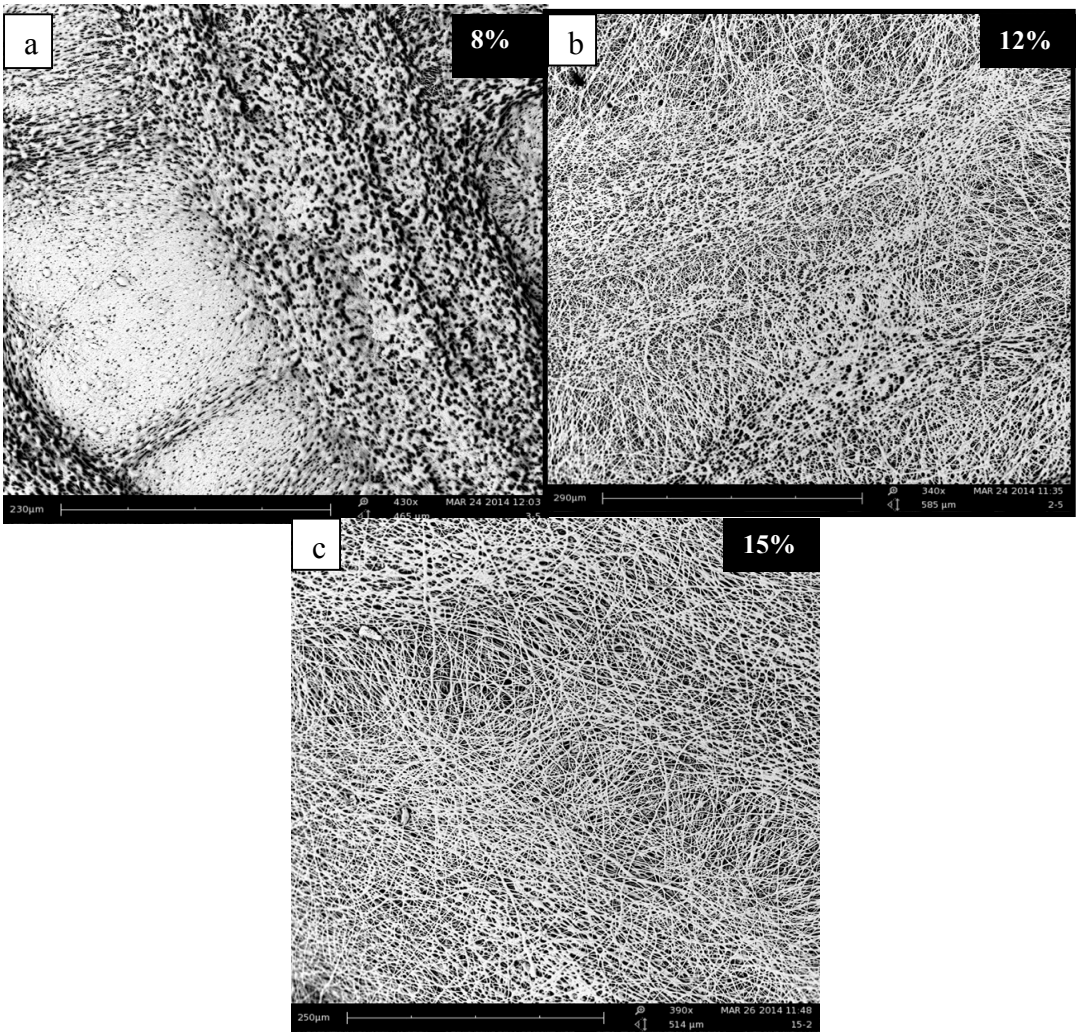

Figure 4. 1 SEM micrographs of electrospun webs showing the effect of different polymer solution concentrations (w/v) (10 kV, 2 ml/h, 6 cm). (a):8% (magnification 430×), (b): 12% (magnification 340×), (c): 15% (magnification 390×).

4.1.2 Effect of Applied Voltage on Electrospinning

A range of different applied voltages was also investigated so as to determine the optimal voltage for electrospinning the PLCL layer. The images of the electrospun webs collected on the knitted layer were viewed by SEM and shown in Figure 4.2. All three images represent the webs produced with a polymer concentration of 15% (w/v), a flow rate of 2 ml/h and a collection distance of 6 cm. It was observed that as the applied voltage increased form 5 kV to 10 kV, the bead formation was significantly reduced and the fiber diameter was more uniform (Figure 4.2(a) and 4.2(b)). More specifically, at 5 kV the fibers showed a tendency to aggregate and fuse together as seen in Figure 4.2 (a), where the fiber diameter was less uniform. However, by increasing the applied voltage to 15 kV, electrospun fibers acquired a more fused appearance without any improvement in fiber uniformity or rate of production (Figure 4.2(c)). This is probably explained by the increased mass flow rate from the needle to the collection mandrel leading to the need for more time for complete solvent evaporation if all other variables, such as concentration, flow rate and collecting distance, were kept constant.

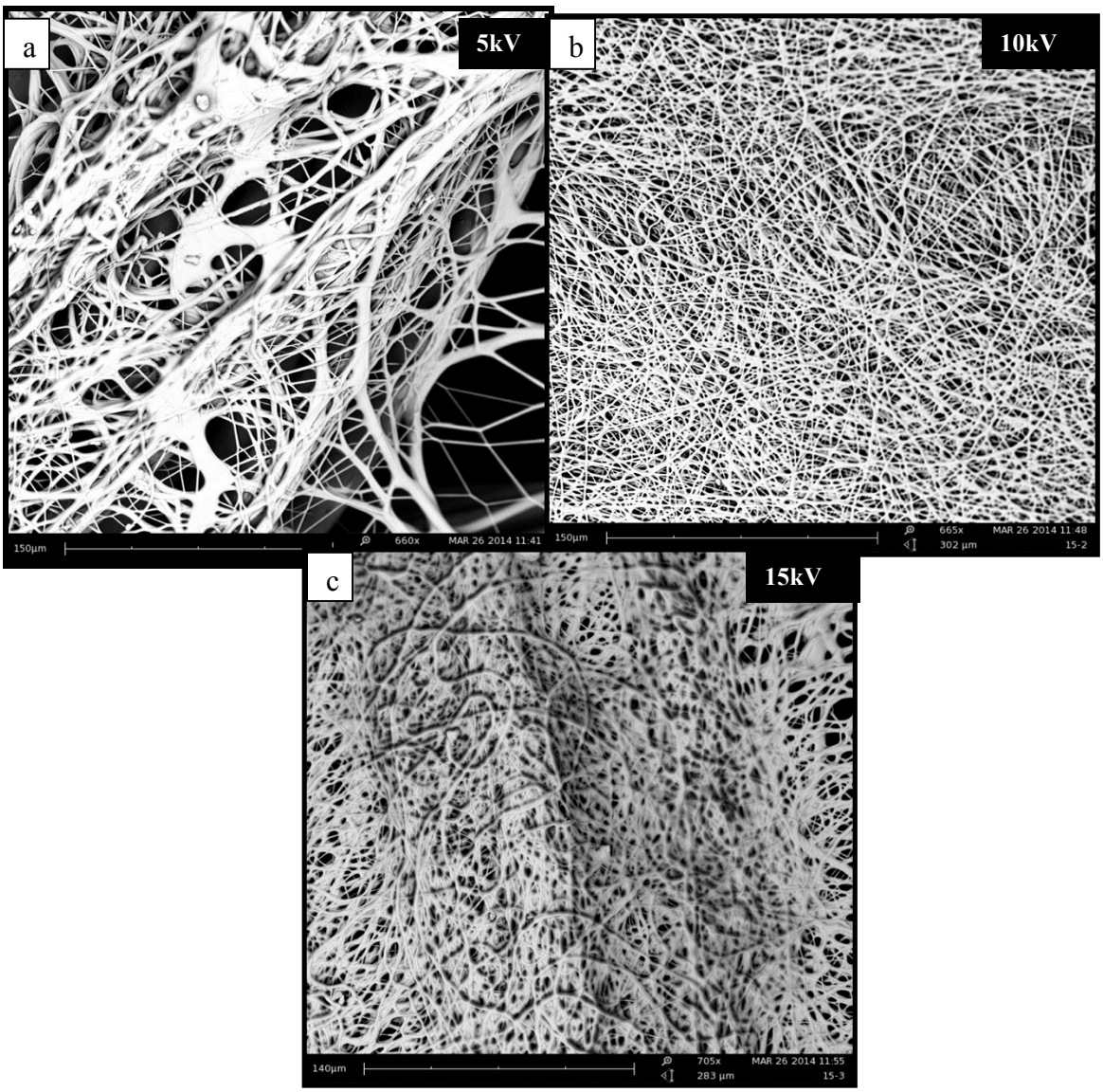

Figure 4. 2 SEM micrographs of electrospun webs showing the effect of applied voltage (15% (w/v), 2 ml/h, 6 cm). (a):5 kV (magnification 660×), (b): 10 kV (magnification 665×), (c): 15 kV (magnification 705×).

4.1.3 Effect of the Collecting Distance on Electrospinning

To select the optimum collection distance in combination with the other two variables, namely polymer concentration and applied voltage, three distances, 3 cm, 6 am and 10 cm between the needle tip and the rotating mandrel were tested at different solution concentrations. Again the appearance of SEM images of the electrospun webs were viewed and compared in Figure 4.3 and 4.4. When the polymer concentration was 8% (w/v) and the applied voltage was 10kV, by increasing the collection distance from 6 cm to 10 cm, the formation of beads and the fusing of fibers were significantly decreased (Figure 4.3). The same result was observed for the electrospun webs fabricated from a 15% (w/v) polymer solution under 15kV of applied high voltage. In this case, more uniform fibers were formed at a collection distance of 6 cm compared to 3cm (Figure 4.4). In general, increasing collection distance can enhance the uniformity of the electrospun fibers and avoid defects by providing sufficient time and distance for the solvent to evaporate and the polymer to dry. Alternatively, it may be necessary to shorten the distance if a larger fiber diameter or an aligned fiber orientation is required depending on the application (Ou, 2011; Fuh, 2012; Tuck, 2012).

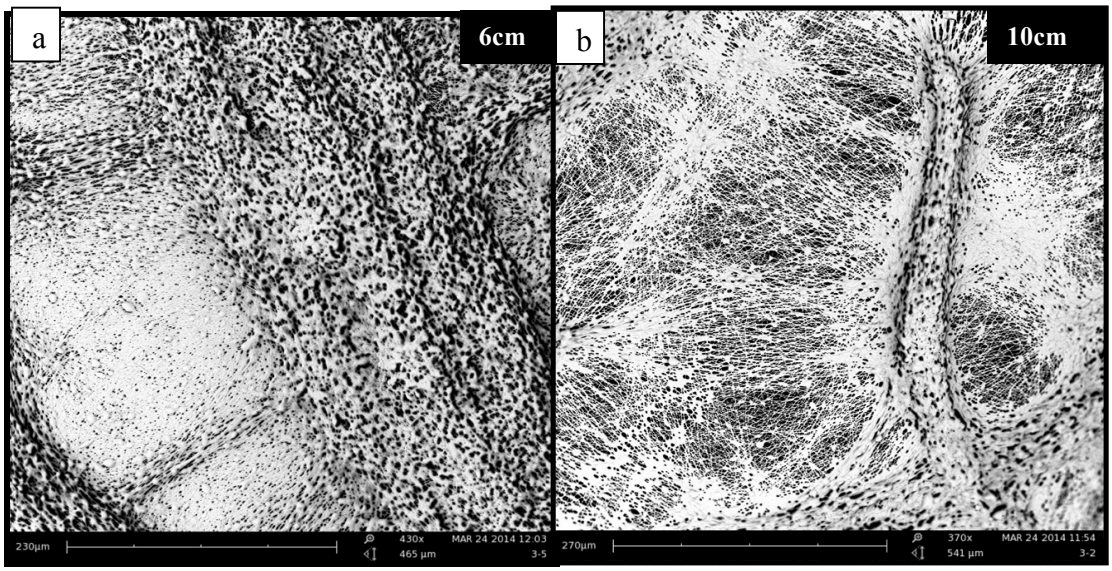

Figure 4. 3 SEM micrographs of electrospun webs showing the effect of collection distance (8% (w/v), 2ml/h, 10kV). (a):6 cm (magnification 430×), (b): 10 cm (magnification 370×).

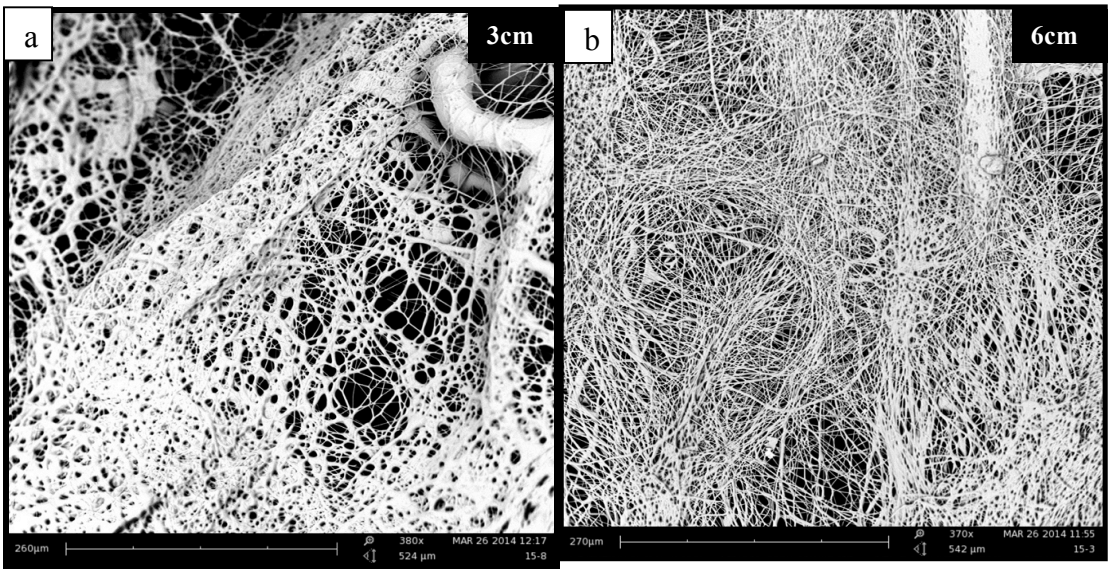

Figure 4. 4 SEM micrographs of electrospun webs showing the effect of collection distance (15% (w/v), 2ml/h, 15kV). (a): 3 cm (magnification 380×), (b): 6 cm (magnification 370×).

Based on the preliminary results discussed above, the optimum parameters selected for producing the PLCL electrospun layer are listed in Table 4.1.

Table 4. 1 Experimental parameters for electrospun layer fabrication

Parameters for electrospinning	
Polymer concentration	15 %(w/v)
Applied voltage	10 kV
Distance between needle tip and rotating mandrel	6 cm
Mandrel rotation speed	200 rpm
Flow rate	2 ml/h

The PLCL electrospun fibers were deposited directly onto the weft knitted tubular structure and collected for 25-30 minutes so as to obtain the desired thickness. After turning the bilayer tube inside out, the electrospun layer formed the luminal surface and then the structure was impregnated with collagen/elastin followed by genipin cross-linking. Photographs of the series of small diameter tubular vessels with approximately 3.2 mm inner diameter, except for the knitted only samples, are shown in Figure 4.5.

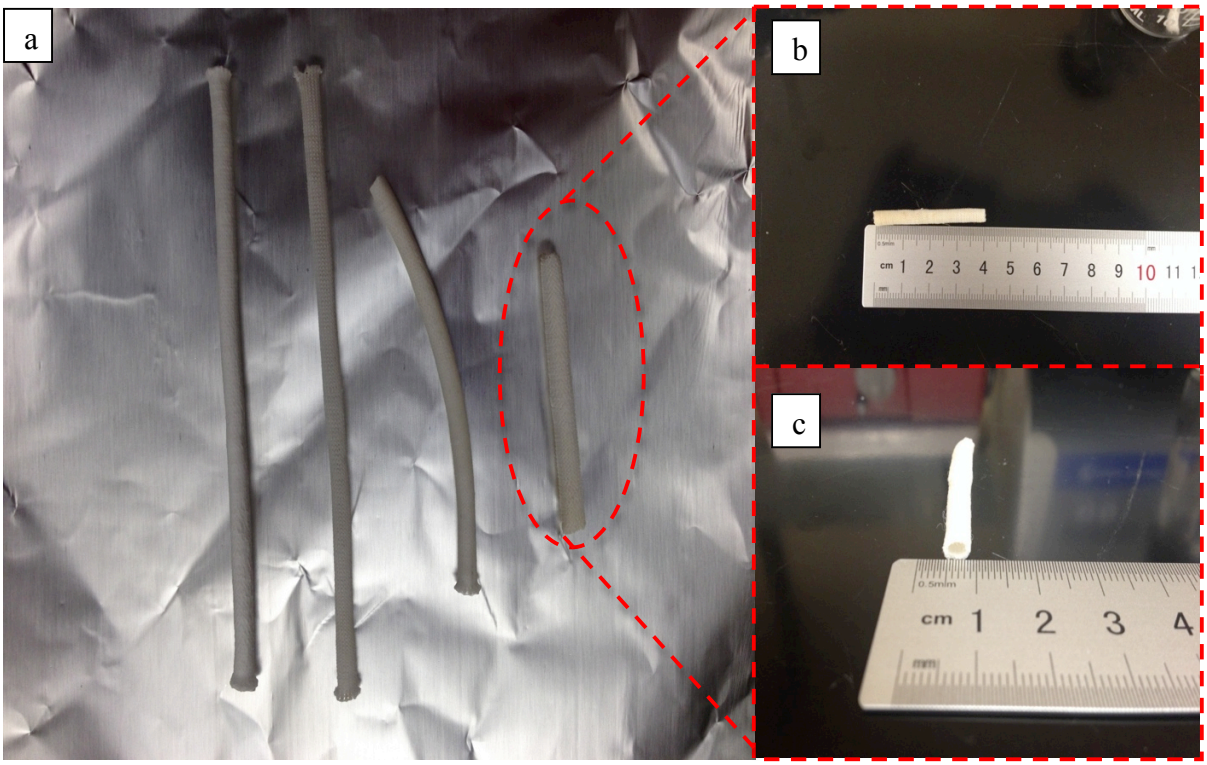

Figure 4. 5 Photographs of the different small diameter vascular grafts. (a): From left to right: knitted tube with external electrospun layer; knitted tube after genipin crosslinked collagen/elastin impregnation; knitted tube with external electrospun layer following crosslinked impregnation; and external knitted tube with internal electrospun layer following crosslinked impregnation. (b) and (c): View of the bilayer graft with external knitted structure and internal electrospun layers plus crosslinked impregnation.

4.1.4 Morphology of Small Diameter Vascular Grafts

The morphology of the series of tubular vessel structures was investigated using SEM at magnifications between 300-400x (Figure 4.6). The two layers in the bilayer structure were observed to be attached to each other as seen from the cross-sectional images in Figure 4.6 (a). Additionally, it was observed that the electrospun fibers served as the "bridge" connecting the two layers together (see arrows in Figure 4.6 (a)). The thin electrospun layer presented a porous and randomly oriented fibrous web in the circumferential plane (Figure 4.6 (d)). For the external weft knitted layer, the collagen/elastin component had penetrated well between the yarns and the filaments during the impregnation process as shown in Figure 4.6 (c), compared with before impregnation (Figure 4.6(b)). Figure 4.6 (d) and (e) display the difference in appearance of the electrospun layer before and after collagen/elastin impregnation and genipin crosslinking. And apparently, the average pore size at the surface diminished significantly.

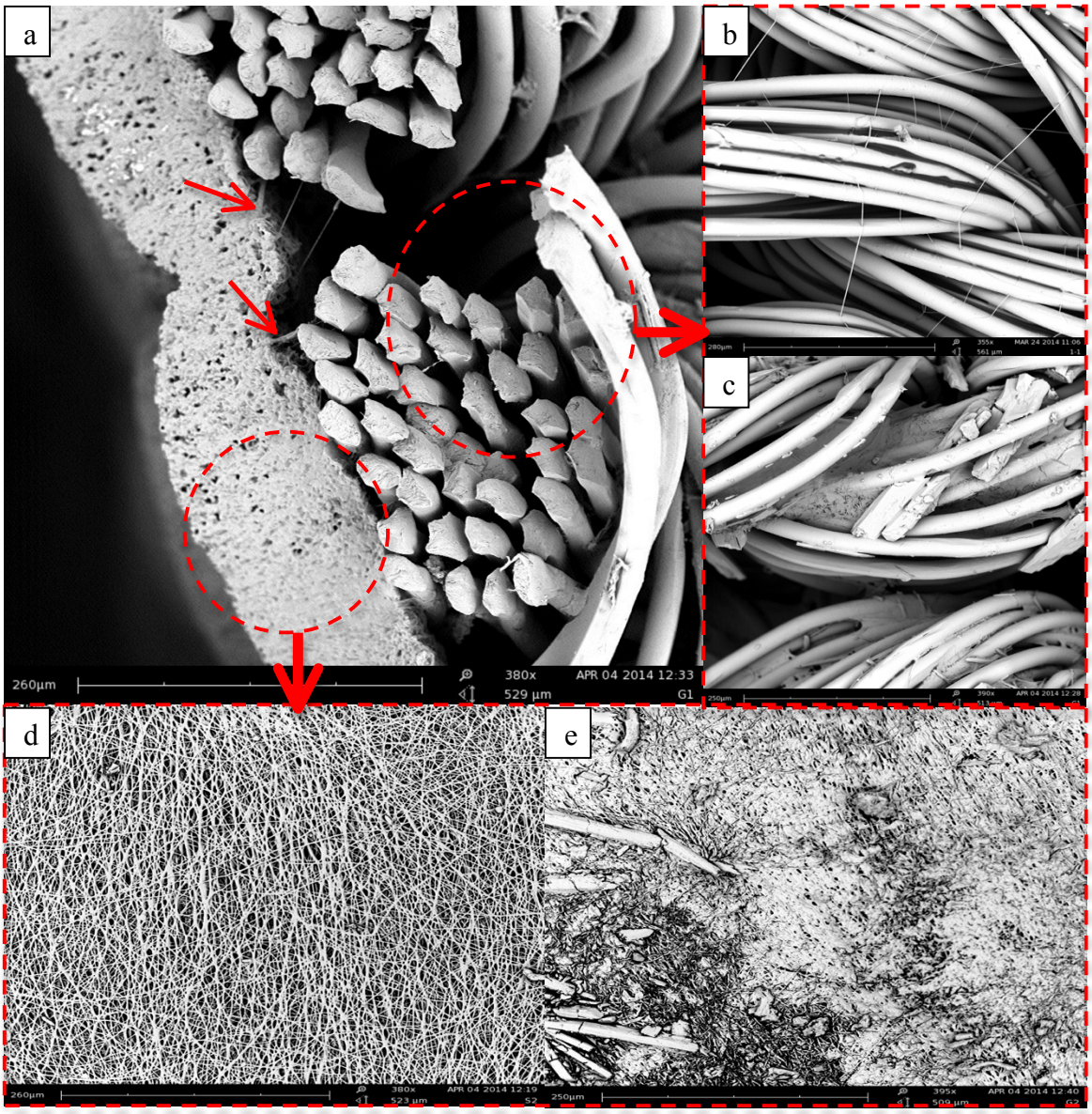

Figure 4. 6 SEM images showing the morphology of the bilayer vessel graft with inside electronspun layer and outside weft knitted structure impregnated with crosslinked collagen/elastin. (a) Transverse section of vessel graft, magnification: 380×. (b)-(c): outside knitted layer before and after impregnation and crosslinking, magnification: 350× and 390 ×. (d)-(e): inside electrospun layer before and after impregnation and crosslinking, magnification: 380×and 395×.

4.1.5 Wall Thickness of Small Diameter Vascular Graft

The wall thickness of the single knitted tube and two of the bilayer knitted and electrospun tubes was measured from the images obtained by optical microscopy (Figure 4.7) using the image analysis software Image J. A total of 12 thickness measurements were obtained from 3 different images of each sample and the results are shown in Table 4.2. Statistically, there was no significant difference in the wall thickness between the two types of bilayer structures, regardless of whether the electrospun layer was on the inside or outside. However, as expected, the average wall thickness value for the monolayer PLA knitted structure was significantly different compared to both types of bilayer grafts ($p \leq 0.05$). And given that bilayer grafts were approximately 0.03 mm thicker than the monolayer grafts, this difference corresponds to the thickness of the electrospun layer.

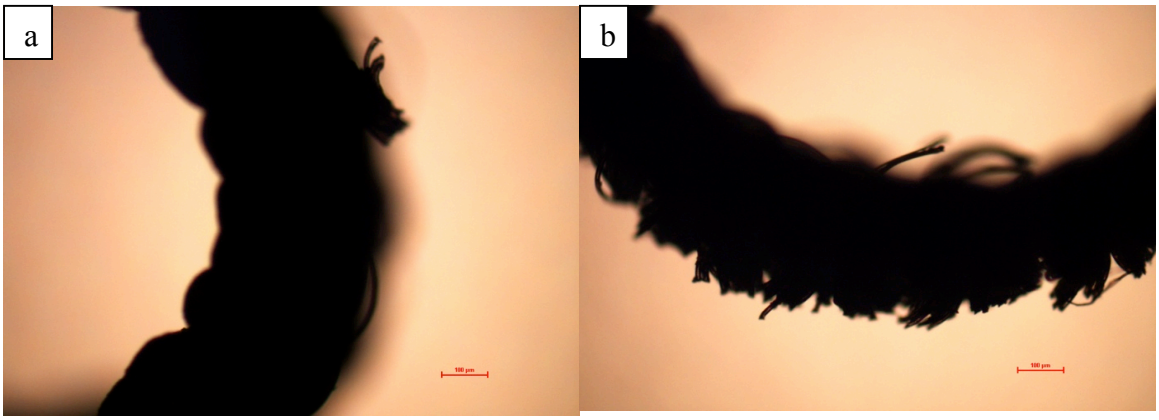

Figure 4. 7 Representative optical microscopy images used for thickness measurements. (a) Transverse image of bilayer vascular graft, magnification: 100×. (b) Transverse image of single layer knitted graft, magnification: 100×.

Table 4. 2 Thickness results of tubular vascular grafts (mm)

Wall thickness (mm)				
Number	Knitted(outside) /Electrospun (inside) /impregnation	Knitted(inside) /Electrospun (outside) /impregnation	Knitted /impregnation	Non-impregnated Knitted(inside) /Electrospun (outside)
1	0.333	0.361	0.305	0. 383
2	0.334	0.367	0.299	0. 364
3	0.349	0.310	0.355	0. 339
4	0.290	0.348	0.308	0. 350
5	0.287	0.346	0.272	0. 333
6	0.318	0.332	0.267	0. 316
7	0.369	0.331	0.289	0. 330
8	0.372	0.308	0.291	0. 298
9	0.326	0.311	0.310	0. 332
10	0.327	0.325	0.375	0. 303
11	0.321	0.286	0.297	0. 279
12	0.313	0.319	0.273	0. 297
13	0.367			0. 301
14	0.350			
15	0.358			
16	0.328			
17	0.308			
18	0.341			
Average	0.333	0.329	0.303	0.325
SD	0.025	0.024	0.032	0.030
SE	0.006	0.007	0.009	0. 008
CV%	7.54	7.24	10.7	9.2

4.2 Mechanical Properties

4.2.1 Circumferential Tensile Strength

The circumferential tensile strength of vascular grafts indicates the ability of the tubular structure to support circumferential loading, or pressure, particularly the pulsatile stress resulting from blood flow. It is one of the most important parameter and property for vascular tissue engineering (Kowalski et al, 2012). The circumferential tensile strength of vascular graft should be similar to the native arteries, which has much higher strength in circumferential direction than longitudinal direction (How, 1992). In addition, this is particularly important for those arteries with relatively high rates of blood flow, such as the coronary artery. The following Figures 4.8, 4.9 and 4.10 illustrate the averages and standard deviations for the maximum load, the peak stress and the percent strain at the maximum load respectively for the five small diameter vascular graft samples prepared in this study. It can be seen from Figure 4.8 that both samples with an external electrospun layer and internal knitted layer had a higher average maximum load than the other three groups of samples. Comparing the pairs of samples statistically showed that the bilayer tube with external electrospun plus impregnation had significantly higher circumferential tensile strength than the other samples, except for the samples with the same structure but no impregnation ($p \leq 0.05$). Similarly, after dividing the maximum load by the valid support area (Figure 4.9), impregnated knitted (inside) /electrospun (outside) tubes had a significantly higher peak stress than the single PLA knitted tubes and even the impregnated knitted (outside) /electrospun (inside) samples ($p \leq 0.05$). Hence, the addition of an electrospun layer can

significantly improve the circumferential load resistance properties of the graft, while the use of an added cross-linked impregnation has only a marginal impact on this property. In addition, after turning the sample inside out, the bilayer grafts show a small but significant decease in circumferential strength.

However, the percent strain at the maximum load showed that one layer knitted structures had greater extensibility than all the bilayer samples (Figure 4.10). In particular the single knitted tube had a significantly higher percent strain than the two samples with electrospun outer layer. In other words, the presence of electrospun film was found to restrict the amount of strain to some extent. Meanwhile, the impregnation treatment caused a minor decrease in the extent of the circumferential strain under pressure. The significant decrease in strength for the electrospun inside bilayer graft compared with the electrospun outside bilayer graft may have resulted from the inversion procedure. When the outside elastomeric PLCL electrospun layer was turned inside, it may have become loose so that it would not be under tension when a force in the circumferential direction applied on the bilayer graft. In this case, only the knitted layer supported the whole graft and contributed to the prevention of failure.

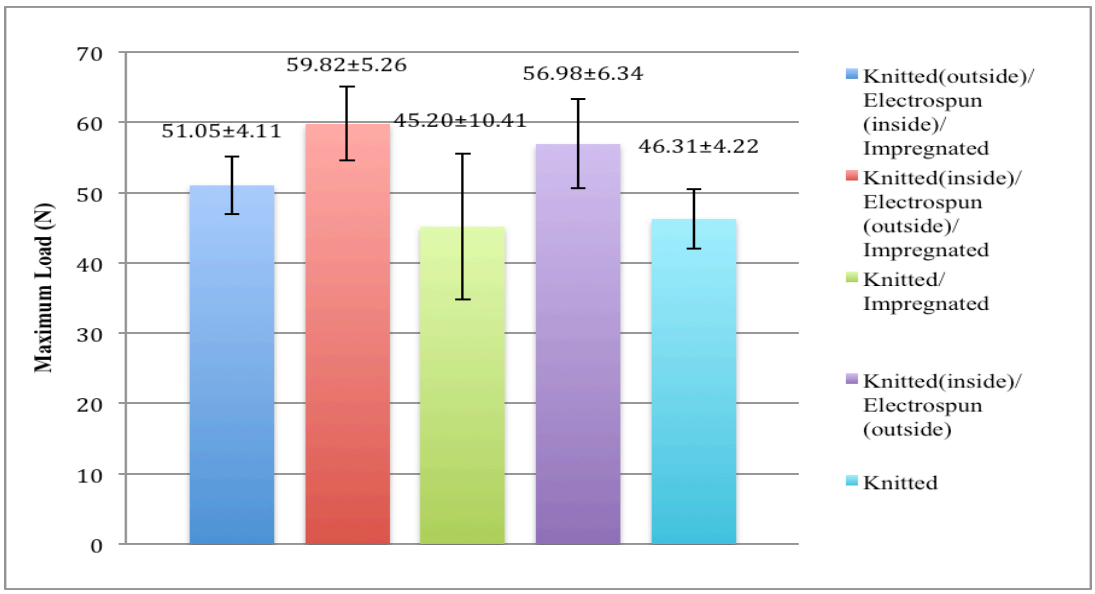

Figure 4. 8 Maximum load of five different vascular grafts in circumferential tensile test

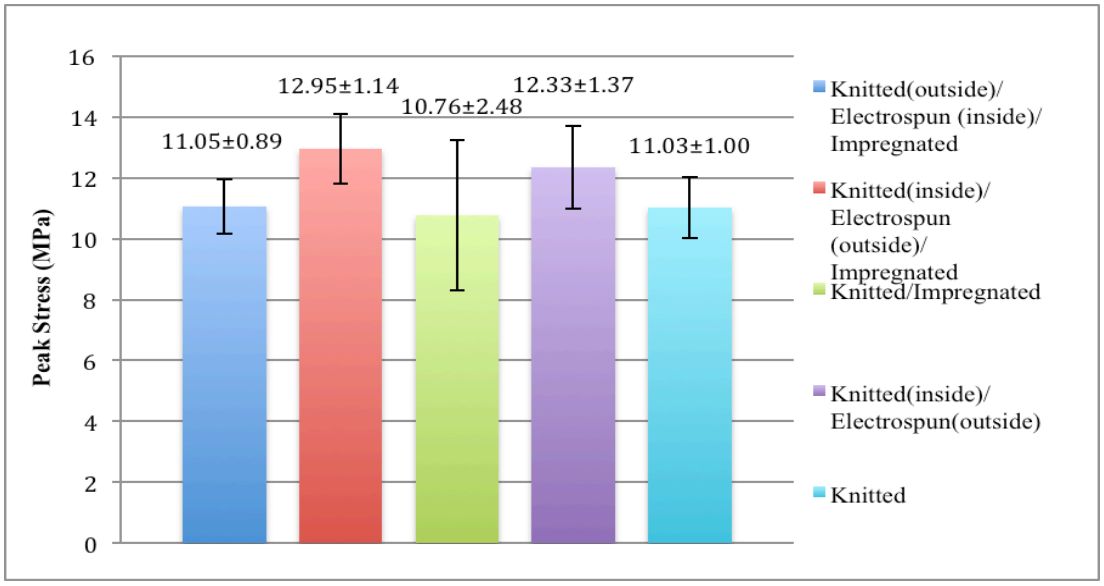

Figure 4. 9 Peak stress of five different vascular grafts in circumferential tensile test

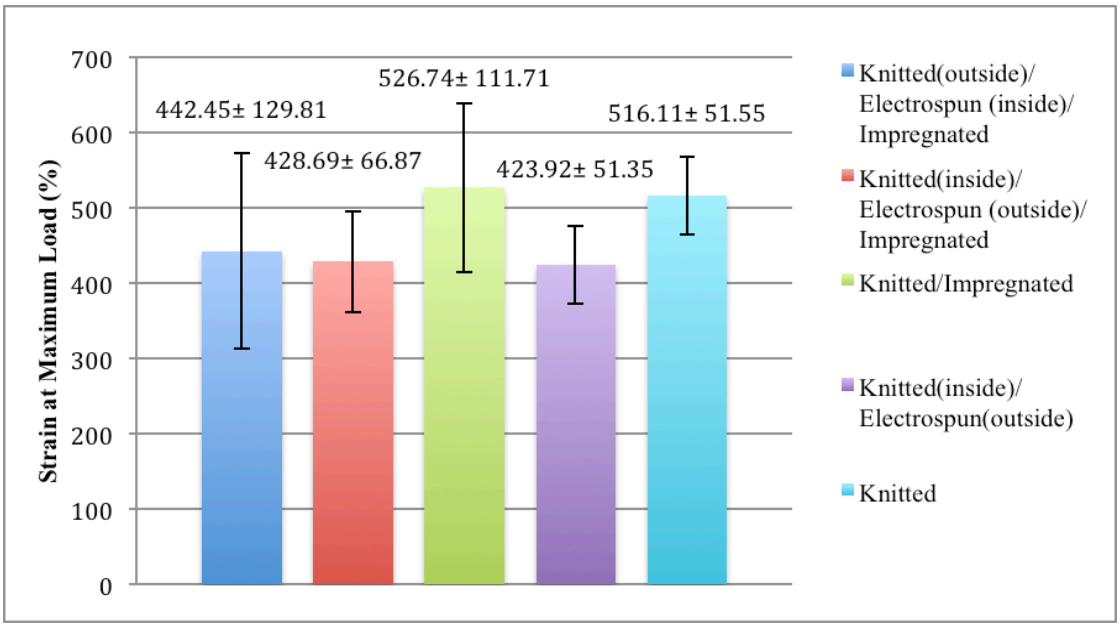

Figure 4. 10 Strain at maximum load of the five different vascular grafts in circumferential tensile test

4.2.2 Burst Strength

The bursting strength reflects the ability of the tubular vascular graft to withstand internal the pressure. The experimental results for the five different graft samples are presented in terms of bursting stress in Figure 4.11 and extension at the peak load in Figure 4.12. In Figure 4.11, the bilayer impregnated knitted (outside)/electrospun (inside) sample appears to have a higher average bursting stress. However, this value is not significantly different from the other three bilayer or impregnated samples. What is important to note is that the bursting stress values for all four bilayer or impregnated samples were significantly higher than for the single layer non-impregnated PLA knitted control graft ($p \leq 0.05$). Thus, either adding an

electrospun layer or impregnating with collagen/elastin or both was found to significantly enhance the bursting strength of the small diameter vascular grafts.

In Figure 4.12, the average extension at peak load for the impregnated knitted (outside)/elecrospun (inside) graft appears to be higher than the other samples. However, none of the average extension at peak load values is significantly different from the rest. Therefore, the addition of an electrospun layer and/ or the collagen/elastin impregnation treatment did not affect the bursting extension of the prototype vascular grafts. In addition, we can conclude that there was no adverse impact on the bursting strength from turning the bilayer grafts inside out.

What was different from the circumferential tensile test, was that the bursting force was applied by the pin perpendicular to the plane of the bilayer flat fabric, either directly to the electrospun layer or to the knitted layer. This is a different direction from the circumferential strength test. So the tension or looseness in the electrospun layer did not impact the bursting test results.

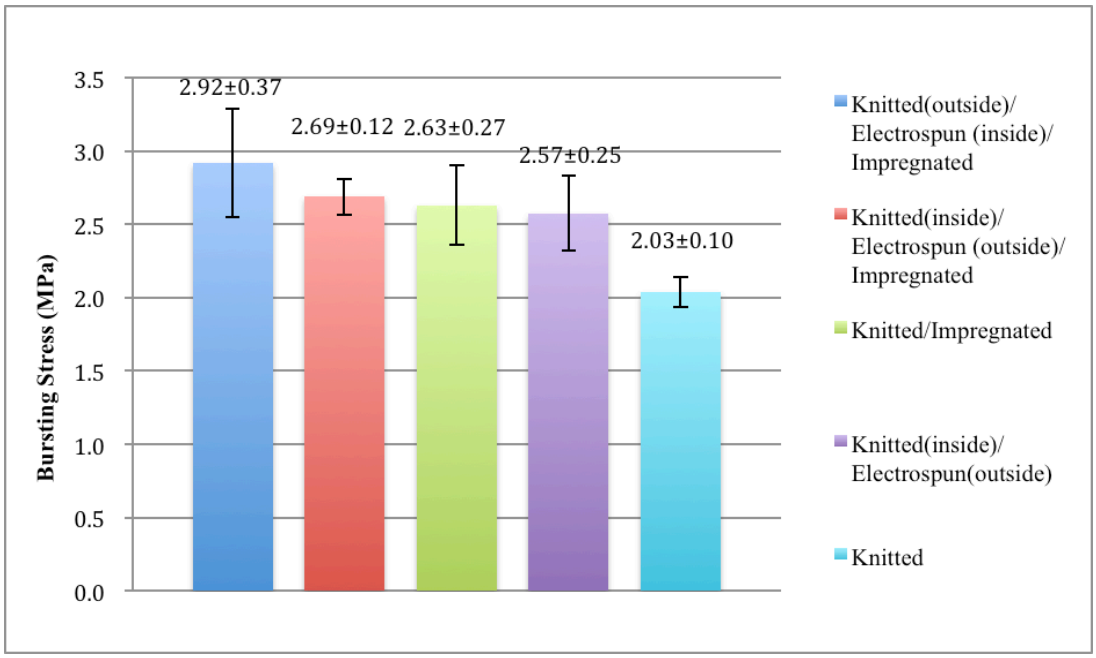

Figure 4. 11 Bursting stress for five different vascular grafts

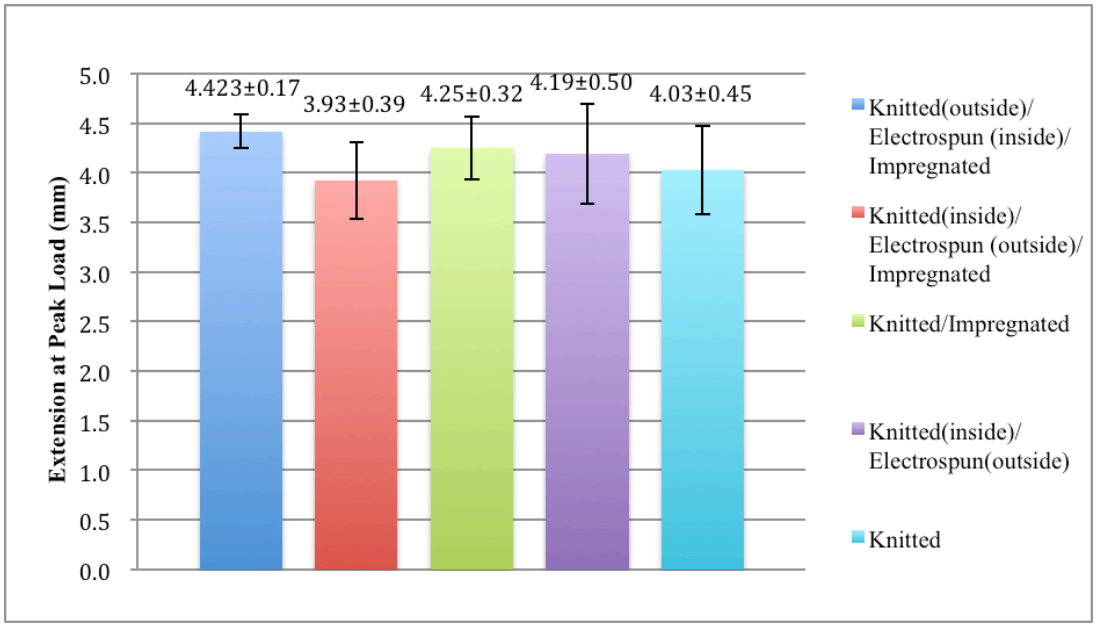

Figure 4. 12 Extension at peak load for five different vascular grafts

4.2.3 Suture Retention Strength

When used for clinical bypass surgery, a small diameter vascular graft is usually installed by suturing one end to the patient's aorta while the other end is attached to the coronary artery with an end to side anastomosis. Thus, the small diameter vascular substitutes are required to have high suture retention strength so as to keep the suture line from moving, fraying or rupturing. Also, a weft knitted structure is known to have a tendency to ravel. It is believed that measurements of suture retention strength can point to whether the application of an electrospun layer and/or collagen/elastin impregnation or both can restrict or even prevent the weft knitted structure from unraveling. Figure 4.13 shows the averages and standard deviations for the suture retention strength of the five prototype samples of small diameter vascular grafts prepared in this study. Clearly, the suture retention strength of the non-impregnated single weft knitted control graft was significantly lower than the other four samples ($p \leq 0.05$). However, there were no significant differences in suture retention performance between any of these four other samples regardless of whether the electrospun layer was on the inside or the outside. Therefore, stabilization of the weft knitted structure, either by applying an electrospun layer or by impregnating and crosslinking a collagen/elastin layer or both, can significantly improve the suture retention strength for the prototype grafts and limit or control the raveling problem for the weft knitted structure. Additionally, turning the bilayer samples inside out had no negative effect on the suture retention strength of the resulting vascular prosthesis. The improved performance is possibly

due to the ability of the electrospun layer and the impregnation of collagen/elastin to stabilize the weft knitted fabric and limit the distortion of the knitted loops when under stress.

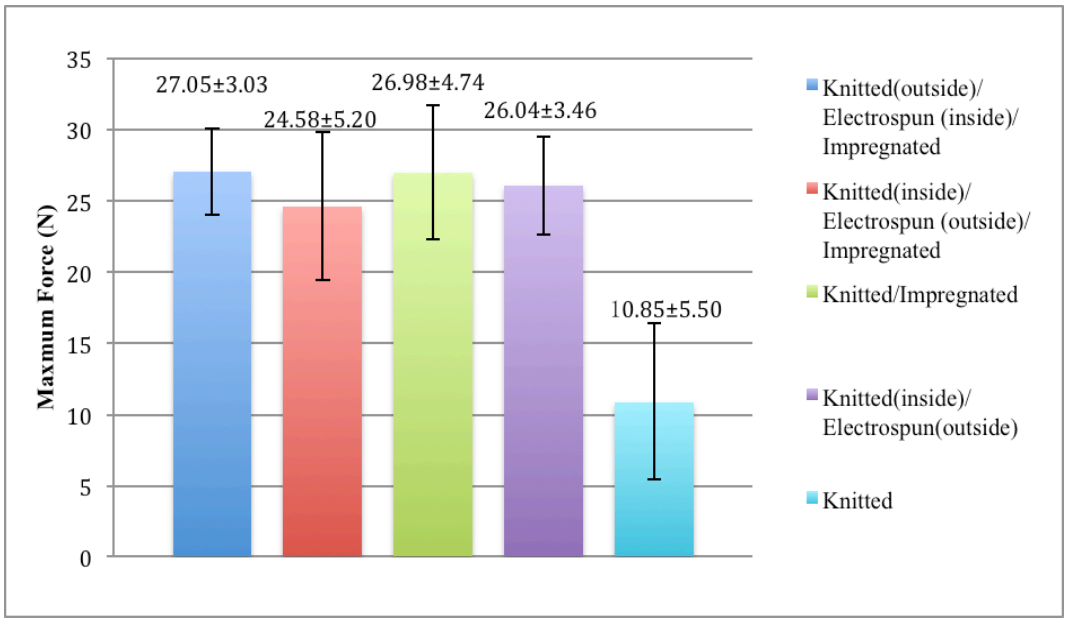

Figure 4. 13 Suture retention strength for five different vascular grafts

4.2.4 Compliance

Compliance refers to the dimensional and volumetric changes in a blood vessel in response to the transmural pressure change during pulsatile blood flow. It also reflects the ability of the vascular graft to expand and increase its volume when the internal pressure in the vessel increases. In this study, the compliance of the five different prototype grafts was tested under dynamic cyclic simulated loading and the results were shown in Figures 4.14 and 4.15.

In Figure 4.14, we can see the general trend where the amount of compliance in most vascular prostheses decreases at a higher applied pressure range. This is because most materials, whether knitted, electrospun or as coated membranes, will experience their maximum displacement at lower loads, and as the applied stress or pressure is increased so the relative amount of strain decreases. The only sample that showed a different trend and did not decrease progressively in compliance with increase of pressure was the knitted (inside)/electrospun (outside)/impregnated sample which has a yield point in the 80-120 mmHg pressure range. The compliance properties among these five prototype grafts are compared in Figure 4.15 at hypotensive, normotensive and hypertensive blood pressure ranges respectively. In the low-pressure range, the single layer knitted/impregnated graft samples had the highest average compliance of all five samples ($p \leq 0.05$). On the other hand, the knitted (inside)/electrospun (outside)/impregnated grafts gave the lowest average compliance value among all five groups ($p \leq 0.05$). The knitted (outside)/electrospun (inside)/impregnated sample had greater compliance than the non-impregnated single knitted structure ($p \leq 0.05$) while sharing the similar average compliance value with the non-impregnated knitted (inside)/electospun (outside) sample.

When the pressure increased to a normotensive range (80-120 mmHg), the compliance value of the knitted (inside)/electrospun (outside)/impregnated sample fell significantly and was far less compliant than the non-impregnated knitted (inside)/electrospun (outside) grafts under the same pressure range ($p \leq 0.05$). This suggests that the impregnated and cross-linked

treatment had a significant effect on the mobility of the yarns and severely limited the structure to respond to the normotensive pressure range.

With the increase in pressure up to the hypertensive (110-150 mmHg) level, only marginal differences in compliance were observed between the five prototype samples. What remained significant was the fact that again, as was observed at the two lower pressure ranges. By turning the knitted (inside)/electrospun (outside)/impregnated graft inside out, a significant increase in average compliance was achieved for the knitted (outside)/electrospun (inside)/impregnated graft structure. The reasons for this phenomenon are not clearly understood, but it may be due to the fact that as an internal layer the PLCL electrospun web was no longer under tension and dilated more readily and provided increased compliance to the bilayer structure as a whole.

In general, these results indicate that an additional electrospun layer of PLCL will limit the amount of compliance offered by this prototype. However this limitation is less severe if the electrospun layer is the inner layer rather than the outer layer of the prototype structure. Nevertheless, none of the five prototype samples exhibited a compliance that is comparable to a native artery with compliance of $5.9 \pm 0.5\%/100\text{mmHg}$ (Salacinski, 2001; Catto, 2014).

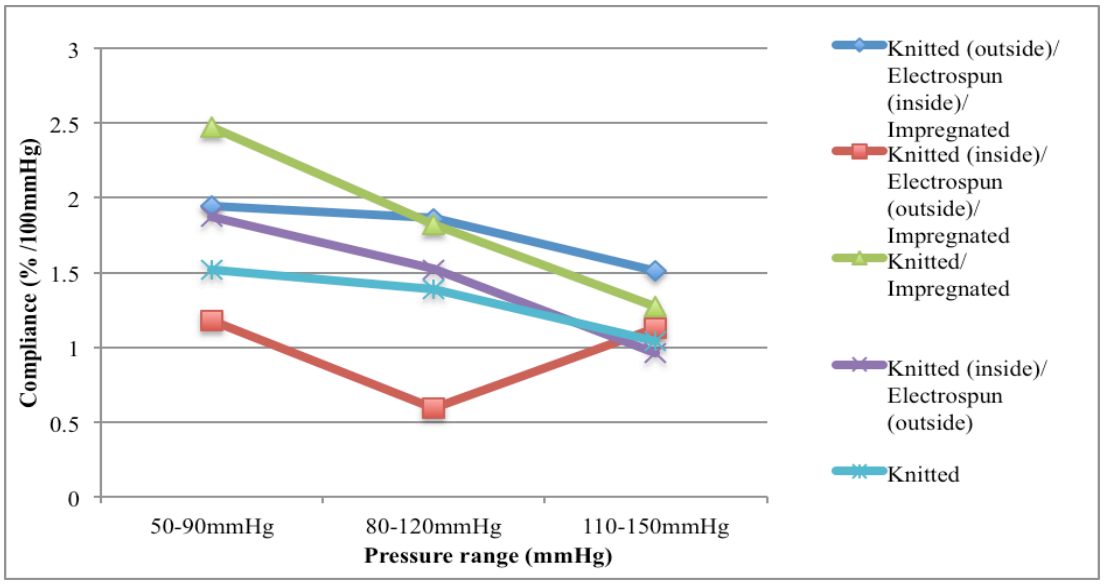

Figure 4. 14 Average compliance values for the five prototype grafts under different pressure ranges

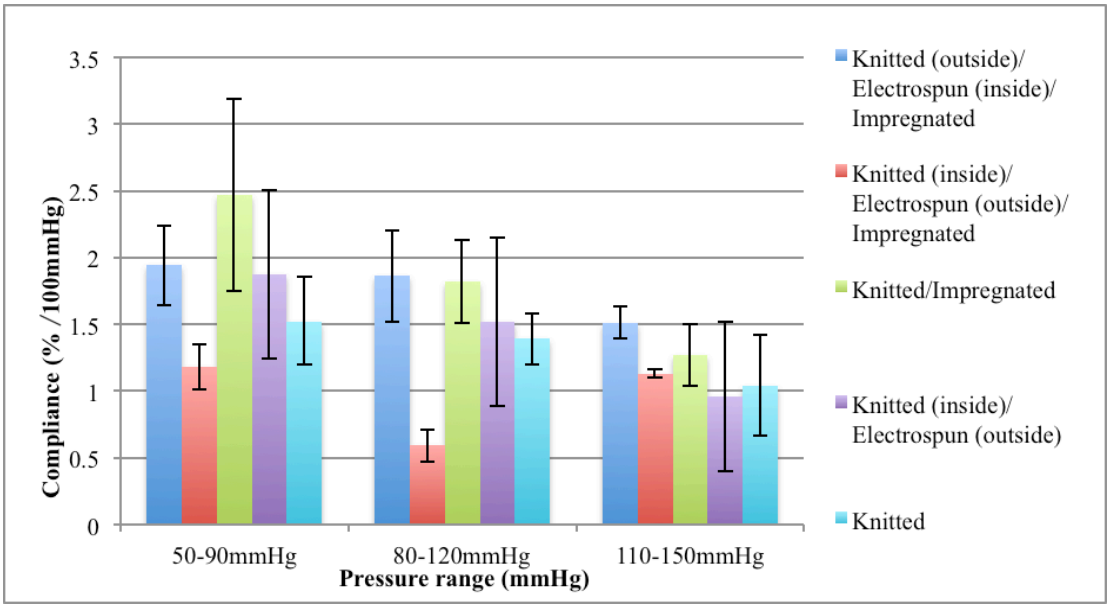

Figure 4. 15 Comparison of compliance values among the five prototype grafts at different pressure ranges (Error bars = ± standard deviation)

4.3 Thrombogenicity

The main reason for failure of small diameter vascular grafts after implantation is usually due to the formation of a blood clot or thrombus which attaches to the luminal wall of the device causing narrowing (stenosis) and eventually blockage (occlusion). One of the reasons for impregnating the vascular grafts in this study with collagen/elastin was to reduce the tendency for thrombus formation and extend the patency rate of the grafts after implantation. In this study, the graft samples were tested in a thromboelastograph (TEG) to determine their tendency to promote thrombus formation when exposed to plasma and whole blood under controlled conditions.

In this test, there are four TEG parameters that represent coagulation activation and clot formation. The parameter "R" represents reaction or incubation time until the formation of fibrin. It is shown as a flat line at the beginning of Figures 4.16 and 4.17. "K" is the clot formation time from the end of "R" until the thrombus creates enough viscoelastic force to deviate the pin by 20 mm, which represents the speed of thrombus formation. The "Angle" is derived from the midline and a line tangent to the slope that determines "K". Both "K" and the "Angle" reveal how fast the thrombus forms during the coagulation phase and are said to describe the kinetics of clot formation. "MA" is the maximum amplitude or widest deviation of the tracing imparted by the viscoelastic properties, or overall strength of the thrombus. The coagulation index (CI) is derived to create a single value that incorporates all of the other parameters to more easily define the hypo- or hypercoagulable tendencies. The formula is provided in Chapter 3.

In Figure 4.16, we can see that when tested in plasma both the impregnated and non-impregnated grafts had more thrombus deposition compared to the empty cup, while the ePTFE graft gave a better performance with lower clot strength ("MA" value). However, the reaction time "R" before the clot started for the impregnated graft was equivalent to that for the ePTFE graft.

Figure 4.17 illustrates typical curves for each prototype graft tested with whole blood. The results indicate that the impregnated graft gave a similar performance of promoting thrombus formation as the commercial ePTFE graft with an equivalent value for "R". However, the "K", "Angle" and "MA" values for the impregnated graft were smaller than that for the ePTFE graft, indicating that the collagen/elastin surface was less thrombogenic than the ePTFE surface (Figure 4.17). On the other hand, the non-impregnated graft showed a distinct tracing which points to unstable clot formation and an increased clot retraction or rate of clot lysis or thrombus unstability caused by separation of the clot from the pin. By reviewing the data in Figure 4.17 it is possible to claim that the impregnated graft had a less thrombogenic performance compare to the ePTFE control with relatively longer "R" and "K" values and lower "Angle" and "MA" values. This is reflected in the CI, which is significantly less or relatively hypocoagulable, for the impregnated graft relative to the commercial ePTFE control.

Tables 4.3 shows the values of all four TEG parameters for the three specimens tested from each sample with different blood from the three donors, while Table 4.4 shows the average of the four TEG parameters compared with previously established normal data from 17 healthy

dog donors. Generally the impregnated samples had lower CI values than the non-impregnated and commercial ePTFE samples (Table 4.3). Furthermore, they were even lower than those for established normal healthy donor samples (Table 4.4).

In summary, the collagen/elastin impregnated grafts exhibited marked decrease in their thrombogenicity with a visibly longer incubation or reaction time "R" compared with the non-impregnated samples. In addition, the impregnated grafts showed an equivalent thrombogenicity to the commercial ePTFE control graft, which has been reported as one of the most inert and "non-thrombogenic" biomaterials due to its electro-negative surface (Campbell, 1975; Ariyoshi, 1997).

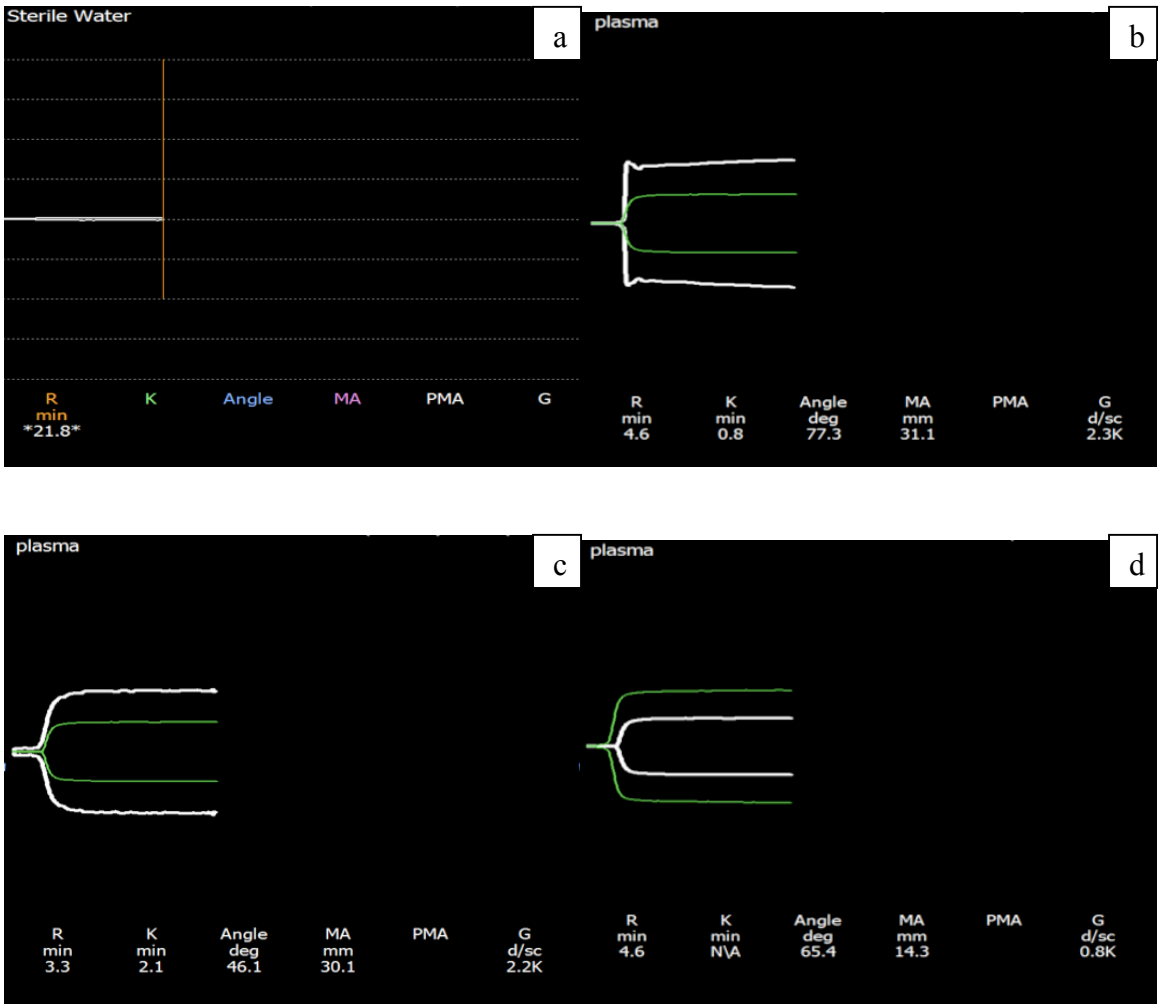

Figure 4. 16 Thromboelastograph curves (a) knitted (outside)/electrospun (inside)/impregnated graft using sterile water as a negative control, demonstrates no effect by the presence of the material alone, (b) knitted (outside)/electrospun (inside)/impregnated graft using citrated canine plasma, (c) knitted (inside)/electrospun (outside) non-impregnated graft using plasma and (d) ePTFE commercial graft using plasma. In image (b) and (C), white tracings show the results with the test material while green tracings show that of the control cup containing no test material. In image (d), the tracings are reversed.

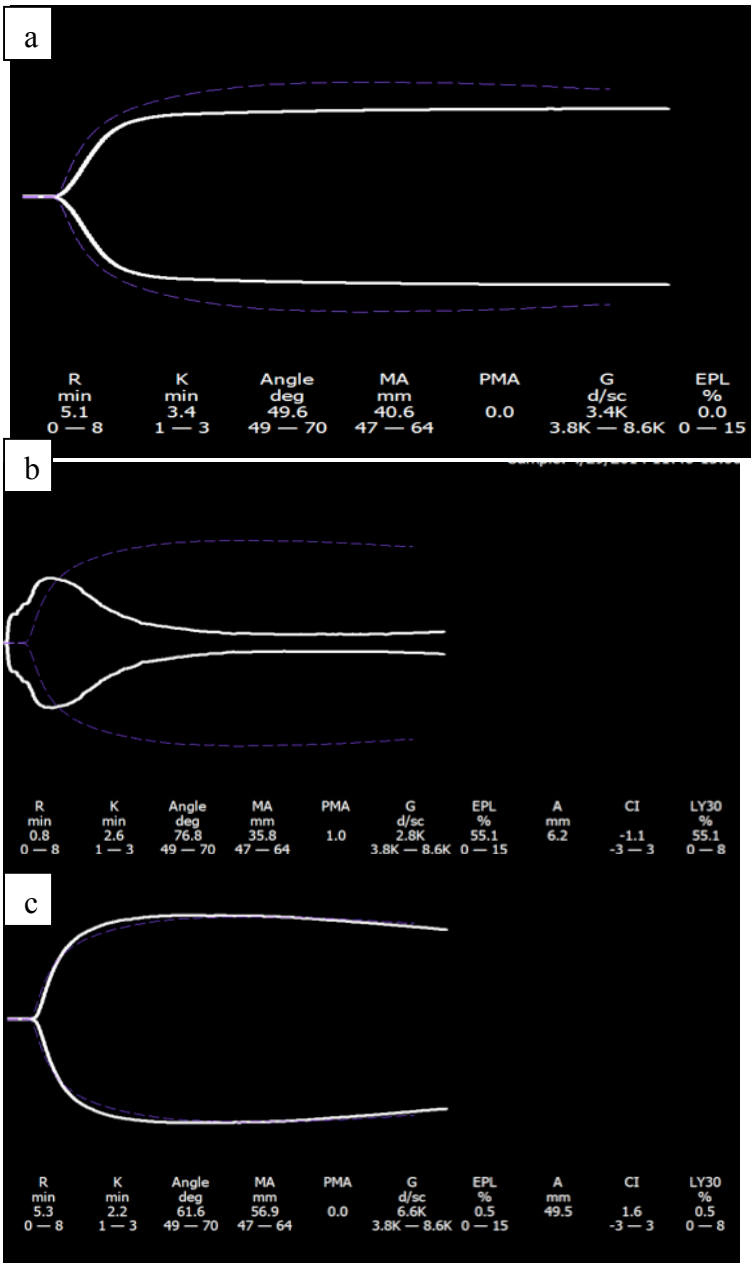

Figure 4. 17 Thromboelastograph curves using citrated canine whole blood: (a) knitted (outside)/electrospun (inside)/impregnated graft, (b) knitted (inside)/electrospun (outside) non-impregnated graft and (c) ePTFE commercial graft. The white tracings indicate the results with the test materials and the purple tracings show the results of the control cup containing no test material.

Table 4. 3 Thromboelastograph test results for three samples of test materials with different donor blood

		R (min)	K (min)	Angle (degree)	MA (mm)	Coagulation index (CI)
Knitted (inside)/ electrospun (outside)/ impregnated graft	Blood 1	5.10	3.40	49.60	40.60	1.16
	Blood 2	4.60	1.80	64.40	57.10	3.46
	Blood 3	2.70	2.00	64.20	47.90	1.71
	Average	4.13	2.40	59.40	48.53	2.11
Non-impregnated knitted (inside)/ electrospun (outside) graft	Blood 1	0.20	4.30	52.40	59.00	3.54
	Blood 2	0.80	2.60	76.80	35.80	-0.83
	Blood 3	2.10	0.80	77.10	64.70	4.09
	Average	1.03	2.57	68.77	53.17	2.27
Commercial ePTFE graft	Blood 1	0.20	N/A	61.40	6.10	N/A
	Blood 2	5.30	2.20	61.60	56.90	3.58
	Blood 3	2.20	1.60	69.70	67.00	4.67
	Average*	3.75	1.90	65.65	61.95	4.13

* Average of commercial ePTFE graft was only calculated from the values tested with blood 2 and blood 3 due to abnormal test results with Blood 1.

Table 4. 4 Comparison of the four parameters and coagulation index (CI) with established normal native samples

TEG variables	TEG values			
	Knitted (inside)/ electrospun (outside)/ impregnated graft	Non-impregnated knitted (inside)/ electrospun (outside) graft	Commercial ePTFE graft	Established normal native samples*
R (min)	4.13	1.03	3.75	4.52
K (min)	2.40	2.57	1.90	2.38
Angle (degree)	59.40	68.77	65.65	59.61
MA (mm)	48.53	53.17	61.95	56.16
Coagulation index (CI)	2.11	2.27	4.13	3.41

* Previously established mean values for recalcified citrated whole blood canine samples established with 17 healthy dogs in Dr. Rita Hanel's lab.

4.4 Biological Performances of Vascular Prostheses

4.4.1 Cytotoxicity by MTT Assay

To evaluate the biological performance of the prototype vascular grafts, an MTT assay was used to investigate the relative cytotoxicity, cell viability and cell proliferation by measuring the number of viable cells attached to the inner lumen of the four different vascular graft prototypes after 1, 3 and 7 days of *in vitro* culture. Please note that non-impregnated PLA

knitted control graft was excluded from this experiment. After 1, 3 and 7 days of endothelial cells culture, the MTT absorbance values were read. The average values and standard deviations are recorded in Table 4.5. Figure 4.18 illustrates the cell proliferation results on the inner lumen of different the grafts at Day 1, 3 and 7. From this figure, the viable cell density for all the four prototype graft samples appears to decrease significantly from Day 1 to Day 3 ($p \leq 0.05$), while, for some samples the cell viability then later increases from Day 3 to Day 7 ($p \leq 0.05$). When comparing the performance of the 3 bilayer samples, namely the knitted (outside)/electrospun (inside)/impregnated sample, the knitted (inside)/electrospun (outside)/impregnated sample and the non-impregnated knitted (inside)/electrospun (outside) sample, no significant difference in cell viability was observed by the MTT assay. Unlike smooth muscle cells, endothelial cells tend to grow as a monolayer on the luminal surface of native arteries. This means that their continual growth may be limited by the amount of the material surface available for cell proliferation or because the cells have already reached confluency. If a certain number of cells died and became detached between Day 1 and Day 3, they would have increased the available surface area providing for the proliferation of live cells along and around the graft after they reach confluency. This may explain the increases in some cell populations from Day 3 to Day 7.

As for the differences in cell viability between the different types of grafts, it is evident from Figure 4.18 that the single layer weft knitted structure had significantly lower cell density compared with other three samples at all 3 time points from 1 to 7 days even through they were all impregnated with collagen and elastin ($p \leq 0.05$). This is most likely due to the very

large pore size of the weft knitted structure. Many of the cells seeded onto the knitted fabric passed through the pores and grew on the surface of culture dish instead of on the fabric. For the bilayer structure, regardless of whether the electrospun layer was on the inside or the outside, the first two types of graft generated similar cell viability results at Days 1, 3 and 7. So not only is the electrospun web of nanofibers suitable for growing a monolayer of endothelial cells because of the remarkably small pore size and pore size distribution, but also the knitted structure containing multifilament yarns can lead to a promising cell proliferation performance due to its really large surface. By comparing the two knitted (inside)/electrospun (outside) grafts with and without impregnation, they gave similar cell viability data according to the MTT assay at Day 7. These results suggest that the collagen/elastin impregnation did not significantly improve cell viability.

Table 4. 5 MTT absorbance results of endothelial cell viablility on vascular grafts.

	Knitted (outside)/ Electrospun (inside)/ Impregnated graft		Knitted (inside)/ Electrospun (outside)/ Impregnated graft		Knitted/ Impregnated graft		Non-impregnated Knitted (inside)/ Electrospun (outside) graft	
	Mean	SD	Mean	SD	Mean	SD	Mean	SD
Day 1	0.222	0.025	0.207	0.015	0.171	0.016	0.222	0.019
Day 3	0.182	0.018	0.176	0.014	0.138	0.005	0.193	0.012
Day 7	0.202	0.011	0.202	0.029	0.139	0.005	0.216	0.020

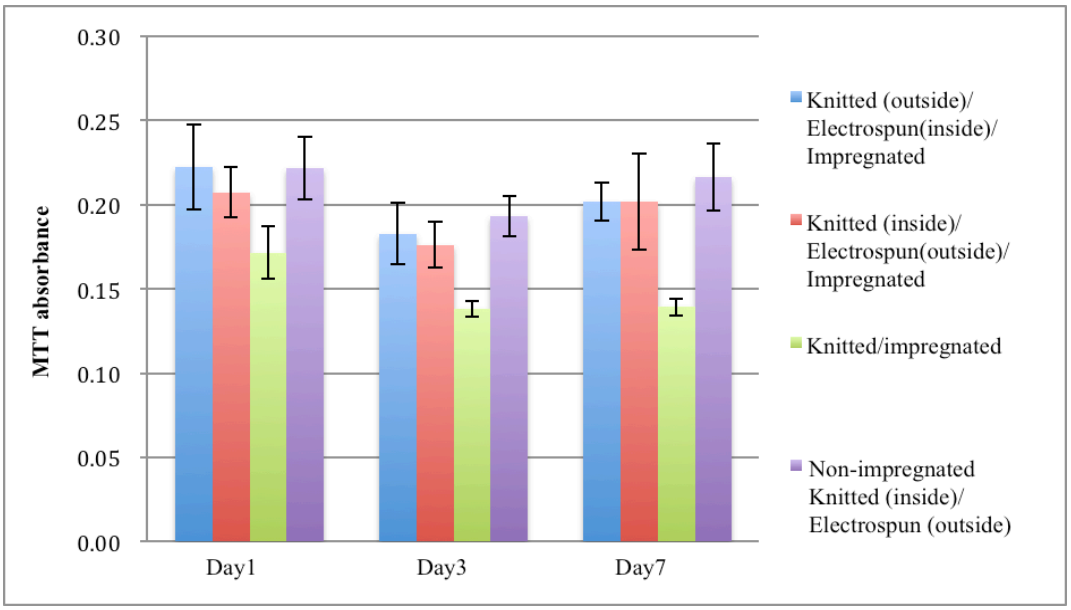

Figure 4. 18 MTT assay results at Day 1, 3 and 7 for four different vascular grafts (Error bars = ± standard deviation).

4.4.2 Cell Proliferation and Distribution by Immunofluorescence Assay

The extent of proliferation and distribution of the endothelial cells on the four different graft structures was investigated by an immunofluorescence assay together with the observation by means of a laser scanning confocal microscope (LSCM). Figures 4.19, 4.20, 4.21 and 4.22 illustrate the cell distributions at Day 7 on four different scaffolds. They included the knitted (outside)/electrospun(inside)/impregnated graft, the knitted(inside)/electrospun (outside)/impregnated graft, the knitted/ impregnated graft and the non-impregnated knitted (inside)/electrospun (outside) graft. Each figure provides a three dimensional image of the cell distribution in the x, y plane by viewing down through the thickness. In addition, there are also images of cell distribution at different levels when viewed in the x, z plane. Figure

4.23 provides transverse views of the four different types of grafts and compares cells distribution through the thickness of each structure.

Figure 4.19 illustrates the cell distribution looking down on the inner lumen of the knitted (outside)/electrospun (inside)/impregnated graft at Day 7. From the fluorescent image (a), we can see that the cells have proliferated relatively uniformly across the entire surface area of the graft. The transverse images (b) and (c) show how the cells grew and proliferated at different levels within the structure.

Figure 4.20 shows the cell distribution looking down on the inner lumen of the knitted (inside)/electrospun (outside)/impregnated graft at Day 7. It is evident that there were fewer cells growing across the observable surface area (image a) compared with the cells on the previous graft sample (Figure 4.19). The same situation is apparent in the transverse images at different scanning depths within the structure (images b and c), with fewer cells appearing on the PLA multifilament yarns. This result suggests that the electrospun web can promote better endothelial cell proliferation and distribution than the weft knitted tubular fabric. In Figure 4.20 (a), there appears to be some other fluorescent materials that were stained by DAPI. These are seen as noncircular blue spots or abnormal aggregates (identified by arrows) and may be the unidentified residuals of the impregnation and/or crosslinking processes.

Figure 4.21 displays the cell distribution looking down on the inner lumen of the single layer knitted/impregnated graft with collagen/elastin coating at Day 7. The distribution of small blue spots representing the cell nuclei is similar to the previous image (Figure 4.20), pointing to the fact that fewer cells were observed after 7 days of culture compared with the knitted

(outside)/electrospun (inside)/impregnated sample. Again the presence of a number of unidentified fluorescent blue spots (identified by arrows) suggests that there were residuals or contaminant following the impregnation and/or cross-linking processes. If these blue spots were associated with cell-stained nuclei, such observations would not be consistent with the results observed by the MTT assay (Figure 4.18).

Figure 4.22 presents the cell distribution looking down on the inner lumen of the knitted (inside)/electrospun (outside) non-impregnated graft structure at Day 7. Note that the number of blue viable cell nuclei observed on this sample appear to be more than on the two previous kinds of grafts. This observation is in general agreement with the MTT assay results presented in Figure 4.18. It is difficult to assess the uniformity of the cell distribution in any given viewing area, but it is clear from Figure 4.22 that there are no fluorescent shapeless unidentified blue spots that make the overall assessment more difficult to accomplish.

Figure 4.23 provides a series of transverse views of the four prototype samples after cell culture for 7 days with endothelial cells. In contrast to the uniform cell distribution across the luminal surface as observed with the knitted(outside)/electrospun(inside)/ impregnated grafts (Figure 4. 19), the transverse view through the thickness of the sample in the z direction shows that the viable cells follow a wave formation, which reflects the shape of the weft knitted fabric (Figure 4.23 a). In Figure 4.23 b) and c), we can also see some unidentified blue spots (identified by arrows) in the cross sectional view of the knitted(inside)/electrospun(outside)/impregnated graft and the single layer knitted/ impregnated graft. The transverse view through the section of the knitted (inside)/

electrospun(outside)/ non-impregnated graft also has a wavy shaped cell distribution, indicating the tendency for cell proliferation to follow the curvature of the knitted structure (Figure 4.23 d). However, the wavy shape in this case is less distinct. Note that the overall scanned depth of the cell seeded graft fabrics was different for the different samples, which reflected the different thicknesses of the monolayer and bilayer graft walls. The overall depth of cell growth and proliferation were approximately 120, 300, 350, and 250 μm for the four graft samples respectively. As previously indicated in Table 4.2, the wall thicknesses of the monolayer and bilayer grafts are approximately 300 μm and 330 μm respectively. It is evident that the endothelial cells did not proliferate through the electrospun layer on the inner surface of the graft, and the depth of 120 μm is likely due to the curvature of the graft surface. While it was observed in the grafts with an inner knitted layer, regardless of whether the collagen/elastin had been added or not, the depth measurements indicate that the cells grew through the knitted layer but were stopped and failed to penetrate the electrospun layer. Clearly, the existence of an electospun outer layer or inner layer limited the depth of cell penetration, compared with the graft sample made with a single layer knitted construction with no electrospun layer.

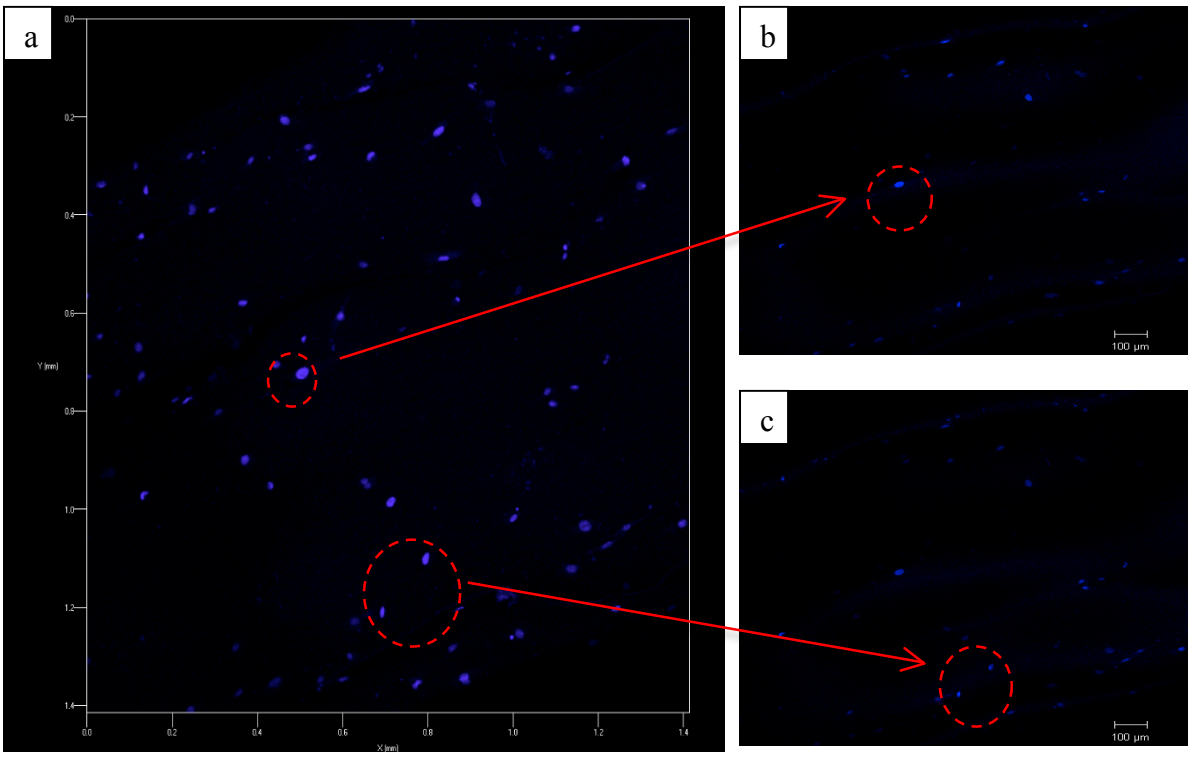

Figure 4. 19 LSCM images of DAPI stained cells seeded on the inner lumen of the knitted (outside)/electrospun (inside)/impregnated vascular graft at Day 7. The cell nuclei appear blue. (a) 3D image of cell distribution through entire thickness of the graft in the x, y plane (Magnification: 10×). (b) and (c) 2D images of cell distribution at two different levels through the thickness in the vertical plane (Magnification: 10×)

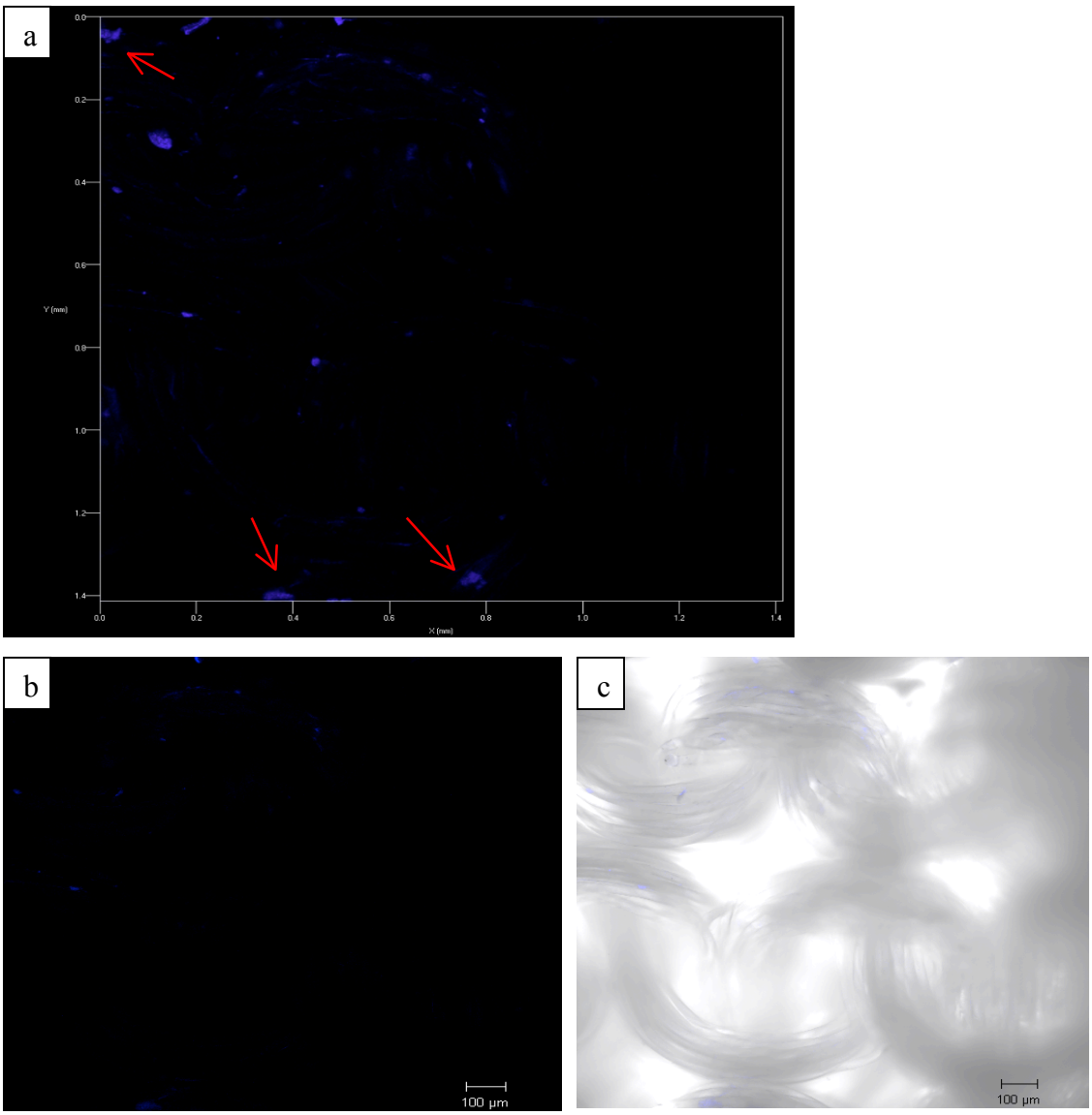

Figure 4. 20 LSCM images of DAPI stained cells seeded on the lumen of the knitted (inside)/electrospun (outside)/impregnated vascular graft at Day 7. The cell nuclei appear blue. (a) 3D image of cell distribution through the entire thickness of the graft in the x, y plane (Magnification: 10×) (Arrows indicate the abnormal spots). (b) 2D image of cell distribution in one vertical plane through the thickness (Magnification: 10×). (c) 2D image of cell distribution on the knitted structure in the same vertical plane as (b) after gamma correction (Magnification: 10×).

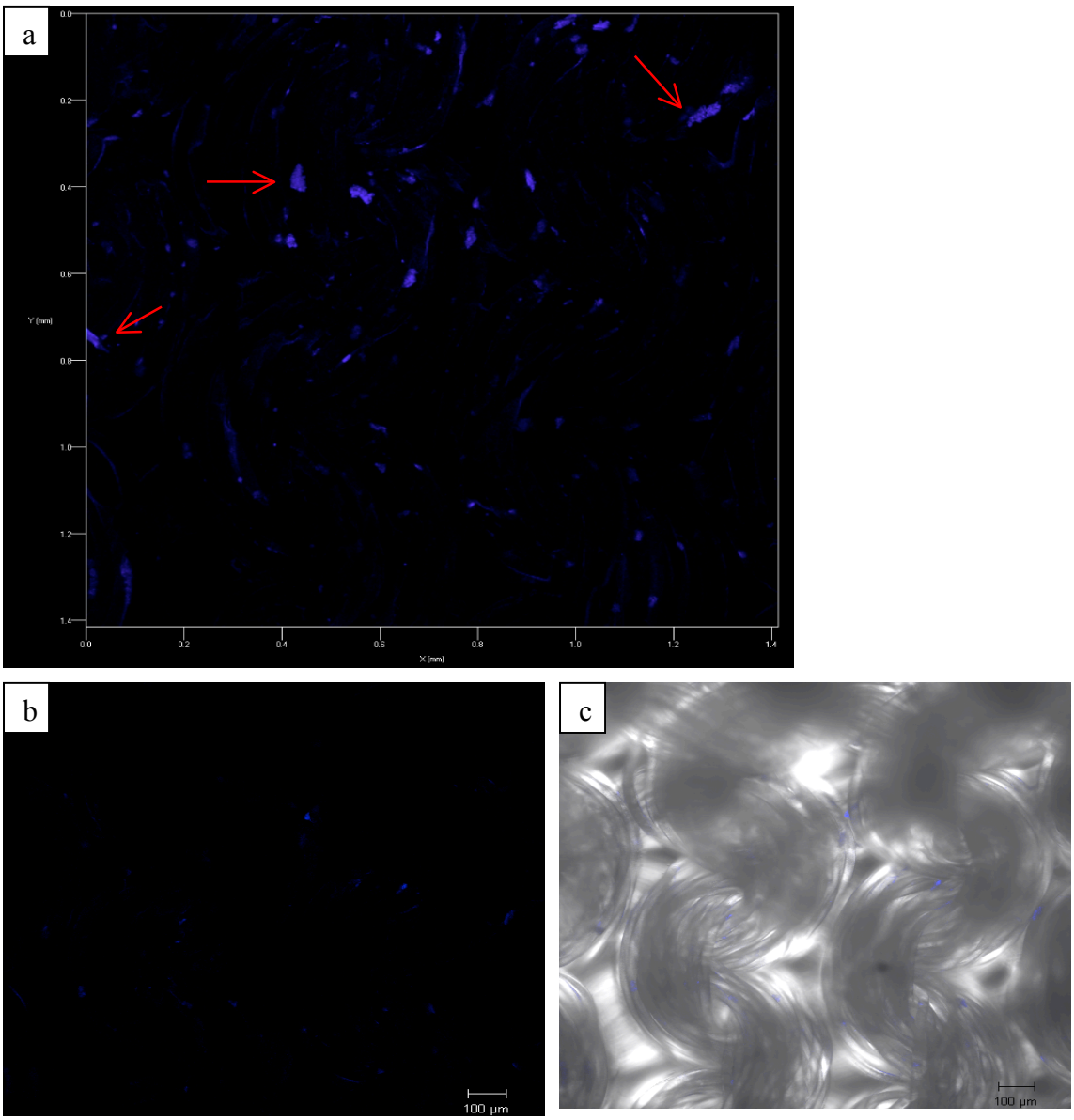

Figure 4. 21 LSCM images of DAPI stained cells seeded on the lumen of knitted /impregnated vascular graft at Day 7. The cell nuclei appear blue. (a) Image of cell distribution through the entire thickness of the graft in the x, y plane (Magnification: 10×) (arrows indicate the abnormal spots). (b) 2D image of cell distribution in one vertical plane through the thickness (Magnification: 10×). (c) 2D image of cell distribution on the knitted structure in the same vertical plane as (b) after gamma correction (Magnification: 10×).

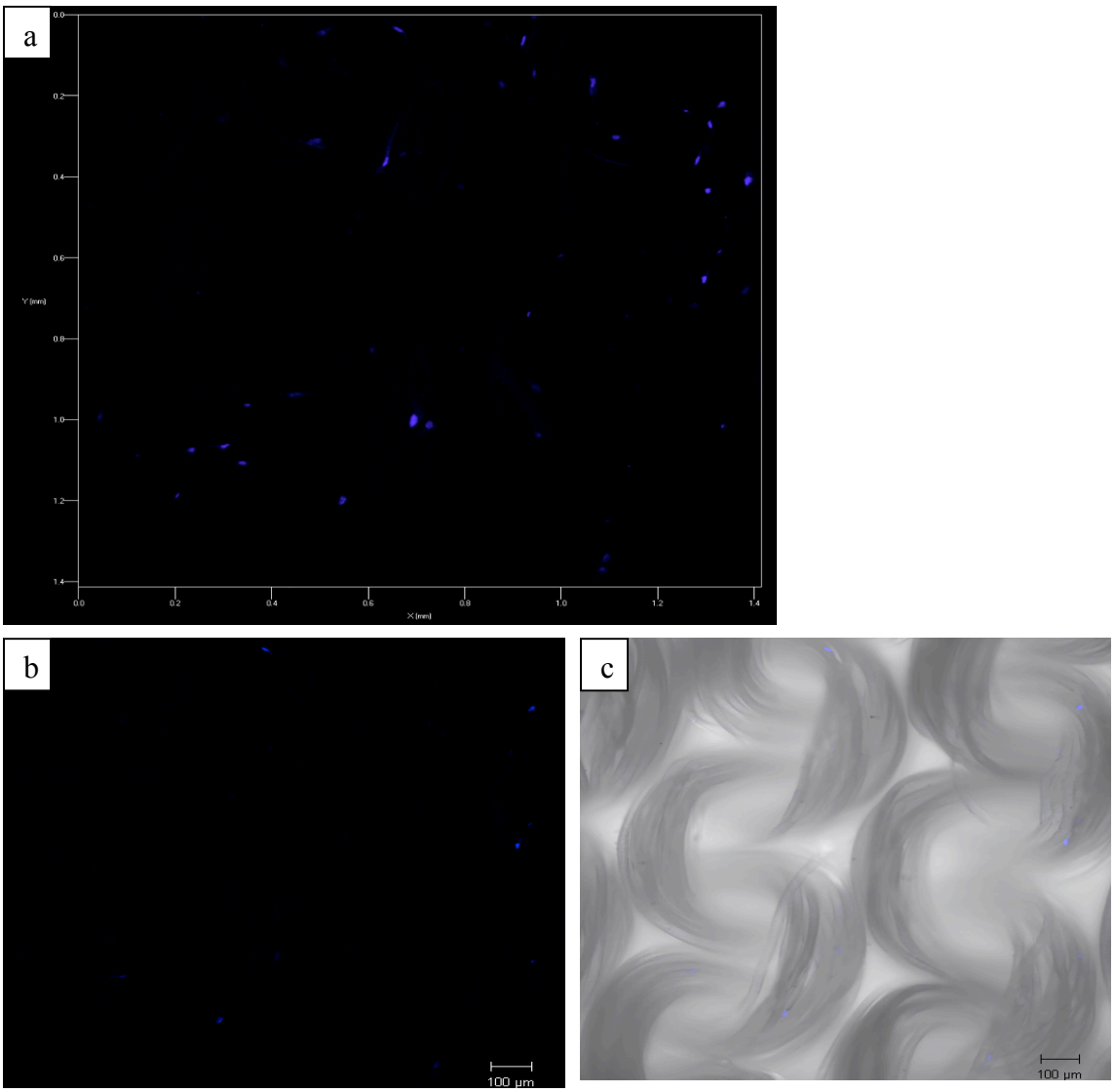

Figure 4. 22 LSCM images of DAPI stained cells seeded on the lumen of the non impregnated knitted (inside) /electrospun (outside) vascular graft at Day 7. The cell nuclei appear blue. (a) Image of cell distribution through the entire thickness of the graft in the x, y plane (Magnification: 10×). (b) 2D image of cell distribution in one vertical plane through the thickness (Magnification: 10×). (c) 2D image of cell distribution on the knitted structure in the same vertical plane as (b) after gamma correction (Magnification: 10×).

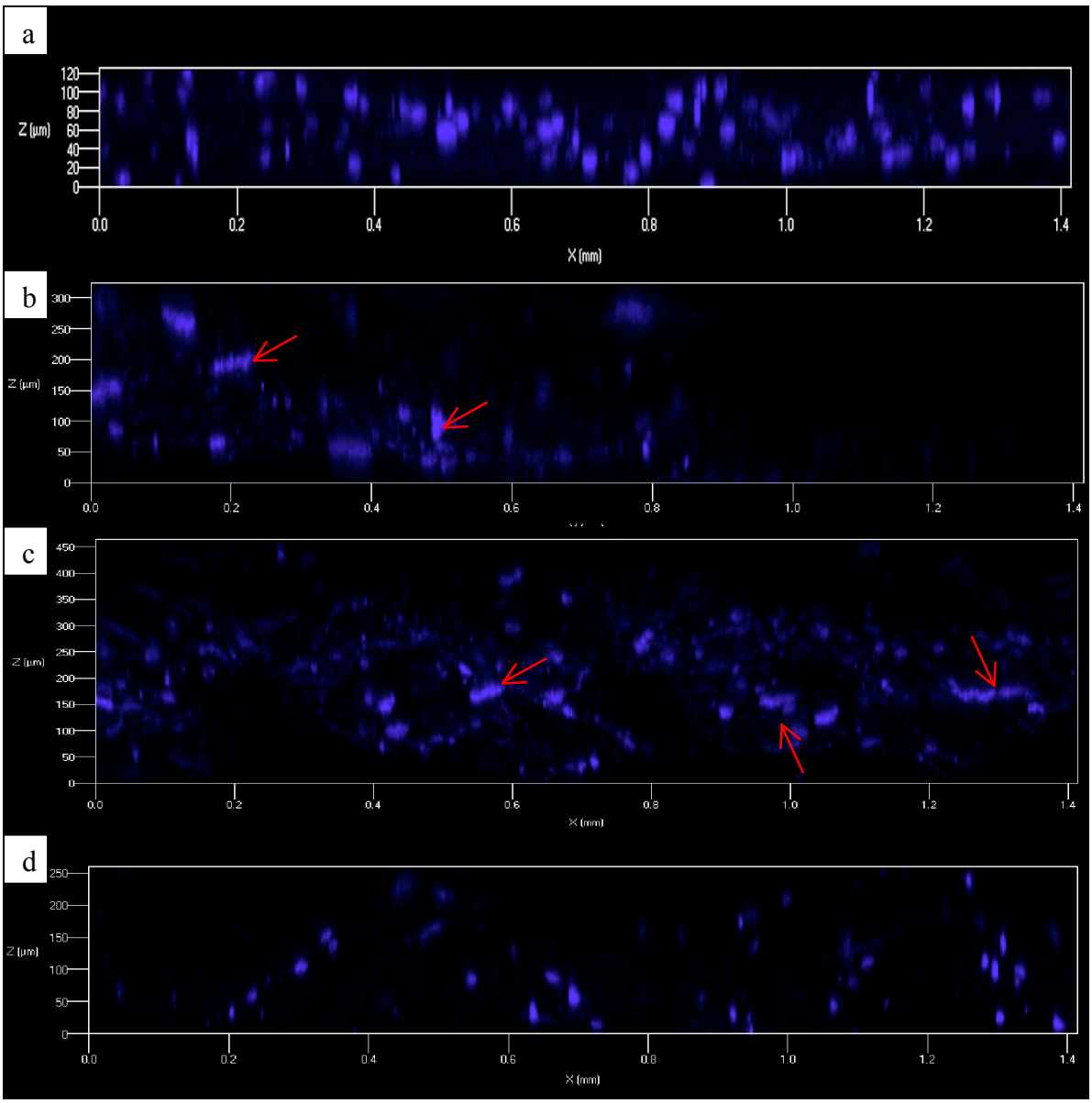

Figure 4. 23 LSCM images showing the proliferation of DAPI stained cells at Day 7 along the thickness of the four different prototype grafts in transverse view. The cell nuclei appear in blue. (a) Knitted (outside)/electrospun (inside)/impregnated graft (Magnification: 10×); (b) Knitted (inside)/electrospun (outside)/impregnated graft (10×) (arrows indicate the abnormal spots); (c) Knitted /impregnated graft (10×) (arrows indicate the abnormal spots); (d) Non-impregnated knitted (inside)/electrospun (outside) graft (10×).

4.4.3 Cell Morphology and Attachment by SEM

To characterize the level of cell attachment and to observe the cell morphology after attachment, scanning electron microscopy (SEM) was used to capture the surface appearance of the graft samples after cell culture for 7 days at 500× and 1000× magnification. The SEM micrographs show the endothelial cells spread out and flattened onto the electrospun surface. Some are displaying pseudopodia and probing the relatively flat surface, which suggests a positive actin fiber response (Figure 4.24) (Malek & Izumo, 1996). Additionally, we can see from Figure 4.24, some fusing or degradation occurring at the surface probably caused by the collagen/elastin impregnation. Figure 4.25 illustrates cell attachment on collagen/elastin coated PLA multifilament fibers in the knitted structure. With these micrographs, it is much harder to distinguish between the cells and the coating. Even so, it is possible to identify some aggregation or clusters of cells attached to different filaments. In contrast, there are more confirmed cell aggregates or clusters on the PLA filaments without an impregnation or a coating in Figure 4.26. It is undoubtedly possible for endothelial cells to attach and proliferate on both electrospun PLCL membranes and weft knitted PLA structures. However, in this study the observable number of viable cells are consistent with the observations by LSCM, namely, that endothelial cells are not able to grow and proliferate rapidly and generate a large cell population within 7 days of cell culture, indicating that longer culture periods may be necessary for better characterization in the future.

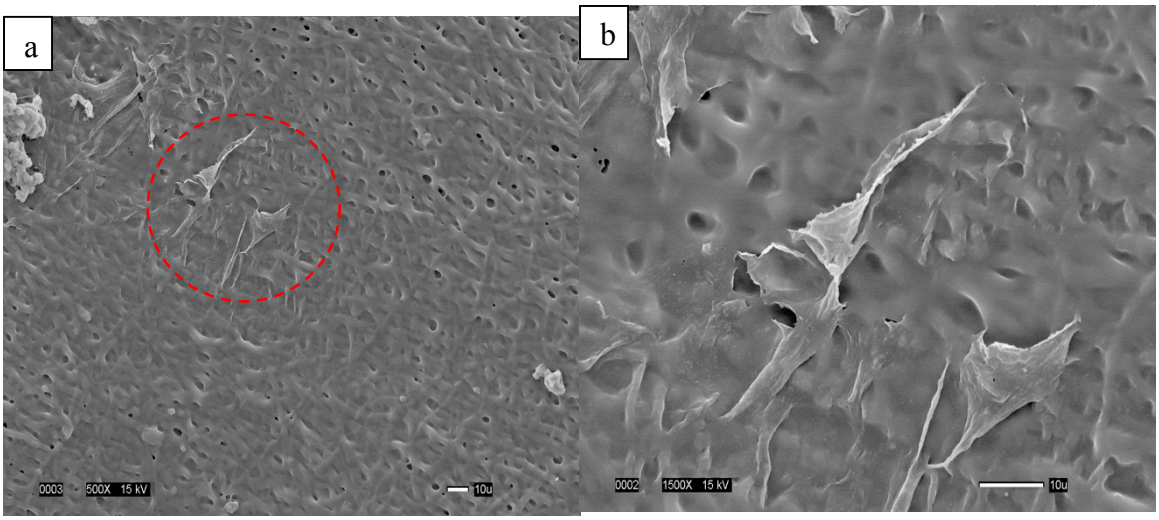

Figure 4. 24 SEM micrographs of cells cultured on the collagen/elastin impregnated PLCL electrospun layer for 7 days. (a) Cell attachment and morphology under low magnification (500×). (b) Cell attachment and morphology under high magnification (1000×).

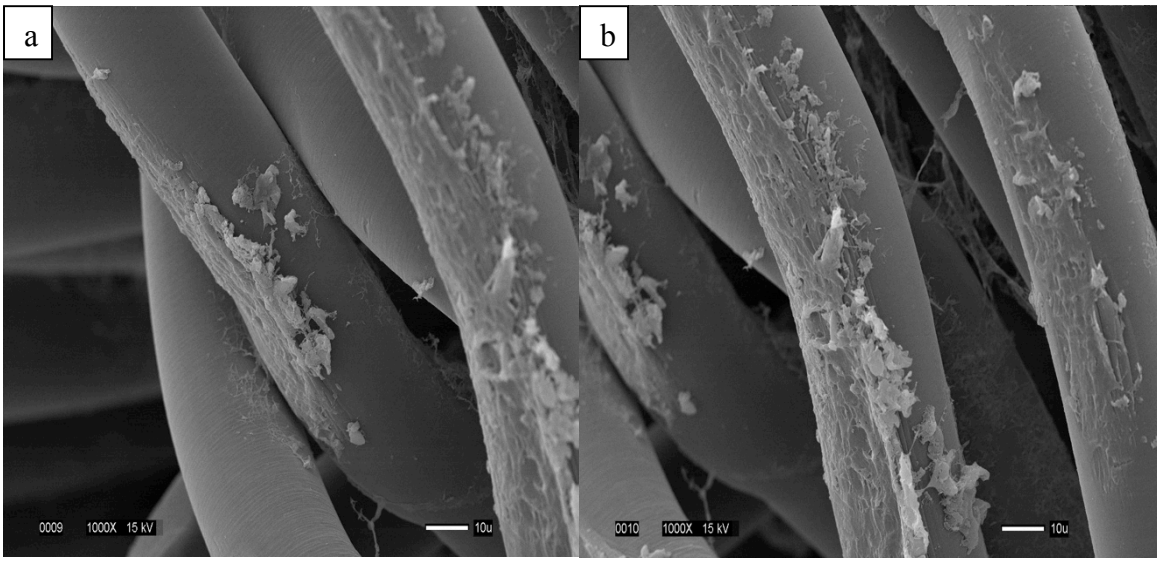

Figure 4. 25 SEM micrographs of cells cultured on the collagen/elastin impregnated PLA weft knitted structure for 7 days. (a) and (b) Cell attachment to different filaments under high magnification (1000×).

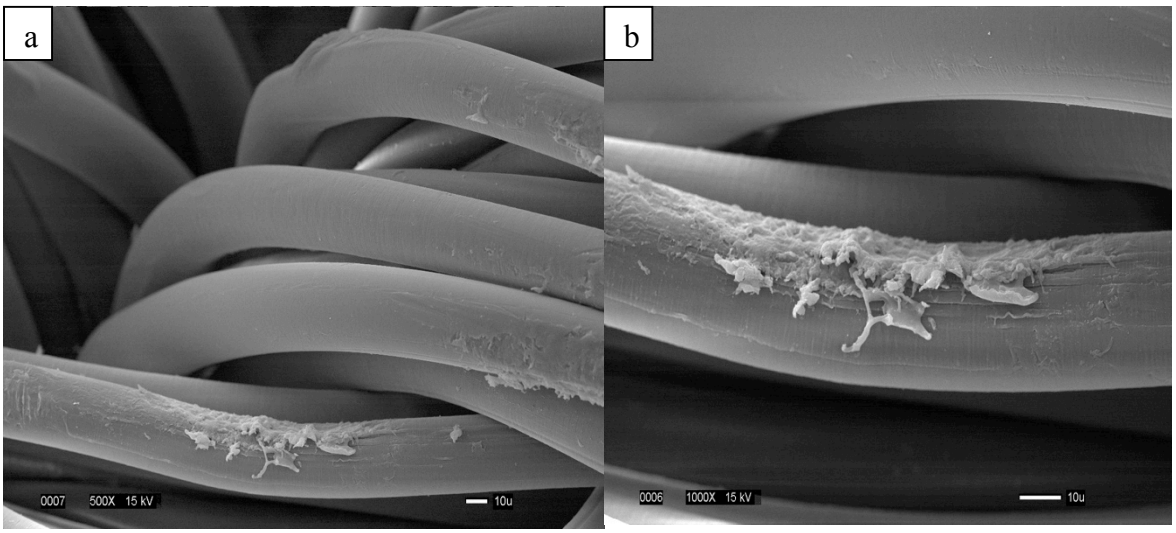

Figure 4. 26 SEM micrographs of cells cultured on PLA filaments without any coating for 7 days. (a) Cell attachment under low magnification (500×). (b) Cell attachment under high magnification (1000×).

CHAPTER 5

CONCLUSIONS AND FUTURE WORK

5.1 Conclusions

In summary, a bilayer small diameter prosthesis with an inner layer of electrospun fibers and an outside weft knitted structure was successfully fabricated so as to achieve the first goal of this study. In addition, the mechanical and biological performance of this bilayer structure achieved a satisfactory performance.

First of all, in the fabrication stage, the use of weft knitting technology is feasible for small diameter vascular grafts because it enables direct fabrication of a tubular structure without the need for a seam. The diameter of the tube can be adjusted according to the number and spacing (gauge) of the needles and the tensions applied to the feed yarn and the fabric takedown. These parameters can also control the loop length and hence the pore size, which can be stabilized by heat setting.

During electrospinning the tubular weft knitted fabric was fitted tightly onto a high speed rotating mandrel, so that the PLA knitted surface served as the collector for a thin PLCL electrospun web. This process was successful in providing adequate attachment and adherence between the knitted and electrospun layers. In fact the manual procedure of turning the bilayer structure inside out using a needle and thread ensured that the attachment between the two layers was maintained. In addition, the bilayer graft with the knitted(outside)/electrospun(inside) structure demonstrated that endothelial cells could attach

and proliferate on the inner lumen of graft. Viewing under SEM confirmed that the collagen/elastin mixture was successfully impregnated into the structure and penetrated between the PLA filaments and the PLCL electrospun fibers, followed by efficient crosslinking with genipin.

The second objective was to investigate the mechanical performance of the prototype samples and to determine whether the additional electrospun layer or the collagen/elastin impregnation could improve the mechanical properties of the cardiovascular prostheses in terms of their circumferential tensile strength, bursting strength, compliance and suture retention strength. Both the addition of an electrospun layer and the impregnation procedure generated an increase in circumferential tensile stress to a value as high as 12.95 ±1.14MPa. However this tensile stress saw a marginal drop to 11.05±0.89MPa when the two-layer structure was turned inside out ($p \leq 0.05$). Compared with two layer electrospun grafts, the single knitted layer, whether impregnated or not, maintained a higher circumferential strain. In addition, no improvement in the strength of the grafts was observed as a result of collagen/elastin impregnation.

Similarly, the bursting strength of either the two-layer electrospun or the impregnated sample or both was at least 0.5 MPa higher than the bursting strength of the non-impregnated single layer knitted graft ($p \leq 0.05$). And in a similar manner for the suture retention performance, the force applied to the two layer grafts in order to break the suture was at least 14 N higher than that for the non-impregnated single layer knitted graft ($p \leq 0.05$). What is more, the suture retention test results revealed that the raveling problem associated with weft knitted

structures has been reduced to a large extent by either adding a thin electrospun layer or by applying the collagen/elastin impregnation process.

With respect to graft compliance, the existence of an additional elastomeric electrospun layer did not increase the compliance of the bilayer graft. In fact with increased internal pressure the diameter expansion of the graft with the electrospun layer was observed to be more limited. But, it improved significantly when the electrospun layer was turned inside. By applying the collagen/elastin impregnation, the compliance of the grafts improved significantly at the two lower pressure ranges. Having said that, it is clear that significant improvements are still needed in the future so that the compliance of a small diameter vascular prosthesis can mimic more closely that of a native artery.

Last but not least, the essential biological performance of the graft samples included their thrombogenicity, *in vitro* viability, cell attachment and proliferation. For thrombogenicity, collagen/elastin impregnation has been shown to be an effective way to minimize thrombus formation, and so is a promising strategy to improve the thromboresistance of small diameter vessels. And based on our experimental results, the non-impregnated graft has the tendency to generate a thrombus in a comparatively short time. Endothelial cell attachment and growth on the PLCL electrospun layer showed a preference for proliferating as a monolayer with a more uniform distribution. Also, the weft knitted layer provided the pattern and structure to promote cell proliferation and migration through the thickness of the fabric, resulting in a multilayer cell population. However, during the short 7-day culture period, no significant improvement in cell growth was observed with the collagen/elastin impregnation of the grafts.

Therefore, the inclusion of a second PLCL electrospun layer could improve circumferential tensile strength, bursting stress, and suture retention strength, but limited the compliance for bilayer small diameter vascular grafts. The procedure of turning the bilayer tubular structure inside out, while improving the suture retention strength and compliance did not significantly reduce the mechanical properties of the prototype vascular grafts. And it promoted a more uniform monolayer of endothelial cell proliferation on the electrospun layer inside graft. The impregnated collagen/elastin protein coating with genipin crosslinking was found to be able to improve mechanical properties excluding circumferential tensile strength and to reduce the thrombogenicity of the graft.

5.2 Future Work

According to the results and the limitations of this study, there are several recommendations in terms of graft design and the experimental design that need to be considered for further investigation of small diameter vascular grafts.

To enhance their performance mechanically and biologically, future work should focus on:

1) Designing an electrospun layer with aligned fibers. Based on the literature review of electrospinning techniques for vascular substitutes, we plan to produce a bilayer graft with an aligned electrospun layer of fibers oriented in the axial direction for better guidance of endothelial cells so they can proliferate axially along the inner lumen of the graft.

2) Activate the PLA knitted graft surface so as to immobilize by covalent bonding the

collagen/elastin protein mixture rather than impregnating it on the surface. SEM and LSCM imaging indicated that significant amounts of residual "contaminants" were present after impregnation and crosslinking, which are likely to have had a negative impact on the experimental results. PLA has some limitations for cell growth. For instance, it has an inert hydrophobic surface and so is difficult to attach reactive groups and proteins like collagen/elastin. However, the PLA surface can be activated by UV light and radio frequency plasma so as to increase the feasibility of surface modification, graft polymerization and protein immobilization.

3) Apply a suitable adhesive for better attachment between the two layers of the graft. We have observed a tendency for the two different structural layers, the electrospun layer and the weft knitted layer, to separate, particularly during the inside out turning procedure, and then subsequently during implantation this may become problematic. Therefore a suitable biosafe adhesive, such as a tissue adhesive, may facilitate the two layers achieving greater adhesion.

4) Seed endothelial cells on the lumen of the vascular grafts and then culture them in a bioreactor. a confluent layer of endothelial cells is essential to ensure a non-thrombogenic surface that will promote revascularization. Seeded endothelial cells as a component of a vascular substitute will minimize thrombus formation and extend patency.

To improve the characterization methods and complete a comprehensive vascular graft study according to the ISO standard, future work should include the following studies:

1) Live/dead viability assay is planned to investigate the number of live and dead cells growing and proliferating on the graft after different periods of *in vitro* culture. Live cells appear green, while dead cells are red under fluorescence microscopy after staining with a DAPI live/dead assay. Additionally, we plan to culture smooth muscle cells (SMCs) on the outer layer, so as to determine whether the weft knitted structure with its circumferential pattern is able to promote circumferentially oriented cell growth and improve radial compliance. This may involve co-culturing two different cell lines simultaneously.

2) *In vivo* animal studies and clinical trials are most important and essential to evaluate the clinical capability of new and novel vascular prostheses in terms of handling and implantation, healing, tissue regeneration and the maintenance of physiologic function in the circulatory system. When undertaking such *in vivo* trials it is important to determine the healing response of the host to the prosthesis as well as the material and structural response of the prosthesis to the host's biological environment. The assessment of patency and prosthesis explant pathology need to be included in the studies.

REFERENCES

Aldenhoff, Y. B., van der Veen, F. H., Woorst, J., Habets, J., Poole–Warren, L. A., & Koole, L. H. (2001). Performance of a polyurethane vascular prosthesis carrying a dipyridamole (Persantin®) coating on its lumenal surface. *Journal of Biomedical Materials Rresearch, 54*(2), 224-233.

Almine, J. F., Bax, D. V., Mithieux, S. M., Nivison-Smith, L., Rnjak, J., Waterhouse, A., ... & Weiss, A. S. (2010). Elastin-based materials. *Chemical Society Reviews, 39*(9), 3371-3379.

Alobaid, N., Salacinski, H. J., Sales, K. M., Hamilton, G., & Seifalian, A. M. (2005). Single stage cell seeding of small diameter prosthetic cardiovascular grafts. *Clinical Hemorheology and Microcirculation, 33*(3), 209-226.

Anderson, J.L., Adams, C.D., Antman, E.M., Bridges, C.R., Califf, R.M., Casey, D.E., … Wright, R.S. (2011). 2011 ACCF/AHA focused update incorporated into the ACC/AHA 2007 guidelines for the management of patients with unstable angina/non-ST elevation myocardial infarction. *Journal of the American College of Cardiology, 123*, e426-e579

Baudis, S., Ligon, S. C., Seidler, K., Weigel, G., Grasl, C., Bergmeister, H., ... & Liska, R. (2012). Hard-block degradable thermoplastic urethane-elastomers for electrospun vascular prostheses. *Journal of Polymer Science Part A: Polymer Chemistry, 50*(7), 1272-1280.

Bi, L., Cao, Z., Hu, Y., Song, Y., Yu, L., Yang, B., ... & Han, Y. (2011). Effects of different cross-linking conditions on the properties of genipin-cross-linked chitosan/collagen scaffolds for cartilage tissue engineering. *Journal of Materials Science: Materials in Medicine, 22*(1), 51-62.

Bian, W., Li, D., Lian, Q., Li, X., Zhang, W., Wang, K., & Jin, Z. (2012). Fabrication of a bio-inspired beta-tricalcium phosphate/collagen scaffold based on ceramic stereolithography and gel casting for osteochondral tissue engineering. *Rapid Prototyping Journal, 18*(1), 68-80.

Boccafoschi, F., Habermehl, J., Vesentini, S., & Mantovani, D. (2005). Biological performances of collagen-based scaffolds for vascular tissue engineering. *Biomaterials, 26(*35), 7410-7417.

Bosiers, M., Deloose, K., Verbist, J., Schroë, H., Lauwers, G., Lansink, W., & Peeters, P. (2006). Heparin-bonded expanded polytetrafluoroethylene vascular graft for femoropopliteal and femorocrural bypass grafting: 1-year results. *Journal of Vascular Surgery, 43*(2), 313-318.

Buttafoco, L., Boks, N. P., Engbers-Buijtenhuijs, P., Grijpma, D. W., Poot, A. A., Dijkstra, P. J., ... & Feijen, J. (2006). Porous hybrid structures based on P(DLLA-co-TMC) and collagen for tissue engineering of small-diameter blood vessels. *Journal of Biomedical Materials Research Part B: Applied Biomaterials, 79*(2), 425-434.

Caves, J. M., Kumar, V. A., Wen, J., Cui, W., Martinez, A., Apkarian, R., ... & Chaikof, E. L. (2010). Fibrillogenesis in continuously spun synthetic collagen fiber. *Journal of Biomedical Materials Research Part B: Applied Biomaterials, 93*(1), 24-38.

Cen, L., Liu, W., Cui, L., Zhang, W., & Cao, Y. (2008). Collagen tissue engineering: development of novel biomaterials and applications. *Pediatric Research, 63*(5), 492-496.

Chang, Y., Tsai, C. C., Liang, H. C., & Sung, H. W. (2001). Reconstruction of the right ventricular outflow tract with a bovine jugular vein graft fixed with a naturally occurring crosslinking agent (genipin) in a canine model. *The Journal of Thoracic and Cardiovascular Surgery, 122*(6), 1208-1218.

Chong, M.S., Lee, C.N., & Teoh, S.H. (2007) Characterization of smooth muscle cells on poly(epsilon-caprolactone) films. *Materials Science and Engineering C, 27*, 309–312.

Chlupac, J., Filova, E., Bacakova, L. (2009). Blood vessel replacement: 50 years of development and tissue engineering paradigms in vascular surgery. *Physiological Research, 58*, 119-139.

Chung, S., Moghe, A.K., Montero, G.A., Kim, S.H., & King, M.W. (2009). Nanofibrous scaffolds electrospun from elastomeric biogradable poly (L-lactide-co--caprolactone) copolymer. *Biomedical Materials, 4*: doi015019

Chung, S., Ingle, N.P., Montero, G.A., Kim, S.H., & King, M.W. (2010). Bioresorbable elastomeric vascular tissue engineering scaffold via melt spinning and electrospinning. *Acta Biomaterialia, 6*, 1958-1967.

Chvapil, M. (1977). Collagen sponge: theory and practice of medical applications. *Journal of Biomedical Materials Research, 11*(5), 721-741.

Cleland, J. L., Duenas, E. T., Park, A., Daugherty, A., Kahn, J., Kowalski, J., & Cuthbertson, A. (2001). Development of poly-(D, L-lactide–coglycolide) microsphere formulations containing recombinant human vascular endothelial growth factor to promote local angiogenesis. *Journal of Controlled Release, 72*(1), 13-24.

Daamen, W. F., Van Moerkerk, H. T. B., Hafmans, T., Buttafoco, L., Poot, A. A., Veerkamp, J. H., & Van Kuppevelt, T. H. (2003). Preparation and evaluation of molecularly-defined collagen–elastin–glycosaminoglycan scaffolds for tissue engineering. *Biomaterials, 24*(22), 4001-4009.

Deutsch, M., Meinhart, J., Zilla, P., Howanietz, N., Gorlitzer, M., Froeschl, A., ... & Grabenwoeger, M. (2009). Long-term experience in autologous in vitro endothelialization of infrainguinal ePTFE grafts. *Journal of Vascular Surgery, 49*(2), 352-362.

DeRosa, K. E., Siriwardane, M. L., & Pfister, B. J. (2011, April). Design and characterization of a controlled wet spinning device for collagen fiber fabrication for neural tissue

engineering. In Bioengineering Conference (NEBEC), 2011 IEEE 37th Annual Northeast (pp. 1-2). Troy, NY.

De Valence, S., Tille, J. C., Giliberto, J. P., Mrowczynski, W., Gurny, R., Walpoth, B. H., & Möller, M. (2012). Advantages of bilayered vascular grafts for surgical applicability and tissue regeneration. *Acta Biomaterialia, 8*(11), 3914-3920.

Dodge, J. T., Brown, B. G., Bolson, E.L., & Dodge, H. T. (1992). Lumen diameter of normal human coronary arteries: Influence of age, sex, anatomic variation, and left ventricular hypertrophy or dilation. *Circulation, 86*, 232-246.

Donahue, S. M., & Otto, C. M. (2005). Thromboelastography: a tool for measuring hypercoagulability, hypocoagulability, and fibrinolysis. *Journal of Veterinary Emergency and Critical Care, 15*(1), 9-16.

Engelberg, I., & Kohn, J. (1991). Physico-mechanical properties of degradable polymers used in medical applications: a comparative study. *Biomaterials, 12*(3), 292-304.

Enomoto, S., Sumi, M., Kajimoto, K., Nakazawa, Y., Takahashi, R., Takabayashi, C., ... & Sata, M. (2010). Long-term patency of small-diameter vascular graft made from fibroin, a silk-based biodegradable material. *Journal of Vascular Surgery, 51*(1), 155-164.

Fleser, P. S., Nuthakki, V. K., Malinzak, L. E., Callahan, R. E., Seymour, M. L., Reynolds, M. M., ... & Shanley, C. J. (2004). Nitric oxide–releasing biopolymers inhibit thrombus

formation in a sheep model of arteriovenous bridge grafts. *Journal of Vascular Surgery, 40*(4), 803-811.

Fox, S. I. (1993). *Human Physiology*. 4th ed. Dubuque, Iowa: W.C. Brown.

Fowkes, F. G. R., Rudan, D., Rudan, I., Aboyans, V., Denenberg, J. O., McDermott, M. M., ... & Criqui, M. H. (2013). Comparison of global estimates of prevalence and risk factors for peripheral artery disease in 2000 and 2010: a systematic review and analysis. *The Lancet, 382*(9901), 1329-1340.

Fuh, Y. K., Chen, S., & Jang, J. S. (2012). Direct-write, well-aligned chitosan-poly (ethylene oxide) nanofibers deposited via near-field electrospinning. *Journal of Macromolecular Science, Part A, 49*(10), 845-850.

Gelse, K., Pöschl, E., & Aigner, T. (2003). Collagens—structure, function, and biosynthesis. *Advanced Drug Delivery Reviews, 55*(12), 1531-1546.

Goissis, G., Marcantonio , E., Marcantônio, R. A. C., Lia, R. C. C., Cancian, D. C., & Carvalho, W. M. D. (1999). Biocompatibility studies of anionic collagen membranes with different degree of glutaraldehyde cross-linking. *Biomaterials, 20*(1), 27-34.

Greisler, H. P., Endean, E. D., Klosak, J. J., Ellinger, J., Dennis, J. W., Buttle, K., & Kim, D.U. (1988). Polyglactin 910/polydioxanone bicomponent totally resorbable vascular prostheses. *Journal of Vascular Ssurgery, 7*(5), 697-705.

Greisler, H.P., Tattersall, C.W., Henderson, S.C., Cabusao, E.A., Garfield, J.D., Kim, D.U. (1992). Polypropylene small-diameter vascular grafts. *Journal of Biomedical Material Research, 26*, 1383–1394.

Grijpma, D. W., Zondervan, G.J., & Pennings, A.J.(1991). High molecular weight copolymers of L-lactide and ε- caprolactone as biodegradable elastomeric implant materials. *Polymer Bulletin, 25*(3), 327-333.

Heise, M., Schmidmaier, G., Husmann, I., Heidenhain, C., Schmidt, J., Neuhaus, P., & Settmacher, U. (2006). PEG-hirudin/iloprost coating of small diameter ePTFE grafts effectively prevents pseudointima and intimal hyperplasia development. *European Journal of Vascular and Endovascular Surgery, 32*(4), 418-424.

Hernandez, L. (2010). An overview of PCI vs CABG for Severe Coronary Artery Disease. Missouri State University. n.d. Retrieved from: http://www.cvr.ir/articles/surgery/An%20overview%20of%20PCI%20vs%20CABG%20for%20Severe%20Coronary%20Artery%20Disease.pdf

Hirsch, A. T., Haskal, Z. J., Hertzer, N. R., Bakal, C. W., Creager, M. A., Halperin, J. L., ... & Riegel, B. (2006). ACC/AHA 2005 guidelines for the management of patients with peripheral arterial disease (lower extremity, renal, mesenteric, and abdominal aortic). *Journal of the American College of Cardiology, 47*(6), e1-e192.

Hoffman Jr, H., &Schankereli, K. (1992). U.S. Patent No. 5,108,424. Washington, DC: U.S. Patent and Trademark Office.

How, T. V. (1992). Mechanical properties of arteries and arterial grafts. *Cardiovascular biomaterials*, 1-35, Springer London.

Huang, C., Geng, X., Qinfei, K., Xiumei, M., Al-Deyab, S. S., & El-Newehy, M. (2012). Preparation of composite tubular grafts for vascular repair via electrospinning. *Progress in Natural Science: Materials International, 22*(2), 108-114.

Inoguchi, H., Kwon, I.K., Inoue, E., Takamizawa, K., Maehara, Y., & Matsuda, T. (2006). Mechanical responses of a compliant electrospun poly(L-lactide-co-ε-caprolactone) small-diameter vascular graft. *Biomaterials, 27*(8), 1470-1478.

Institute of Medicine (US) Committee. (2010). *Promoting Cardiovascular Health in the Developing World: A Critical Challenge to Achieve Global Health.* Fuster, V., & Kelly, B.B. (Eds.). Washington, DC: National Academic Press.

Izhar, U., Schwalb, H., Borman, J. B., Hellener, G. R., Hotoveli-Salomon, A., Marom, G., ... & Cohn, D. (2001). Novel synthetic selectively degradable vascular prostheses: a preliminary implantation study. *Journal of Surgical Research, 95*(2), 152-160.

Jamshidian, M., Tehrany, E. A., Imran, M., Jacquot, M., & Desobry, S. (2010). Polylactic acid: production, applications, nanocomposites, and release studies. *Comprehensive Reviews in Food Science and Food Safety, 9*(5), 552-571.

Jeong, S.I., Kim, B.S., Kang, S.W., Kwon, J.H., Lee, Y.M., Kim, S.H., & Kim, Y.H. (2004). In vivo biocompatibilty and degradation behavior of elastic poly(l-lactide-co-ε-caprolactone) scaffolds. *Biomaterials, 25*, 5939–5946.

Johns Hopkins Medicine. (n.d. (a)). Coronary artery disease (ischemic heart disease). Retrieved from http://www.hopkinsmedicine.org/heart_vascular_institute/conditions_treatments/conditions/coronary_artery.html

Johns Hopkins Medicine. (n.d. (b)). Percutaneous Coronary Intervention (PCI), Coronary Angioplasty, and Stent Placement. Retrieved from http://www.hopkinsmedicine.org/healthlibrary/test_procedures/cardiovascular/percutaneous_transluminal_coronary_angioplasty_ptca_and_stent_placement_92,P07981/

Jordan, S. W., & Chaikof, E. L. (2007). Novel thromboresistant materials. *Journal of Vascular Surgery, 45*(6), A104-A115.

Jun, H. W., Taite, L. J., & West, J. L. (2005). Nitric oxide-producing polyurethanes. *Biomacromolecules, 6*(2), 838-844.

Jung, Y., Kim, S.H., You, H.J., Kim S.H., Ha Kim Y., Min B.G. (2008). Application of an elastic biodegradable poly(L-lactide-co-e-caprolactone) scaffold for cartilage tissue regeneration. *Journal of Biomaterial Science Polymer,19*, 1073–85.

Kalyanasundaram, A. (April 5, 2012). "Comparison of Revascularization Procedures in Coronary Artery Disease". Drugs, Diseases, and Procedures. Medscape. Retrieved from http://emedicine.medscape.com/article/164682-overview#a1

Kannan, R. Y., Salacinski, H. J., Butler, P. E., Hamilton, G., & Seifalian, A. M. (2005). Current status of prosthetic bypass grafts: a review. *Journal of Biomedical Materials Research Part B: Applied Biomaterials, 74*(1), 570-581.

Kapadia, M. R., Popowich, D. A., & Kibbe, M. R. (2008). Modified prosthetic vascular conduits. *Circulation, 117*(14), 1873-1882.

Kapfer, X., Meichelboeck, W., & Groegler, F. M. (2006). Comparison of carbon-impregnated and standard ePTFE prostheses in extra-anatomical anterior tibial artery bypass: a prospective randomized multicenter study. *European Journal of Vascular and Endovascular Surgery, 32*(2), 155-168.

King, M. W. (1991). Designing fabrics for blood vessel replacement. *Canadian Textile Journal, 108*(4), 24-30.

King, M. W., Gupta, B.S., & Guidoin, R. (Eds.). (2013). *Biotextiles As Medical Implants.* Cambridge, UK: Woodhead Publishing.

Kong, X., Han, B., Li, H., Liang, Y., Shao, K., & Liu, W. (2012). New biodegradable small-diameter artificial vascular prosthesis: A feasibility study. *Journal of Biomedical Materials Research Part A, 100*(6), 1494-1504.

Konig, G., McAllister, T. N., Dusserre, N., Garrido, S. A., Iyican, C., Marini, A., ... & L'Heureux, N. (2009). Mechanical properties of completely autologous human tissue engineered blood vessels compared to human saphenous vein and mammary artery. *Biomaterials, 30*(8), 1542-1550.

Kowalski, K., Mielicka, E., & Jasińska, I. (2012). Modelling and Analysis of the Circumferential Forces and Susceptibility of Vascular Prostheses to Internal Pressure Changes. *Fibres & Textiles in Eastern Europe,* 87-91.

Krijgsman, B., Seifalian, A. M., Salacinski, H. J., Tai, N. R., Punshon, G., Fuller, B. J., & Hamilton, G. (2002). An assessment of covalent grafting of RGD peptides to the surface of a compliant poly(carbonate-urea) urethane vascular conduit versus conventional biological coatings: its role in enhancing cellular retention. *Tissue Engineering, 8*(4), 673-680.

Kumar, V. A., Caves, J. M., Haller, C. A., Dai, E., Liu, L., Grainger, S., & Chaikof, E. L. (2013). Collagen-based substrates with tunable strength for soft tissue engineering. *Biomaterials Science, 1*(11), 1193-1202.

Kwon, I.K., Kidoaki, S., & Matsuda, T. (2005). Electrospun nano-to microfiber fabrics made of biodegradable copolyesters: structural characteristics, mechanical properties and cell adhesion potential. *Biomaterials, 26*(18), 3929-3939.

Laube, H. R., Duwe, J., Rutsch, W., & Konertz, W. (2000). Clinical experience with autologous endothelial cell–seeded polytetrafluoroethylene coronary artery bypass grafts. *The Journal of Thoracic and Cardiovascular Surgery, 120*(1), 134-141.

Lee, S. H., Kim, B. S., Kim, S. H., Choi, S. W., Jeong, S. I., Kwon, I. K., ... & Kim, Y. H. (2003). Elastic biodegradable poly(glycolide-co-caprolactone) scaffold for tissue engineering. *Journal of Biomedical Materials Research Part A, 66*(1), 29-37.

Lee, S. J., Liu, J., Oh, S. H., Soker, S., Atala, A., & Yoo, J. J. (2008). Development of a composite vascular scaffolding system that withstands physiological vascular conditions. *Biomaterials, 29*(19), 2891-2898.

Li, C., Hill, A., & Imran, M. (2005). In vitro and in vivo studies of ePTFE vascular grafts treated with P15 peptide. *Journal of Biomaterials Science, Polymer Edition, 16*(7), 875-891.

Li, H., Feng, F., Bingham, C. O., & Elisseeff, J. H. (2012). Matrix metalloproteinases and inhibitors in cartilage tissue engineering. *Journal of Tissue Engineering and Regenerative Medicine, 6*(2), 144-154.

Lunt, J. (1998). Large-scale production, properties and commercial applications of polylactic acid polymers. *Polymer Degradation and Stability, 59*(1), 145-152.

Malek, A. M., & Izumo, S. (1996). Mechanism of endothelial cell shape change and cytoskeletal remodeling in response to fluid shear stress. *Journal of Cell Science, 109*(4), 713-726.

Marelli, B., Achilli, M., Alessandrino, A., Freddi, G., Tanzi, M. C., Farè, S., & Mantovani, D. (2012). Collagen-reinforced electrospun silk fibroin tubular construct as small calibre vascular graft. *Macromolecular Bioscience, 12*(11), 1566-1574.

McClure, M. J., Sell, S. A., Simpson, D. G., Walpoth, B. H., & Bowlin, G. L. (2010). A three-layered electrospun matrix to mimic native arterial architecture using polycaprolactone, elastin, and collagen: a preliminary study. *Acta Biomaterialia, 6*(7), 2422-2433.

McClure, M. J., Simpson, D. G., & Bowlin, G. L. (2012). Tri-layered vascular grafts composed of polycaprolactone, elastin, collagen, and silk: Optimization of graft properties. *Journal of the Mechanical Behavior of Biomedical Materials, 10,* 48-61.

Mekhail, M., Wong, K. K. H., Padavan, D. T., Wu, Y., O'Gorman, D. B., & Wan, W. (2011).Genipin-cross-linked electrospun collagen fibers. *Journal of Biomaterials Science, Polymer Edition, 22(*17), 2241-2259.

Memorial Health System.(2009). Femoral Popliteal Bypass Surgery – Patient Guide. Memorial Health System, Colorado Springs, CO., 1-25. Retrieved from http://www.memorialhealthsystem.com/wps/wcm/connect/48ef7500429f678a93b6b3d7c469fd0f/MHS_FemoralPoplitealBypassSurgery_eBook.pdf

Ming-Che, W., Pins, G. D., & Silver, F. H. (1994). Collagen fibres with improved strength for the repair of soft tissue injuries. *Biomaterials, 15*(7), 507-512.

Naghavi, N., de Mel, A., Alavijeh, O. S., Cousins, B. G., & Seifalian, A. M. (2013). Nitric oxide donors for cardiovascular implant applications. *Small, 9*(1), 22-35.

National Heart, Lung, and Blood Institute (NHLBI). 2012. Morbidity & Mortality: 2012 Chart Book on Cardiovascular, Lung, and Blood Diseases. National Institutes of Health, Bethesda, Maryland, US. Retrieved from website: http://www.nhlbi.nih.gov/resources/docs/2012_ChartBook_508.pdf

Nicolas, F. L., & Gagnieu, C. H. (1997). Denatured thiolated collagen: II. Cross-linking by oxidation. *Biomaterials, 18*(11), 815-821.

Niklason, L. E., Abbott, W., Gao, J., Klagges, B., Hirschi, K. K., Ulubayram, K., ... & Langer, R. (2001). Morphologic and mechanical characteristics of engineered bovine arteries. *Journal of Vascular Surgery, 33*(3), 628-638.

Niklason, L. E., Gao, J., Abbott, W. M., Hirschi, K. K., Houser, S., Marini, R., & Langer, R. (1999). Functional arteries grown in vitro. *Science, 284*(5413), 489-493.

Nishibe, T., O'Donnel, S., Pikoulis, E., Rich, N., Okuda, Y., Kumada, T., ... & Yasuda, K. (2001). Effects of fibronectin bonding on healing of high porosity expanded polytetrafluoroethylene grafts in pigs. *The Journal of Cardiovascular Surgery, 42*(5), 667-673.

Norgren, L., Hiatt, W. R., Dormandy, J. A., Nehler, M. R., Harris, K. A., & Fowkes, F. G. R. (2007). Inter-society consensus for the management of peripheral arterial disease (TASC II). *European Journal of Vascular and Endovascular Surgery, 33*(1), S1-S75.

Ou, K. L., Chen, C. S., Lin, L. H., Lu, J. C., Shu, Y. C., Tseng, W. C., ... & Chen, C. C. (2011). Membranes of epitaxial-like packed, super aligned electrospun micron hollow poly (l-lactic acid)(PLLA) fibers. *European Polymer Journal, 47*(5), 882-892.

Pektok, E., Nottelet, B., Tille, J. C., Gurny, R., Kalangos, A., Moeller, M., & Walpoth, B. H. (2008). Degradation and healing characteristics of small-diameter poly(ε-caprolactone) vascular grafts in the rat systemic arterial circulation. *Circulation, 118*(24), 2563-2570.

Ramakrishna, S., Fujihara, K., Teo, W. E., Yong, T., Ma, Z., & Ramaseshan, R. (2006). Electrospun nanofibers: solving global issues. *Materials Today, 9*(3), 40-50.

Ravi, S., & Chaikof, E. L. (2010). Biomaterials for vascular tissue engineering. *Regenerative Medicine, 5*(1), 107-120.

Rotmans, J. I., Heyligers, J. M., Verhagen, H. J., Velema, E., Nagtegaal, M. M., de Kleijn, D. P., ... & Pasterkamp, G. (2005). In vivo cell seeding with anti-CD34 antibodies successfully accelerates endothelialization but stimulates intimal hyperplasia in porcine arteriovenous expanded polytetrafluoroethylene grafts. *Circulation, 112*(1), 12-18.

Seifalian, A. M., Tiwari, A., Hamilton, G., & Salacinski, H. J. (2002). Improving the clinical patency of prosthetic vascular and coronary bypass grafts: the role of seeding and tissue engineering. *Artificial Organs, 26*(4), 307-320.

Shalumon, K. T., Chennazhi, K. P., Nair, S. V., & Jayakumar, R. (2013). Development of small diameter fibrous vascular grafts with outer wall multiscale architecture to improve cell penetration. *Journal of Biomedical Nanotechnology, 9*(7), 1299-1305.

Shum-Tim, D., Stock, U., Hrkach, J., Shinoka, T., Lien, J., Moses, M. A., ... & Mayer Jr, J. E. (1999). Tissue engineering of autologous aorta using a new biodegradable polymer. *The Annals of Thoracic Surgery, 68*(6), 2298-2304.

Siriwardane, M. L., DeRosa, K. E., Collins, G. L., & Pfister, B. J. (2012, March). An in vitro 3-D model of collagen-based fiber constituents for peripheral nerve conduits. Proceedings from : *2012 38th Annual Northeast Bioengineering Conference (NEBEC).*Philadelphia, PA: IEEE.

Song, Y., Feijen, J., Grijpma, D. W., & Poot, A. A. (2011). Tissue engineering of small-diameter vascular grafts: a literature review. *Clinical hemorheology and Microcirculation, 49*(1), 357-374.

Sung, H. W., Chang, Y., Liang, I. L., Chang, W. H., & Chen, Y. C. (2000). Fixation of biological tissues with a naturally occurring crosslinking agent: fixation rate and effects of pH, temperature, and initial fixative concentration. *Journal of Biomedical Materials Research, 52*(1), 77-87.

Taylor, L.M., Edwards, J.M., & Porter, J.M. (1990). Present status of reversed vein bypass grafting: five-year results of a modern series. *Journal of Vascular Surgery, 11*, 193–206.

Thomas, L. V., Lekshmi, V., & Nair, P. D. (2013). Tissue engineered vascular grafts—Preclinical aspects. *International Journal of Cardiology, 167*(4), 1091-1100.

Tuck, S. J., Leach, M. K., Feng, Z. Q., & Corey, J. M. (2012). Critical variables in the alignment of electrospun PLLA nanofibers. *Materials Science and Engineering: C, 32*(7), 1779-1784.

Tura, A. (Eds.). 2003. *Vascular grafts: Experiment and modeling.* Southampton, UK: WIT Press.

Vinila, B. H., Sridevi, N. S., & Kumaraswamy, R. (2013). A study on the internal diameter of femoral artery and level of origin of profunda femoris artery. *International Journal of Biological & Medical Research, 4*(1), 2867-2869

Walpoth, B. H., Rogulenko, R., Tikhvinskaia, E., Gogolewski, S., Schaffner, T., Hess, O. M., & Althaus, U. (1998). Improvement of patency rate in heparin-coated small synthetic vascular grafts. *Circulation, 98*(19 Suppl), II319-23.

Wang, X.W., Lin, P., Yao, Q.Z., & Chen, C.Y. (2007). Development of small-diameter vascular grafts. *World Journal of Surgery, 31,* 682–689.

Wang, S., Zhang, Y., Yin, G., Wang, H., & Dong, Z. (2009). Electrospun polylactide/silk fibroin–gelatin composite tubular scaffolds for small-diameter tissue engineering blood vessels. *Journal of Applied Polymer Science, 113*(4), 2675-2682

WebMD,LLC. (n.d.). Heart Disease and Coronary Artery Bypass Surgery. Retrieved from: http://www.webmd.com/heart-disease/treating-coronary-artery-bypass

Weinberg, C. B., & Bell, E. (1986). A blood vessel model constructed from collagen and cultured vascular cells. *Science, 231*(4736), 397-400.

Wolf, Y. G., Kobzantsev, Z., & Zelmanovich, L. (2006). Size of normal and aneurysmal popliteal arteries: A duplex ultrasound study. *Journal of Vascular Surgery, 43*(3), 488-492.

World Health Organization (WHO). 2008. The Global Burden of Disease: 2004 update. Geneva: World Health Organization.

World Health Organization (WHO). 2013. Cardiovascular Diseases (CVDs). Retrieved from website: http://www.who.int/mediacentre/factsheets/fs317/en/

Xu, C. Y., Inai, R., Kotaki, M., & Ramakrishna, S. (2004). Aligned biodegradable nanofibrous structure: a potential scaffold for blood vessel engineering. *Biomaterials, 25*(5), 877-886.

Yin, A., Zhang, K., McClure, M. J., Huang, C., Wu, J., Fang, J., . . . El-Newehy, M. (2013). Electrospinning collagen/chitosan/poly(L-lactic acid-co-ε-caprolactone) to form a

vascular graft: Mechanical and biological characterization. *Journal of Biomedical Materials Research Part A, 101A*(5), 1292-1301.

Yoo, J. S., Kim, Y. J., Kim, S. H., & Choi, S. H. (2011). Study on genipin: a new alternative natural crosslinking agent for fixing heterograft tissue. *The Korean Journal of Thoracic and Cardiovascular Surgery, 44(*3), 197-207.

Zhao, J., Qiu, H., Chen, D. L., Zhang, W. X., Zhang, D. C., & Li, M. (2013). Development of nanofibrous scaffolds for vascular tissue engineering. *International Journal of Biological Macromolecules, 56,* 106-113.

Zhang, Y. Z., Su, B., Venugopal, J., Ramakrishna, S., & Lim, C. T. (2007). Biomimetic and bioactive nanofibrous scaffolds from electrospun composite nanofibers. *International Journal of Nanomedicine, 2*(4), 623.

Zhang, Z., Kuijer, R., Bulstra, S. K., Grijpma, D. W., & Feijen, J. (2006). The in vivo and in vitro degradation behavior of poly(trimethylene carbonate). *Biomaterials, 27*(9), 1741-1748.

Zhu, N., & Chen, X. (2013). Biofabrication of tissue scaffolds. In R. Pignatello (Ed.). *Advances in Biomaterials Science and Biomedical Applications.* Retrieved from: http://www.intechopen.com/books/advances-in-biomaterials-science-and-biomedical-applications/biofabrication-of-tissue-scaffolds

Zong, X., Kim, K., Fang, D., Ran, S., Hsiao, B. S., & Chu, B. (2002). Structure and process relationship of electrospun bioabsorbable nanofiber membranes. *Polymer*, *43*(16), 4403-4412.